

**AN INVESTIGATION INTO LOW SPEED
REAR IMPACTS OF AUTOMOBILES**

By

ROBERT WILLIAM THOMSON

B.Sc., The University of Calgary, 1987

**A THESIS SUBMITTED IN PARTIAL FULFILLMENT OF
THE REQUIREMENTS FOR THE DEGREE OF
MASTER OF APPLIED SCIENCE**

in

**THE FACULTY OF GRADUATE STUDIES
DEPARTMENT OF MECHANICAL ENGINEERING**

We accept this thesis as conforming
to the required standard

THE UNIVERSITY OF BRITISH COLUMBIA

SEPTEMBER 1990

© Robert William Thomson, 1990

In presenting this thesis in partial fulfilment of the requirements for an advanced degree at the University of British Columbia, I agree that the Library shall make it freely available for reference and study. I further agree that permission for extensive copying of this thesis for scholarly purposes may be granted by the head of my department or by his or her representatives. It is understood that copying or publication of this thesis for financial gain shall not be allowed without my written permission.

Department of Mechanical Engineering
The University of British Columbia
Vancouver, Canada

Date Jan 22/91

ABSTRACT

A substantial number of whiplash injuries are reported for motor vehicle accidents which produce little or no structural damage to the automobile. These injuries are predominantly associated with rear-end type accidents affecting passengers of the struck vehicle. Since passengers of the striking vehicles are not reporting as many injuries for the same accidents, occupant and vehicle dynamics experienced during low speed-rear impacts were proposed to be a major source of the whiplash claims.

A review of previous research revealed that little information exists for this type of accident. In general, vehicle safety research and government regulations have been directed towards occupant mortality - not injury - in frontal collisions. Occupant dynamics research has been limited to sled testing, using modified seat structures, or out-of-date vehicle models. Full scale, rear impact, crash testing has concentrated on high impact speeds (above 30 km/h) where significant structural deformation occurs.

A research program was designed to investigate the occupant and vehicle dynamics during low speed - rear impacts. Experimental research was undertaken to document the structural performance of vehicles, noting the impact speeds necessary to initiate the crush mechanisms in the rear portion of the vehicle. To facilitate this testing, a pendulum impactor, based on the government test procedures, was designed and built to consistently reproduce impact speeds below 20 km/h.

A total of 56 rear impact tests were conducted with 1977-1982 Volkswagen Rabbits. The vehicle wheels were locked to represent a vehicle stopped in traffic - the most commonly reported whiplash producing accident. An anthropometric test dummy was used to represent a front seat passenger during the tests. High speed video recordings of the tests were digitized to

provide kinematic information on the occupant and vehicle response. Accelerometers were incorporated into the last 24 tests to monitor the acceleration levels at the bumper mount, seat mount and within the dummy.

Information obtained from this testing suggested that permanent structural damage was only visible when an impact speed between 14 and 15 km/h was experienced by the vehicle. Very little frame deformation occurs for impact speeds below this value. Below this threshold, the vehicle frame can be considered rigid; vehicle response being dominated by the compliance of the bumper and suspension systems as well as sliding of the locked wheels. The accompanying occupant response was a differential rebound of the head and shoulders off the seatback and head restraint. This relative motion between the head and torso was evident in each test and increases the potential for injury. Typical occupant response observed consisted of an initial loading and deflection of the seatback due to the occupant's inertia followed by the release of this stored spring energy as the occupant was catapulted forward. It is this elastic behaviour of the seatback which is the likely cause of whiplash injury. Resulting head velocities were found to be in the order of 1.5 - 2 times the resulting vehicle speed. Initial occupant postures which increased the distance between the torso and seatback tended to increase the dynamic loading experienced by the passenger.

Analytical modelling of the vehicle was initiated as the groundwork for full occupant-vehicle simulation. A finite element model of the vehicle frame, bumper, and suspension was created. Previously obtained empirical information suggested that a non-linear bumper and suspension system connected to a rigid frame would be an acceptable approximation. A parametric analysis of bumper stiffness and braking conditions was conducted in a 30 simulation matrix. General kinematic trends of the tests were observed in the simulations, however, limitations in the material properties introduced a much stiffer response than that experimentally observed.

Results from this study show that little protection is offered to an occupant during a rear end collision. Impact energy management within the vehicle may not be adequate to prevent injury. Improved occupant protection requires the highly elastic behaviour of the vehicle frame and seatback to be attenuated. This will eliminate the amplification of vehicle motion through the seatback to the occupant.

TABLE OF CONTENTS

ABSTRACT	ii
TABLE OF CONTENTS	v
LIST OF TABLES	viii
LIST OF FIGURES	ix
ACKNOWLEDGMENTS	xii
CHAPTER 1 INTRODUCTION	1
1.1 THE WHIPLASH INJURY	2
1.2 THE ROLE OF THE VEHICLE DURING A COLLISION	7
1.3 RESEARCH OBJECTIVES	9
CHAPTER 2 LITERATURE REVIEW	12
2.1 OVERVIEW	12
2.2 INJURY AND IMPACT TOLERANCE	14
2.2.1 INJURY MECHANISMS	14
2.2.2 HUMAN VOLUNTEER STUDIES	15
2.2.3 CADAVER STUDIES	20
2.2.4 ANIMAL STUDIES	21
2.2.5 MODELLING	22
2.2.5.1 MECHANICAL MODELS	23
2.2.5.2 NUMERICAL MODELS	30
2.3 VEHICLE SIMULATIONS	32
2.3.1 LUMPED MASS MODELS	33
2.3.2 FINITE ELEMENT METHODS	36
2.3.3 HYBRID SYSTEM	39
2.4 SAFETY EQUIPMENT	39
2.4.1 SEATBACKS AND HEAD RESTRAINTS	40
2.4.1.1 DEPLOYABLE HEAD RESTRAINTS	44
2.4.2 BUMPERS	45
2.5 FULL SCALE TESTING	46
2.6 SUMMARY	51
CHAPTER 3 EXPERIMENTAL TESTING	53
3.1 LOW SPEED IMPACT TEST FACILITY	53
3.1.1 INSTRUMENTATION	55
3.1.2 TEST MATERIALS	61

3.2 PROCEDURES: SERIES I	61
3.3 PROCEDURES: SERIES II	64
3.4 TESTING SCHEDULE	66
3.5 DATA FORMATS AND PROCESSING	68
3.5.1 SERIES I	69
3.5.2 SERIES II	71
3.5.2.1 VIDEO PROCESSING	71
3.5.2.2 ACCELEROMETER PROCESSING	73
CHAPTER 4 DATA ANALYSIS AND RESULTS	75
4.1 SERIES I TESTING: VEHICLE PERFORMANCE	75
4.2 SERIES I TESTING: OCCUPANT RESPONSE	79
4.3 SERIES I TESTING: DISCUSSION	87
4.4 SERIES II TESTING: VEHICLE RESPONSE	89
4.5 SERIES II TESTING: OCCUPANT RESPONSE	106
4.6 DISCUSSION (SERIES I AND II)	109
CHAPTER 5 COMPUTER MODELLING OF THE VEHICLE	111
5.1 INTRODUCTION	111
5.2 VEHICLE MODEL CONSTRUCTION	112
5.3 IMPLEMENTATION OF THE MODEL	116
5.4 SIMULATION CONDITIONS	118
5.5 SIMULATION RESULTS	120
5.6 ERROR ANALYSIS	128
5.7 DISCUSSION OF MODELLING PROGRAM	130
CHAPTER 6 CONCLUSIONS AND RECOMMENDATIONS	132
6.1 OCCUPANT SAFETY IMPROVEMENTS	136
6.2 WHIPLASH RESEARCH RECOMMENDATIONS	138
6.2.1 EXPERIMENTAL STUDY	138
6.2.2 NUMERICAL MODELLING PROGRAM	140
6.2.3 RECOMMENDATIONS FOR FUTURE WORK	140
APPENDIX A PENDULUM DESIGN	144
APPENDIX B FEM MODEL DEFINITION	148
APPENDIX C SOFTWARE DESCRIPTIONS	153
APPENDIX D VEHICLE INFORMATION	155
Geometric and Mass Properties of the Test Vehicles	155
Suspension Parameters	158
Bumper Characteristics	160

APPENDIX E PHOTOGRAMMETRY	163
APPENDIX F CANADIAN MOTOR VEHICLE SAFETY STANDARDS	164
CMVSS 202	165
CMVSS 215	168
REFERENCES	174
BIOGRAPHICAL INFORMATION	181

LIST OF TABLES

Table 3.1: Matrix of Series I Testing (1988)	67
Table 3.2: Matrix of Series II Testing (1989)	68
Table 4.1: Bumper Performance in Series I Testing	77
Table 4.2: Bumper Performance - Series II	95
Table 5.1: Bumper Stiffness Simulations	119
Table 5.2: Performance of Computer Modelled Bumper	122
Table 5.3: Calculated Energies During Impact	129
Table 6.1: Suggested Improvements to Low Speed Impact Test Facility	139
Table D.1: Inertial Measurements of 1979 Rabbits	155
Table D.2: Mass Properties of a Modified 1977 VW Rabbit	155
Table D.3: General Dimensions of 1980 Volkswagen Rabbit	156
Table D.4: Spring Characteristics of Volkswagen Suspension	158
Table D.5: Absorbed Energy for Different Impact Speeds	162

LIST OF FIGURES

Figure 1.1: Components of the Cervical Spine	3
Figure 1.2: Types of Head and Neck Motions	4
Figure 1.3: Hyperextension Caused by a Rear Impact	4
Figure 1.4: Anterior Structures of the Neck	5
Figure 2.1: Occupant (and Vehicle) Coordinate Systems	13
Figure 2.2: Mertz-Patrick Neck Loading Criteria	18
Figure 2.3: Cross-section of the Neck	19
Figure 2.4: Neck Model of Culver et al	24
Figure 2.5: The HSRI Neck Model	25
Figure 2.6: Neck Structure of Emori and Horiguchi	27
Figure 2.7: Mintes and Goldsmith's Head and Neck Model	27
Figure 2.8: Structural Features of Test Dummy Necks	28
Figure 2.9: Performance Characteristics of Hybrid II and III Necks	29
Figure 2.10: Discrete Anatomical Modelling used by Goldsmith et al	31
Figure 2.11: Lumped Mass Model for Rear Impacts	34
Figure 2.12: Rear Structure with Corresponding Lumped Mass Model	35
Figure 2.13: Influence of Impact Speed on Maximum Neck Extension	43
Figure 2.14: Effect of Impact Speed on Vehicle and Occupant Accelerations	48
Figure 2.15: Test Results of Emori and Horiguchi	50
Figure 3.1: Pendulum Impact Facility	54
Figure 3.2: Typical Video Images	56
Figure 3.3: Instrumentation and Transducer Location	58
Figure 3.4: Occupant Instrumentation	59
Figure 3.5: Optical Shaft Encoder for Speed Trap	60
Figure 3.6: Occupant Positions Studied	63
Figure 3.7: Pneumatic Pendulum Release Mechanism	65
Figure 4.1: Pendulum and Bumper Displacements	76
Figure 4.2: Bumper Isolator Construction	78
Figure 4.3: Vehicle and Occupant Response for a 18.4 kmh Impact	79
Figure 4.4: Vehicle and Occupant Response for a 8.1 kmh Impact	80
Figure 4.5: Typical Occupant Movement	82
Figure 4.6: Loadings of the Occupant's Head and Neck	83
Figure 4.7: Occupant Head Deflections and Accelerations	84
Figure 4.8: Head Rotation	84

Figure 4.9: Occupant Acceleration Relative to the Vehicle	85
Figure 4.10: Effect of Head Restraint on Head Rotation	85
Figure 4.11: Posture Effects on Occupant Displacement	87
Figure 4.12: Errors in the Filtering Process	90
Figure 4.13: Bumper Response for an 8.2 kmh Impact	92
Figure 4.14: Bumper Response for a 12.3 kmh Impact	93
Figure 4.15: Bumper Response for a 13.7 kmh Impact	94
Figure 4.16: Vehicle and Pendulum Velocities for an 8.2 km/h Impact	97
Figure 4.17: Vehicle and Pendulum Velocities for a 12.3 km/h Impact	98
Figure 4.18: Vehicle and Pendulum Velocities for a 13.7 km/h Impact	99
Figure 4.19: Accelerations of the Vehicle and Pendulum for an 8 kmh Impact	101
Figure 4.20: Accelerations of the Vehicle and Pendulum for a 12 kmh Impact	102
Figure 4.21: Accelerations of the Vehicle and Pendulum for a 14 kmh Impact	103
Figure 4.22: Accelerometer Results for an 8.2 kmh Impact	104
Figure 4.23: Accelerometer Results for a 12.3 kmh Impact	104
Figure 4.24: Accelerometer Results for a 13.7 kmh Impact	105
Figure 4.25: Influence of Impact Speed on Peak Seat Mount Accelerations	105
Figure 4.26: Occupant Response During a 13.7 kmh Impact	107
Figure 4.27: Occupant and Vehicle Response During an 8 kmh Impact	108
Figure 4.28: Influence of Impact Speed on Peak Occupant Accelerations	108
Figure 4.29: Influence of Initial Occupant Position on Shoulder Accelerations	109
Figure 5.1: Proposed Computer Model of the Vehicle	113
Figure 5.2: Finite Element Model of the Vehicle	114
Figure 5.3: Comparison of Experimental and Numerical Results	121
Figure 5.4: Vertical Displacements of the Vehicle	122
Figure 5.5: Simulated Dynamics of a Vehicle Struck at 8 km/h	123
Figure 5.6: Simulated Dynamics of a Vehicle Struck at 15 km/h	124
Figure 5.7: Simulated Dynamics of a Free Rolling Vehicle Struck at 8 km/h	126
Figure 5.8: Simulated Dynamics of a Free Rolling Vehicle Struck at 15 km/h	127
Figure A.1: Free Body Diagram of Pendulum	147
Figure D.1: Volkswagen Frame Dimensions	157
Figure D.2: Force / Deflection Curves for Suspension Springs	158
Figure D.3: Damping Characteristics of the Suspension	159
Figure D.4a: Bumper Deflection and Force Response with Time	160
Figure D.4b: Bumper Force/Deflection Response	161
Figure D.5: Approximate Bumper Force/Deflection Curve	161

Figure D.6: Predicted Energy Dissipation	162
Figure E.1: Photographic - Full Size Image Transformation	163

ACKNOWLEDGEMENTS

This project has brought together the efforts of many talented people. The guidance of Dr. Doug Romilly was invaluable throughout this program and it was Dr. Frank Navin's encouragement, along with the resources of the U.B.C. Accident Research Team, that allowed this project to become reality. A special hats off goes to Mike Macnabb who has steered many graduate students (with more on the way) through the system.

The research presented within would not have been possible without the help of Transport Canada Road Safety Directorate (Director General Chris Wilson, P. Eng. and Danius Dalmotas responsible for biomechanics research) whose loan of the Hybrid II Test Dummy, and the equipment grant (File-ASF 3261-113-5) for the accelerometers in Series II were crucial to the testing. Additionally, the staff of the Insurance Corporation of British Columbia Research and Training Center (Bob Wilson, Iain Savill, Joe Micelli, Dave Mitchell, and Larry Kenmare) must be recognized for their efforts in providing space for the pendulum facility and supplying test vehicles. Their expertise in automobiles and constant harassment was greatly appreciated. Thanks also goes to JLR Computing (Everett, Wash.) who is responsible for licensing the ANSYS software at U.B.C. and provided technical support on several occasions. In addition, the Centre for Advance Research and Laboratory for Computer Vision must be acknowledged for access to their facility and especially Stewart Kingdon for his time and effort in developing my Series II digitizing software. Bruce Lehmann is also thanked for providing the filtering software used in processing the Series II data.

Finally, I must thank my parents for all their patience and understanding. In addition, I appreciate all the encouragement from my friends, especially from my favourite editor, Joanne Ellis.

Chapter 1 INTRODUCTION

A substantial rise in reports of 'whiplash' producing accidents in British Columbia has been recently documented by Mercer [1]. Review of these accident reports show that a significant percentage occur with little or no accompanying vehicle damage. A litigious syndrome does not appear to be the sole reason for the increasing numbers of injury claims. An accurate diagnosis of 'whiplash' or neck hyperextension is in many cases symptomatic and subjective as existing evaluation techniques are unable to identify soft tissue injuries. Without observable damage to the occupant and vehicle, difficulties arise in both medical treatment and arbitration of insurance settlements.

All aspects of whiplash injuries attract attention. Doctors disagree on the cause, diagnosis, severity, and treatment. Without the physical evidence of trauma, litigation is based on the credibility of the complainants. Accident reconstructionists (usually engineers or police officers) are often used to comment on the accident. However, these engineering investigations provide little insight after the accident. Low speed collisions produce little if any external vehicle damage and the compliant nature of the interior surface often yields no evidence of occupant contacts inside the vehicle.

There is little information currently available on low speed impacts. Vehicle safety research has historically sidestepped the low speed collision; resources have been directed at high speed collisions where occupant mortality is of concern. The resulting advances in safety systems and medical techniques have reduced the fatality rate in automotive accidents. However, traffic deaths are being replaced by increasing reports of less severe - but still debilitating - injuries as the cause of concern.

1.1 - THE WHIPLASH INJURY

The social and financial costs associated with whiplash demand a critical review of the injury. A diagram of the major physiological components of the head and neck are shown in Figure 1.1. The neck is made up of 7 vertebrae identified as C1 (at the head) to C7. The two most superior are also known as the atlas (C1) and the axis (C2). The vertebrae are separated by flexible intervertebral discs which allow small rotations of adjacent vertebrae. The cumulative movements of the vertebral joints produce the types and ranges of motion depicted in Figure 1.2. Two important areas are the atlanto-occipital and the atlanto-axial joints which are the largest contributors to the nodding (yes) and rotation (no) movements, respectively.

The actual mechanism of the whiplash injury is still under dispute. The most commonly used explanation is hyperextension (extension of the head beyond normal range of motion) over the seatback, Figure 1.3. In Figure 1.4, rotation of the head and neck rearward elongates the anterior muscle groups and ligaments as well as the anterior aspects of the discs. The larynx and esophagus may also be stretched and traumatized if the head is moved away from the mandible (opening of the mouth). Unfortunately, injuries are also reported by individuals who could not experience hyperextension due to seatback or head restraint restrictions. These injuries may be a result of the neck being rotated (as if looking to the side) before the accident. The normal range of rearward motion is reduced when the head is rotated due to prestraining of ligaments [2],[3]. Attending physicians report that many patients claim they were looking to the side at the time of impact [4]. Other injury mechanisms to explain whiplash have been developed and are mentioned in the review of previous research (Chapter 2).

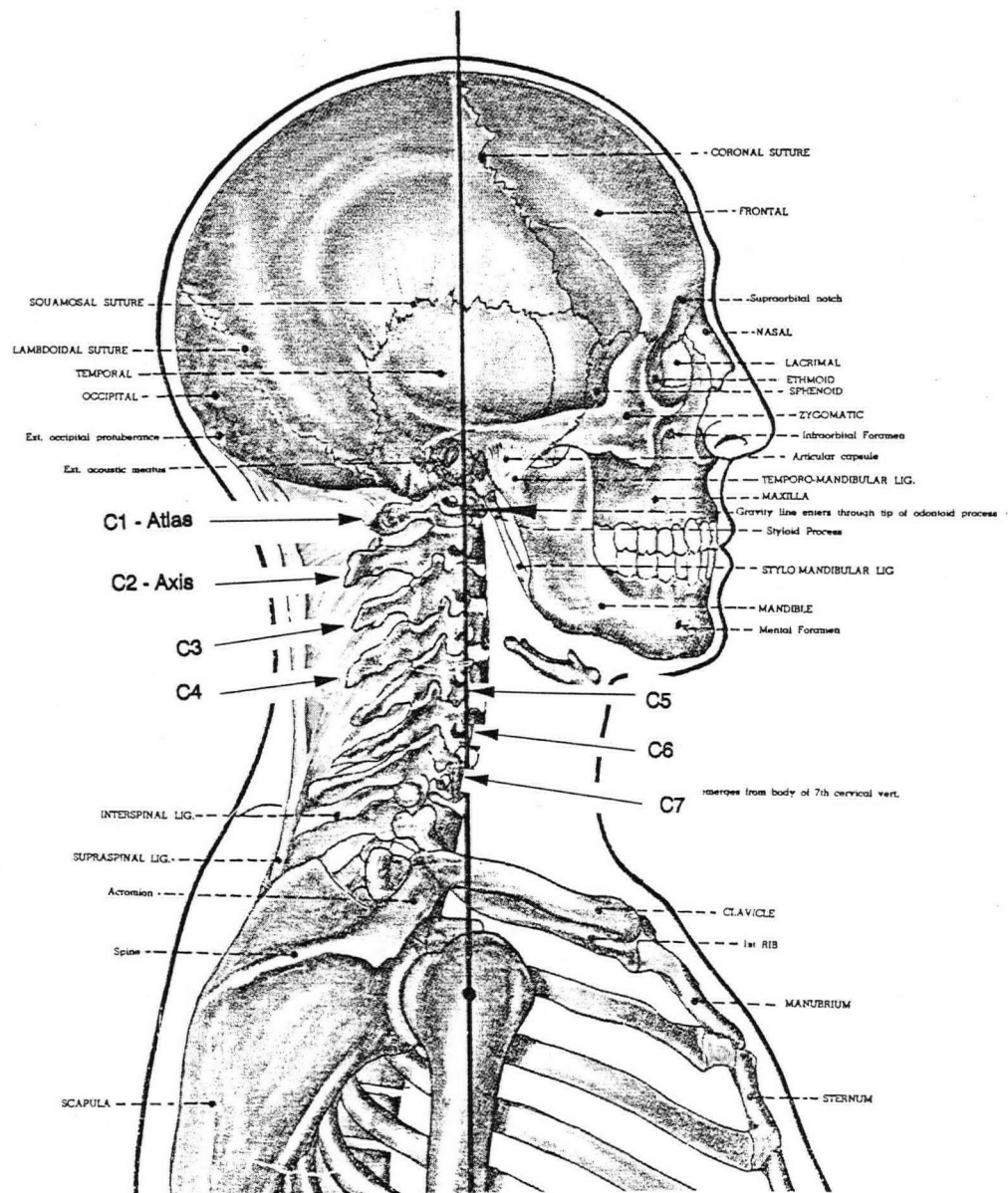


Figure 1.1: Components of the Cervical Spine
(adapted from [5])

The symptoms of whiplash vary between individuals even for similar accident conditions. Dizziness, nausea, and a stiff, sore neck are the most common symptoms. As mentioned before, moderate cases may exhibit laceration of the anterior muscles. Damage to intervertebral discs [8] or important nerves lying within muscle fibers may also arise. This nerve damage may lead to weakness and fatigue in the upper extremities and may interfere with the patient's vocation.

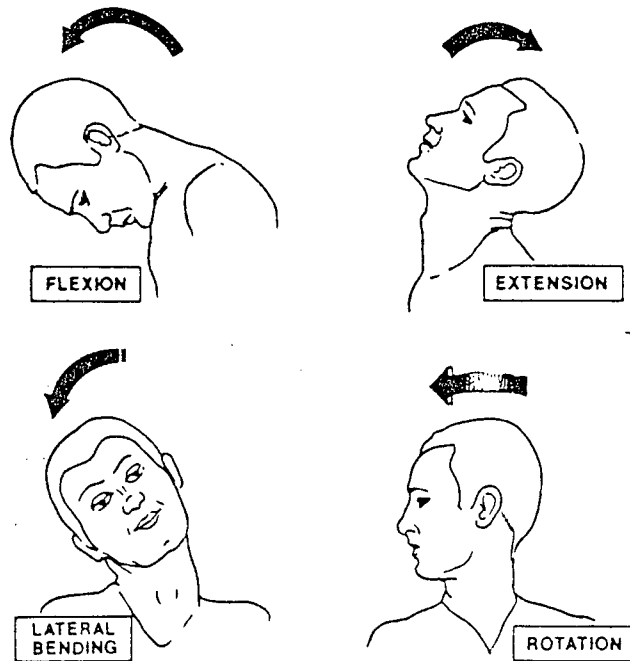


Figure 1.2: Types of Head and Neck Movements
(from [7])

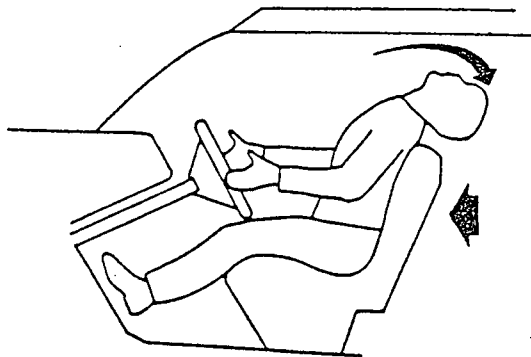
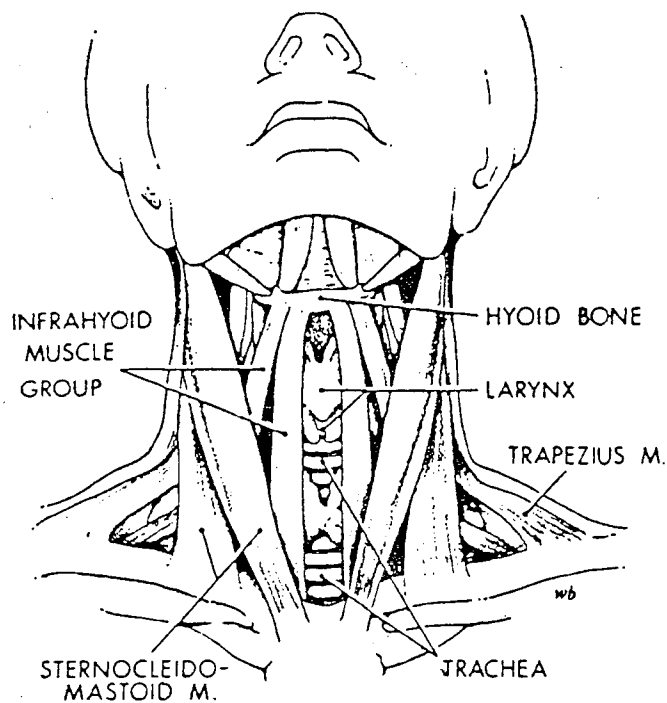


Figure 1.3: Hyperextension Caused by a Rear Impact
(from [8])

More severe cases of whiplash can exhibit ligament and intervertebral damage, but bone fractures are limited to extreme cases of whiplash. The majority of sufferers experience pain in the anterior aspect of the neck when first treated. They may subsequently develop pain posteriorly which can persist longer and is usually associated with the long term debilitating effects of whiplash [4].



- The anterior visceral compartment bounded on the side by the sternocleidomastoid muscles. The larynx and trachea are found on the midline

Figure 1.4: Anterior Structures of the Neck
(adapted from [3])

The injuries received do not necessarily manifest themselves immediately, nor are they restricted to short term duration. Severy [9] reports that symptoms may take from 24 hours to 3

weeks to develop. Information presented at a whiplash symposium sponsored by the Chiropractic Society of British Columbia suggested that treatment of whiplash injuries can last for years without any appreciable reduction in severity and add a psychological element as the patient grows concerned with the long recuperation time. Concerns about predisposition to degenerative arthritis [10] and increased risk of injury in a subsequent accident may also affect the injured individual [6].

There has been a number of surveys observing the presence of whiplash in accidents. The results show that this injury is over-represented in rear end type accidents. Passengers reporting neck injuries are almost exclusively found in the struck vehicle while occupants of the striking vehicle suffered less severe or no injuries. Documentation of the head restraint's introduction shows a reduction in the severity of injury, but the number of reported injuries was not significantly affected. Part of this problem can be attributed to the adjustable head restraint which is often not properly positioned for the occupant.

Whiplash is not confined to North America alone, Emori [11] reports that 40% of automotive related injuries in Japan are whiplash and claim 30% of all insurance payment claims. The Insurance Corporation of British Columbia reported that in 1989, bodily injury claims were responsible for \$600 million of the \$1 billion paid in total claims. It is estimated that whiplash claims make up 1/3 of these injury costs.

Most of the growing concern with whiplash injuries is the low level of vehicle damage. Whiplash injury costs in B.C. probably exceed the associated repair costs for the vehicle when the insurance claim, medical costs, and lost wages are considered. A balance between the "repair bills" of car versus occupant is necessary. Vehicle structures are better understood and controlled, thus a reduced injury potential at the expense of the vehicle is preferable, since fewer hidden costs will be encountered. The repair cost for a vehicle is related to its performance in

the accident as discussed in the following section.

1.2 - THE ROLE OF THE VEHICLE DURING A COLLISION

An automobile collision involves several dynamic processes. As the vehicles come into contact, the vehicle structures deform converting some of the system's kinetic energy into sound, thermal and strain energies. The deformation is defined by the vehicle's stiffness characteristics while the recoverable deformation is a function of its elastic properties. At high impact speeds, relatively little elastic recovery occurs and the vehicle generally behaves as a plastic body. At low impact speeds, however, plastic behaviour may be absent allowing more of the total impact energy available to be recovered in elastic rebound. For the occupant, the best 'ride down' or deceleration profile occurs when the vehicle behaves as a plastic body where large structural deformations reduce the overall acceleration. This creates a major dilemma for the manufacturer, occupant and insurer. Each would like the vehicle to provide the maximum protection for the occupant with the minimum material damage to the vehicle during a collision. As the vehicle becomes stiffer, the vehicle damage costs are reduced as less permanent deformation takes place. However, the occupant now experiences a more violent ride down which increases the potential for injury. To illustrate this concept, one particular vehicle tested at the U.B.C. Accident Research facility showed no structural damage after striking a rigid barrier at 15 km/h and was indicative of a predominantly elastic response. The overall change in velocity, ΔV , experienced by an occupant in this vehicle would have been approximately 30 km/h due to the nearly equal and opposite rebound velocity which resulted after the barrier impact. If this vehicle had behaved in a fully plastic manner upon impact, the same occupant would have experienced a ΔV of only 15 km/h. Thus, based on an assumption of equal impact times during both collisions, the average acceleration experienced by the occupant in the elastic vehicle would be approximately twice that of the plastic vehicle. This theory implies that vehicles not sustaining damage in low speed impacts can produce correspondingly higher

dynamic loadings on their occupants than those which plastically deform under the same or possibly more severe impact conditions. Kipp [12] used this approach to simulate high speed, plastic impacts with low speed, elastic impacts.

Much of the existing literature on road safety addresses vehicle and occupant dynamics in the moderate to high speed range (greater than 50 km/h). This is a result of many countries having set vehicle performance standards based on 50 km/h frontal barrier impacts. However, the majority of accidents occur below this speed. According to a Transport Canada publication [13], in urban areas where travel speeds are below 50 km/h (on average), 250% more injuries occur than in rural areas where highway speeds are typical. Obviously there are higher traffic volumes in developed areas, and vehicle standards should address the commonly encountered accident types.

Government compliance regulations (Canadian Motor Vehicle Safety Standards, CMVSS; Federal Motor Vehicle Safety Standards, FMVSS, in the U.S.) governing the performance of the automobile structure in moderate vehicle speed situations (5 - 50 km/h) is limited to an 8 km/h bumper standard listed in Appendix F (CMVSS 215 [14]). This criteria requires that the safety features of the automobile (doors, hood latches, lights, etc) suffer no degradation in performance when the vehicle is subjected to 8 km/h pendulum impacts on both sets of bumpers. The only specification on occupant dynamics below the barrier impact speed is a requirement that the head cannot rotate more than 45 degrees over the head rest, when the occupant and seat are subjected to an 8 g acceleration in the direction of travel. However, this standard can be avoided if the seatback structure can support a moment of 3220 ft-lbs when a static load is applied at the top of the head restraint (CMVSS 202 [19] - Appendix F).

This seatback standard is of particular concern because the seat is a primary safety system in a rear end impact. Inertia of the occupant and the forward motion of the vehicle results in dynamic loading of the seatback structure. Since the occupant is directly loaded by the seat, its characteristics will have a definite influence on occupant injury.

Before leaving vehicle performance, it is important to describe the dynamic parameter used in accident evaluation. The road safety literature makes extensive use of the change in velocity or ΔV . As the vehicles interact, contact forces produce changes in the vehicle's velocities. Because the occupant is contained within the vehicle, it is presumed that they experience the same velocity change. Accident reconstructionists were probably the impetus for this approach. They utilize the physical evidence from the accident (tire marks, vehicle damage and known travel paths) to recreate the accident. The foundation of these recreations is the conservation of momentum and energy which allow the change in velocity to be calculated, but its history during the crash sequence cannot be derived without replicating each accident with instrumented vehicles. Thus, ΔV is the only quantifiable description of accident severity after the event and is also used to describe the occupant's potential for injury.

The limitations of this criteria are obvious. Velocity change is meaningless if the time over which it occurs is omitted. Tarriere et al [15] described this shortcoming with examples of accidents with similar ΔV 's but varying severity due to the different acceleration histories experienced by the vehicle and the occupant.

1.3 - RESEARCH OBJECTIVES

Whiplash has become an increasing problem for the medical community, insurance agencies, accident reconstructionist, and the automobile manufacturer. Conflicting opinions

exist on diagnosis, treatments, injury mechanisms, vehicle performance, preventive measures, and particularly the correlation between vehicle damage and occupant injury. Because of this, the establishment of a standard treatment for an injured individual is impossible.

In general, whiplash injuries constitute a significant portion of the motor vehicle accident casualties. Surveys indicate that they are predominantly associated with occupants of a vehicle struck from behind, ie passengers of the striking vehicle are usually uninjured in the accident. Isolating these rear impacted vehicles, the overall approach of this whiplash research program is to divide the problem into three parts to identify/quantify:

- 1 The impact dynamics and energy transfer from the striking vehicle into the frame of the struck vehicle;
- 2 The mechanisms by which energy is transferred from the bumper, through the vehicle frame to the seat occupied by the passenger; and
- 3 The dynamics of the occupant interaction with the seatback / head restraint which leads to the injury.

Each of these areas confront the investigator with different challenges. The focus of this research program will be on parts 1 and 2, but all three areas will be discussed. The specific objectives of this research are listed.

Critically Review the Research Reported in Previous Projects

Current information available on whiplash research or studies related to the response of vehicles in collisions is reviewed in Chapter 2. This material is assessed for contribution and deficiencies in the understanding of the whiplash injury and is used to provide direction for the testing and analysis used in the current project.

Experimentally Observe Vehicle and Occupant Behaviour During an Impact

An investigation of automobile impacts requires a test facility which can simulate the accident. The pendulum impactor, described in Chapter 3, is developed to provide controllable impact conditions and allow recording of occupant and vehicle dynamics during a collision. Procedures, materials, and instrumentation required for testing are developed and described in Chapter 3.

Analyze the Experimental Results for Significant Events

The data obtained from the test phase is studied to observe the kinematic history of a collision. The interaction of the different components of the vehicle/occupant system must be analyzed to bring out the processes that lead to whiplash injuries. Particular attention is focussed on the bumper's ability to absorb impact energy during the collision and to determine the point at which damage occurs within the vehicle structure. The results of this analysis is presented in Chapter 4.

Numerically Model the System to Parametrically Evaluate the Performance of the Vehicle

Computer modelling is initiated to provide a flexible, parametric analysis tool. A finite element representation of the vehicle is described in Chapter 5. The simulations described in this section are compared with the experimental results for validation of the numerical modelling and are used to evaluate the influence of vehicle components.

Evaluate the Program for Effectiveness

In Chapter 6, a critique of this research project is presented to highlight the contributions made by the study while areas requiring further attention are presented as topics for future research. In addition, suggestions on how this further research could be accomplished are also listed to provide continuity between programs.

Chapter 2 LITERATURE REVIEW

2.1 - OVERVIEW

Whiplash injuries have been the subject of debate for many years. The term was first coined by Dr. Howard Crowe in 1928 to describe the behaviour of the head in a rear end impact, comparing the rapid rearward rotation of the head to the cracking of a whip. Although the whiplash phenomenon has been a part of road safety since then, the first formal engineering investigations did not begin until 1955. Since then, many researchers have used cadavers, animals, human volunteers, anthropometric test dummies (ATD), and mathematical models to study occupant and vehicle rear impact response and whiplash injuries. Although significant resources have been devoted to the problem, we are still far from fully understanding this injury and its causes. Many different theories have been used to describe the injury mechanism and conflicting opinions still exist.

The purpose of this review is to evaluate the research techniques, results, and conclusions of the previous researchers to assist in developing the current research program. The four main divisions that appear in the literature are the areas of injury and impact tolerance research, vehicle simulation, safety systems, and full size instrumented testing. This material is discussed in the following sections to provide a broad and comprehensive knowledge base.

The coordinate systems used in this research are depicted in Figure 2.1. The global (referenced to ground) and local (applied to the component of interest) coordinate systems for the occupant are shown in the diagram. The positive X axis is directed forward, down the occupants line of sight; the Y axis is vertical, positive values oriented upwards; and Z is used to describe lateral motions. Unfortunately, this system is not consistent in the literature reviewed.

The convention employed in this report, as depicted in Figure 2.1, is that of most biomechanic and military researchers, and is also familiar to most engineers. Although not shown, the vehicle's co-ordinate system is identical to that of the occupant.

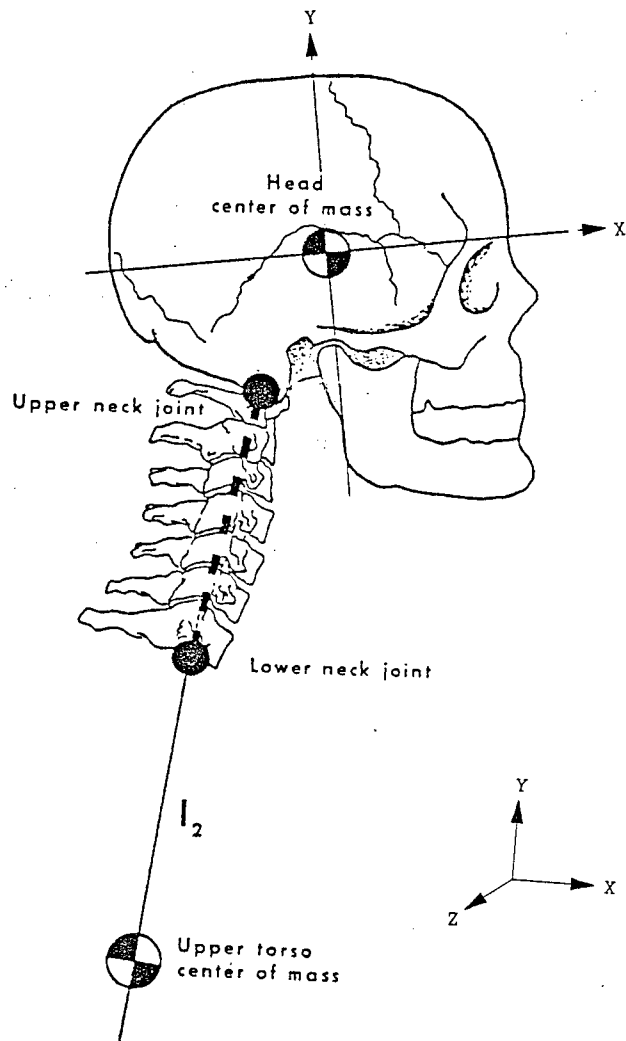


Figure 2.1: Occupant (and Vehicle) Coordinate Systems
(adapted from [16])

2.2 - INJURY AND IMPACT TOLERANCE

2.2.1 - INJURY MECHANISMS

As described earlier, hyperextension of the neck is the most often cited cause of whiplash. Mulligan et al [8] and Mertz [17] give good descriptions of this process. However, the presence of head restraints (after 1968) has limited the amount of extension an occupant may experience. Continuing reports of whiplash injuries suggest that a re-evaluation of the injury mechanism is required.

One important aspect of occupant response is the rebound from the seat. Severy [9] reported that the occupant's head rebounds after the torso has already begun moving forward. However, only the report of States et al [18] comments on this as a possible source of injury. They suggest that this lagging of the head may be extreme enough to force the neck into hyperextension, producing an injury in the presence of a head restraint. Unfortunately, no other researcher has explored this issue further.

Hyperextension may not be required for muscle damage if one uses MacNabb's [6] criteria. He suggests that if the muscle cannot yield to (or support) the deflections, the fibers rupture, independent of the joint angle. This is supported in the many sporting injuries that arise from over-exertion of a muscle group that is fatigued or not prepared for action. The resulting injury produces tenderness and swelling near the affected muscle. When this occurs in the neck region, the numerous nerve roots and bundles present are susceptible to irritation, producing symptoms remote from the injury.

One additional theory from Roaf [19] states that whiplash injuries do not arise out of the hyperextension phase of the response, but during the following flexion. When the occupant rebounds from the seat, their torso is caught by the seatbelt. The head then moves forward past the torso, flexing over the shoulder belt. This could be supported by the numerous complaints of

posterior neck pains. However, in a rear end accident the occupants of the striking car will experience a more violent flexion over the seatbelt, without the initial extension phase. The scarcity of neck injuries among these occupants diminishes the case for this injury mechanism.

Whiplash injuries and accident statistics have been documented by Mercer [1], Mulligan et al [8], States et al [20], O'Neil et al [21] and Garret and Morris [22]. In general, the points brought out in these reports were: 1) rear end impacts are the main cause of whiplash, 2) the introduction of headrests has had some effect on reducing the severity of whiplash injuries but little influence on the frequency of injury, 3) rear impact collisions between 15 and 50 km/h produced essentially the same occupant loading, and 4) occupants can experience differential head and torso movements as they rebound from the seat, possibly causing hyperextension. Investigations to study the different variables presented in these statistics prompted researchers to utilize human volunteers or human analogues in rear impact studies. The different representations have unique strengths and weaknesses and are discussed in the following sections.

2.2.2 - HUMAN VOLUNTEER STUDIES

The first formal research of human response to acceleration loads took place before World War II. Two German doctors Siegfried Ruff and J. Schneider worked for the German Airforce, studying glider landings [23]. Ruff was responsible for first introducing biomechanic testing devices used to study loadings on human subjects. He is responsible for construction of a sled to study impact response, similar to those in use today. The sled test apparatus consisted of a platform to which a test subject was restrained in a chair or seat. The platform was accelerated to a fixed speed and then stopped abruptly to produce a desired deceleration load. Ruff's sled was unique in that he had an X-Ray machine mounted on the sled to monitor occupant skeletal

motions. Similar work was undertaken by Colonel John Stapp [24] in the U.S. His work as an Army doctor exposed him to a number of injuries sustained by pilots who encountered excessive body loadings.

These early researchers were involved in projects for the military and were able to recruit numerous volunteers for their studies. The emphasis was placed on pilot protection during landing or cockpit ejections at flight speed. These two situations produce $-G_x$ and $-G_x + G_y$ accelerations, respectively. Application of these tests to road safety is limited to the frontal impact ($-G_x$). Although this information has been influential to the development of occupant restraints and airbags, studies of occupants exposed to whiplash situations did not appear until the 1960's. Research ethic review committees must have appeared in the early 70's, since volunteer data falls off sharply after this period.

The most important work with human subjects was carried out by Mertz and Patrick [25],[26]. They outlined a criteria, the torque about the occipital condyles, that they proposed would indicate the possibility of a neck injury. Loading corridors for flexion and extension (Figure 2.2) were quantified to allow prediction of injuries. This was also used later as a measure to verify head/neck simulations.

Human volunteers (of varying physical statures) were used to establish a pain threshold. Static tests were used to determine the maximum loads a person would exert on themselves. The static tests were followed by sled tests with low acceleration values to obtain dynamic loading information. Mass characteristics of the volunteers' heads were also altered to observe their influence in these sled tests. In addition, the sled volunteers were instructed to tense or relax their necks during the test so that muscle effects could be observed. The volunteer who experienced the highest recorded neck loading in these test also developed an injury. He

experienced pain down the length of his back and a stiff neck which persisted for several days. Subsequent cadaver tests were used to determine loads required for visible, physical damage to the neck structure.

Mertz and Patrick determined that the neck is much stronger resisting flexion than extension. This is supported by observing a cross-section of the neck (Figure 2.3). The posterior aspect of the neck has an abundance of large muscle groups running the length of its structure. The anterior section cannot accommodate the same amount of fibers, partially due to the presence of the esophagus and larynx. This arrangement produces higher stresses in the anterior muscles, since there is not as much muscle area to share the loads.

This work is important for understanding what loading can induce pain. However, several weaknesses in their study can be isolated. Experimental work of Mertz and Patrick utilized only one occupant posture, a predetermined acceleration pulse and usually a rigid seatback. No references were made to any rebound of the occupant. Some of the specifics of the procedures are not given in the paper but the text and pictures lead one to believe that the occupant sat back against the seat (shoulders contacting the seat), head against the head restraint, and was aware of the impending impact. Although directions were given to induce a specific state of neck muscle tension prior to the test, it is unlikely that the volunteer could fully relax when directed to do so. Also, the range described by the loading corridors is very wide due to the variability between test subjects. This makes it easy for a researcher to meet the criteria when modelling neck response. Unfortunately, the precision and validity of the corridor values have not been verified by independent researchers.

Sled tests by Bowman and Robbins [27] were also conducted on human volunteers. They found that the strength of the neck had a greater effect on head and neck response than the size or mass distribution of the system. This was supported by States et al [18] who reported that

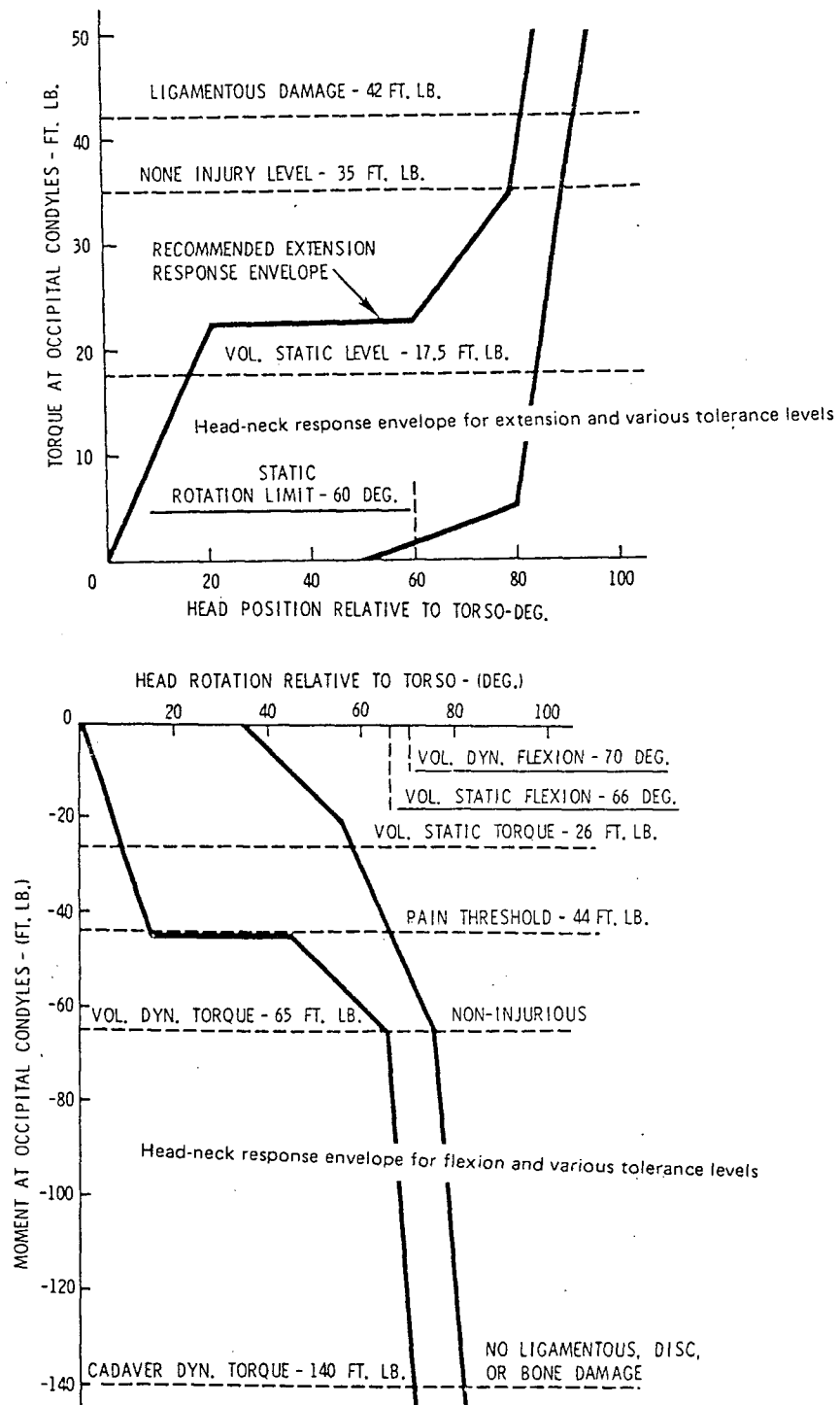


Figure 2.2: Mertz-Patrick Neck Loading Criteria
 (from [26])

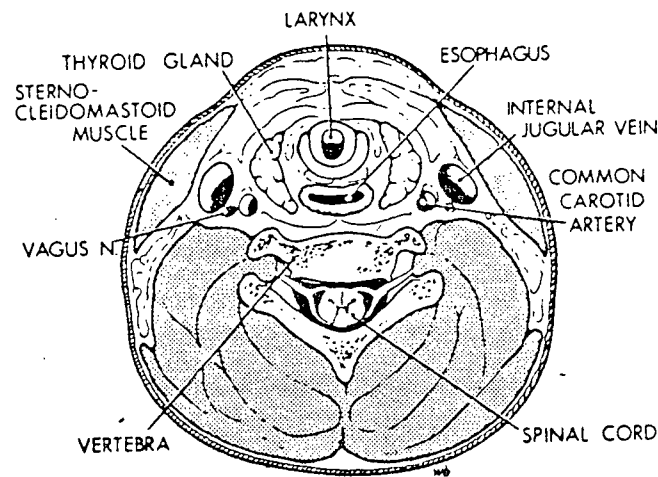


Figure 2.3: Cross-section of the Neck
(from [7])

women are five times as likely to experience a whiplash type injury than men in the same environment. The higher risk for women is a result of the smaller and weaker muscles fibers they have in their necks, compared to men. Subsequent testing by Seemann et al [28] showed that human volunteers can significantly alter their neck response. The researchers noted that the test subjects would tense their neck muscles in anticipation of the sled loading, the trend being more prevalent among those exposed to repeated tests.

A different technique for dynamically loading volunteers was used by Tarriere et al [29] and later by Ewing [30]. The experiments involved swinging a 450 kg pendulum into the shoulders of the subjects at 7.2 km/h to observe hyperextension of the neck. Unfortunately, any comparison of this type of loading to that experienced by a passenger in a struck vehicle is limited. When seated in a vehicle, the occupant is loaded by the seatback acting over the occupant/seat contact area. It appears that these experiments were designed to quantify the head and neck motions only during a rear impact.

The only significant work regarding neuro-muscular response of human necks was conducted by Foust et al [31]. They quantified the range of motion, strength and reflex behaviour in the necks of the test subjects spanning young adults to senior citizens of both sexes. The first two characteristics had been studied previously to understand human anthropometry, but information on reflex response has particular significance for impact tolerance. The researchers studied the response of the head and neck when subjected to a sudden horizontal loading. Information on the muscles was obtained using EMG (electromyogram) equipment, while head dynamics were recorded with accelerometers and film. They determined that approximately 60 ms were required for the muscles to activate and begin responding to the load. This result may be important for analyzing whiplash response, since the muscles may become activated at an inopportune time. Extending this work to whiplash-type loading would likely provide valuable insight into injury mechanisms, since muscle trauma is the most common complaint among the injured.

2.2.3 - CADAVER STUDIES

Several studies have been carried out using human cadavers as test subject. A cadaver provides a conservative value of the ligament and muscle breaking strengths. Their limited performance during impact conditions arise from the lack of muscular response during the event and degradation of the tissues due to age or illness. Still, the cadaver is the only source for meaningful information on hard tissue injuries and provides a factor of safety when these results are applied to living occupants. Mertz and Patrick [26] employed full cadavers in their sled tests to observe bone and ligament injuries. Clemens [32] explored inertial loading of the neck by mounting a cadaver's torso (transected at T10) to a rigid plate attached to the impact sled leaving the head free to contact a head restraint. He discovered that disc type injuries occurred at levels

below which ligament injury was detected suggesting that tissues within the spinal column can be injured before the external components (muscles and ligaments) are affected. This also demonstrates that different tissues have different thresholds of injury, depending on the loading.

2.2.4 - ANIMAL STUDIES

Some work involving animal surrogates was presented by MacNabb [6] where he dropped monkeys (strapped in a seat) down an elevator shaft to simulate rear impacts. Sled testing of primates was presented by Ewing [33] to determine acceleration levels required for severe spinal injuries. Hogson [34] used direct head impacts on monkeys to investigate head injuries and the loading required to induce unconsciousness. These, and similar, animal studies have provided important information on tissue response and the resulting physiological results. However, problems arise when comparing the different animal tissue geometry and strengths to similar human structures. Even the primates have some significant anthropometrical differences that restrict exact comparisons to humans. The communication of injury between the researchers and the animals also limits the information available since most whiplash injuries are symptomatic and not objectively diagnosed.

The important point that comes out of this review of human and animal testing is the lack of useful information available on whiplash injuries. Essentially, only Mertz and Patrick have provided a well documented report on the dynamic behaviour of live human subjects subjected to whiplash loading. Other authors used loading schemes that were not directly applicable to seated occupant response. Even Mertz's tests can be criticized for the use of rigid seatbacks and for not studying occupant posture effects. Only Foust and Seeman have acknowledged the influence of muscle activity, although neither mentioned what effect this has on injury potential in those muscles. And as stated, animal studies have limited applicability to human injuries because of physical differences.

Documentation providing a comprehensive description of whiplash injuries, as well as a parameter that can be used to accurately predict the injury remains to be found. It may not be possible to identify a measure like this, however a better understanding of the injury can be expected with further research.

2.2.5 - MODELLING

There are practical limitations to the use of human and animal subjects for biomechanical studies. Availability, variability, and ethics restrict their use in impact studies. Research oriented towards parametric evaluation of seating position, seat dimensions and characteristics, vehicle performance and other similar variables requires a human surrogate that provides repeatable performance to impact conditions. As a result, mechanical and numerical models have become increasingly popular as material science and computer resources have evolved. The main criticism of this approach is the validity of the model's behaviour since little volunteer data is available. While it is doubtful that a model can be developed to faithfully duplicate human response under the same conditions, the needs of many researchers can be satisfied when consistent performance, referenced to human response, can be achieved.

It is interesting to note that the biofidelity requirements of the government's safety regulations are not well defined. Government regulated compliance testing requires a crash test dummy for determining occupant loading. Unfortunately, the anthropometric dummies employed are based solely on a young male population, with the dynamic neck performance not being satisfied for passengers outside this specific population. The SAE began an anthropometric standard (J962) in the mid 1960's, however its complexity prompted them to cancel the program in 1977. What information is available is limited in terms of age and sex. Additionally, the human volunteer data that is available is narrowly focussed on subjects tested with more complex, sometimes nonrepresentative, restraint systems (for example, data taken

from military research represents individuals restrained with the 4 point harness, compared to the 3 point in all production vehicles). A discussion of the different models, both mechanical and analytical are presented in the following sections.

2.2.5.1 - MECHANICAL MODELS

The early dummies replicated only the range of motion, size and mass of the anatomical components. For example, a 50th percentile male dummy is representative of the average height and weight of the male population (in the U.S.). There was no calibration of dummy to human performance until the late 1960's when the U.S. first introduced the Federal Motor Vehicle Standards (FMVSS). These new regulations required the test dummy to provide qualitative information that could be used as a measure of occupant protection. With this impetus, ATD development became well documented in 1972 when several new dummies were introduced.

As a whiplash investigation tool, the design of the ATD's neck is the primary source of information. The range of motion, static and dynamic loading curves, and general kinematics will be the most important index for comparison to a living human neck response. The position of the neck is convenient as it allows researchers to carry out their work independent of the remaining dummy body. As a result, significant work has been devoted solely to neck models.

Neck models have encompassed many different constructions: one piece rubber components, segments of rubber washers and metal discs, ball and socket joints with rubber stops, and anatomically replicated rubber/plastic representations. A dynamic comparison of dummy to human response had not been made before the neck loading criteria of Mertz and Patrick [26] in 1972. This has since been employed in the development of nearly every mechanical neck model. The obstacles that researchers were still faced with came from the

asymmetric performance of the neck in flexion and extension, nonlinear behaviour during dynamic loading, and a requirement for repeatability and durability to remove any variation between tests.

Examples of the segmented neck models are those developed by Culver et al [35](Figure 2.4) and Melvin et al [36] (Figure 2.5). The neck is composed of a pin or ball and socket joints between round metallic fins. Special rubber resistive elements are placed between the joints to provide resistance to bending. These neck models have been subjected to controlled tests and tend to exhibit stiffer characteristics than those of volunteers.

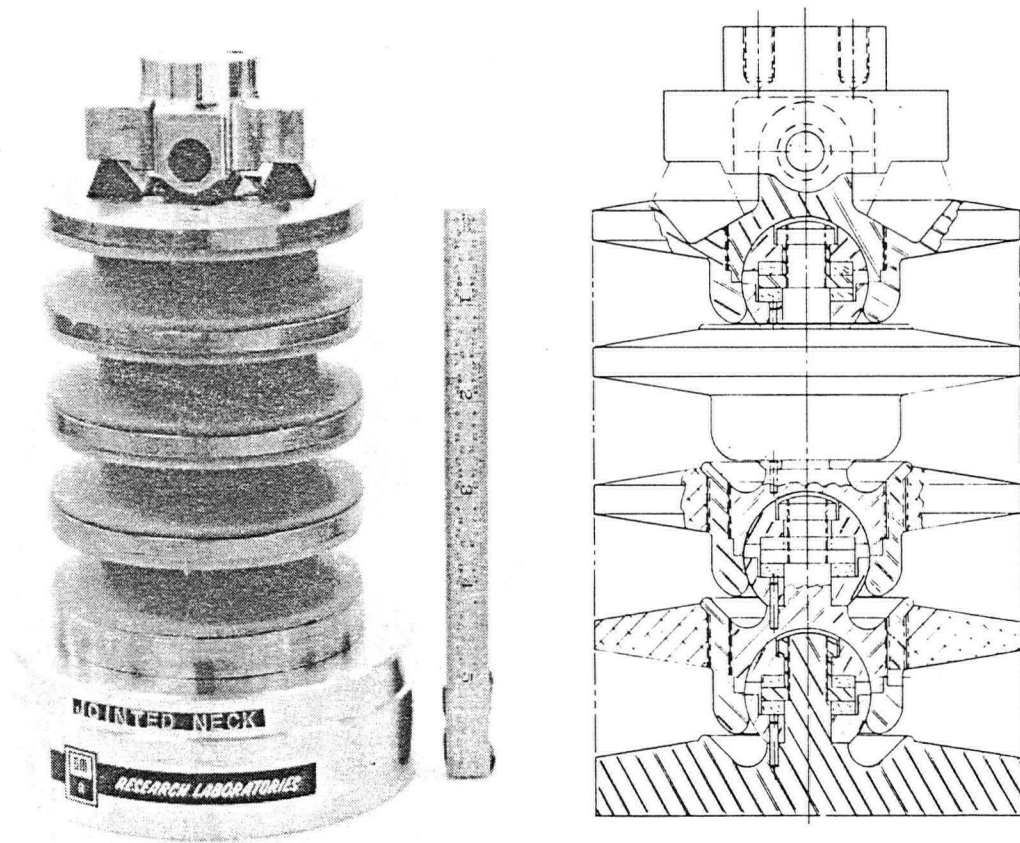


Figure 2.4: Neck Model of Culver et al
(from [35])

Another mechanical neck design was presented by Emori and Horiguchi [17]. Their six segment neck model (Figure 2.6) used aluminum and Teflon cups contained within a rubber tube with axial strength supplied by a central cable. The initial cable tension and the tube wall thickness allows the user to adjust the neck's flexural stiffness. Limited validation testing of the neck restricts interpretation of Emori's test results.

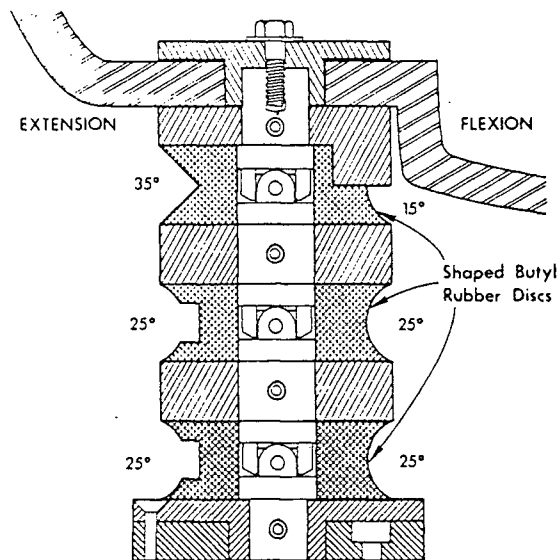


Figure 2.5: The HSRI Neck Model
(from [36])

Mintes and Goldsmith [37] approached neck response by duplicating the anatomy of the head and neck. Ligaments, muscles, discs, and skeletal components were modelled using plastic and rubber components (Figure 2.7). Instrumentation within the model was extensive, allowing the researchers to record deflections and forces in the muscles and ligaments, as well as pressures in the skull and intervertebral discs. The model was fixed to a plate and was not designed to be incorporated into a full body test dummy. This limits its applicability to full scale whiplash testing, since body and seat interactions are not accounted for. This model is useful to observe

the interaction of the neck's components, although the material properties are open to scrutiny.

The most commonly encountered representations of the neck are those of the Hybrid II and Hybrid III test dummies, products of the General Motors research department. The Hybrid II neck (Figure 2.8a - developed in 1972) consists of a tubular rubber neck that attaches at the base of the head and onto the shoulders. This symmetrical neck construction results in similar responses for flexion and extension. The Hybrid III (1976) neck has a more anatomical resemblance with the disk and vertebrae approximations depicted in Figure 2.8b. Not shown is an internal cable which provides axial stiffness to the neck. The rubber disc segments are asymmetrical, providing a better approximation to human performance. Muzzy [38] has shown that the Hybrid II construction has a stiffer response when compared to a volunteer, based on frontal impact simulation. Testing by Foster et al [39] documented the performance of these two necks relative to the Mertz-Patrick results. As shown in Figure 2.9, the Hybrid II exhibits a higher stiffness than volunteer data, while the Hybrid III compares favorably.

Historically, the Hybrid II has been applied to whole body testing, with less emphasis on the specific head and neck motions. In the process, the Hybrid II has proven itself as a reliable test device. More specific and intensive testing of human response has been left to the Hybrid III as it has better (but not perfect) biofidelity and instrumentation options required for refined testing.

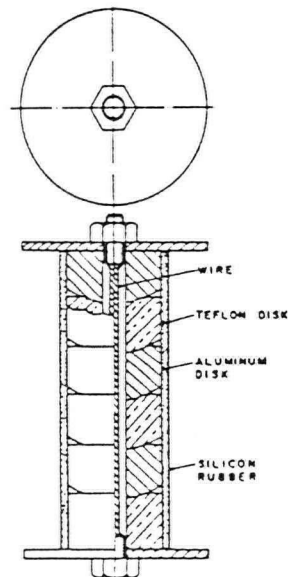


Figure 2.6: Neck Structure of Emori and Horiguchi
(from [17])

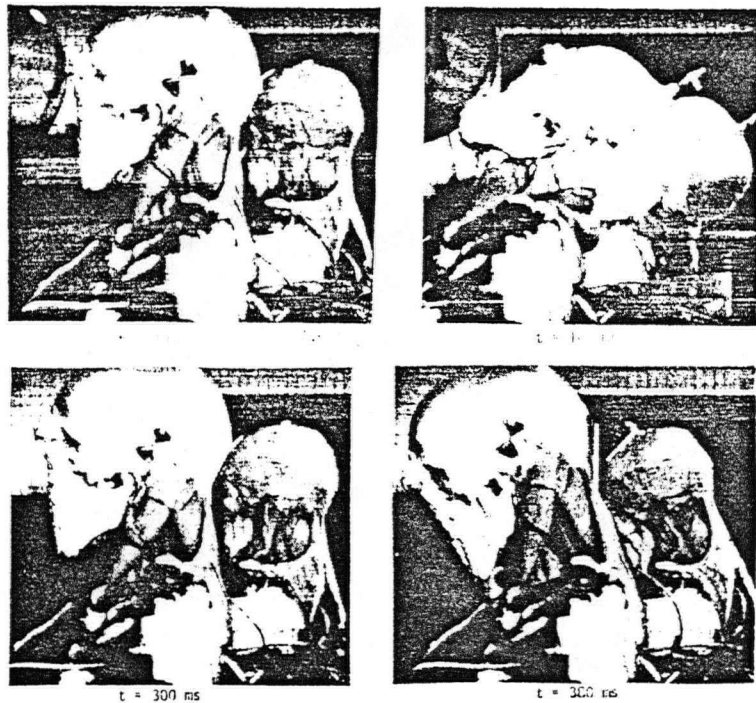


Figure 2.7: Mintes and Goldsmith's Head and Neck Model
(from [37])

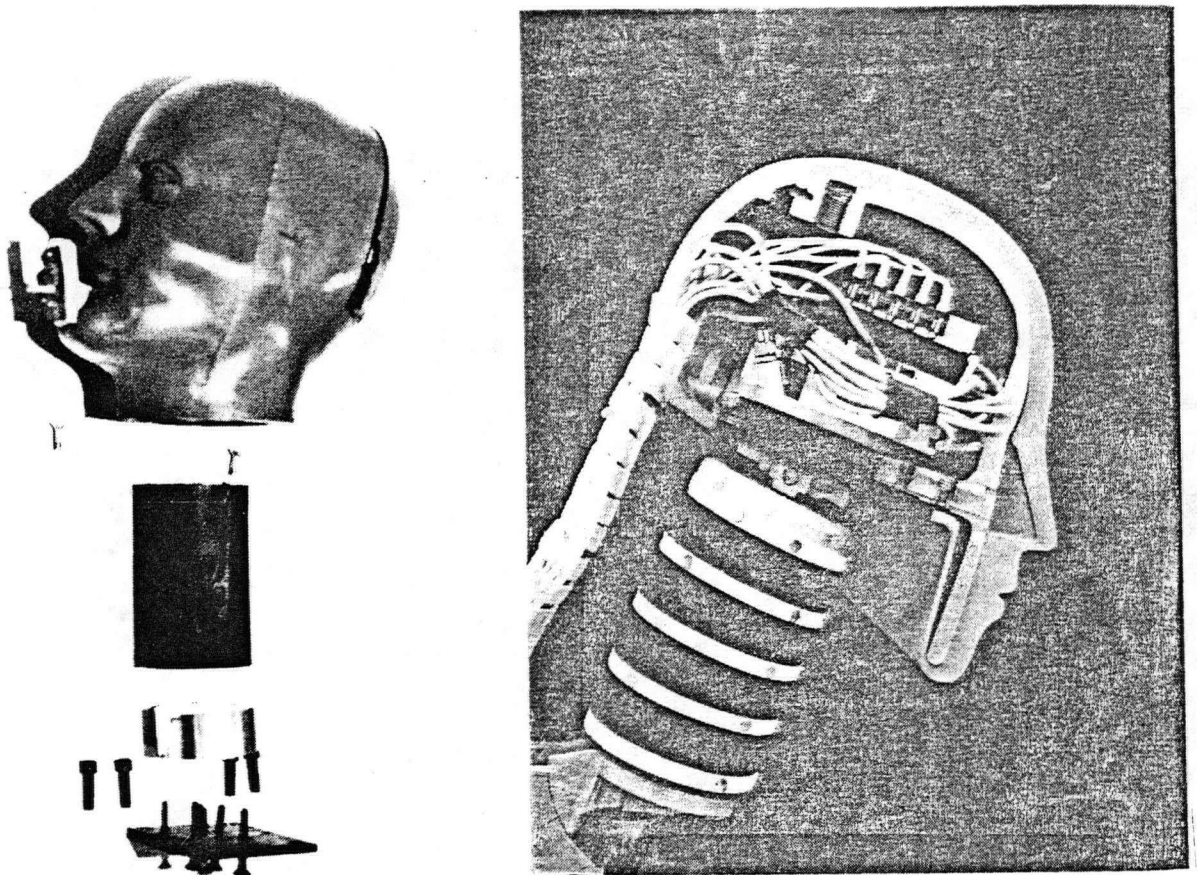
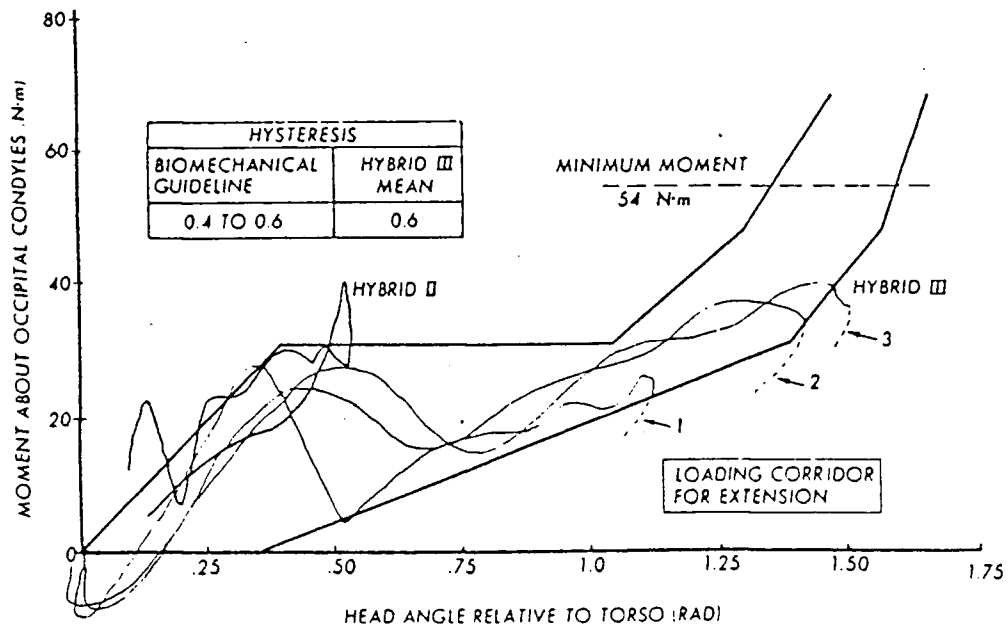


Figure 2.8: Structural Features of Test Dummy Necks
(Left a) - Hybrid II from [38], Right b) - Hybrid III from [40])



Neck extension torque-angle responses are compared to the Hertz et al biomechanical response corridor

Figure 2.9: Performance Characteristics of Hybrid II and III Necks
(from [39])

In summary, the mechanical analogues of the head and neck have some common deficiencies. The most important is a lack of calibration data which limits the comparison of model to human performance. This is of prime importance when human tolerance is being investigated. To date, mechanical necks can only provide a subjective measure of human response. Physiological injuries cannot be identified within a mechanical neck because of their physical differences. In addition, neuro-muscular activity is precluded in all the models reviewed. What a dummy does provide is a durable, consistent approximation of human performance under violent conditions. Overall body motions can be observed which may allow identification of the kinematics leading to possible injury mechanisms.

2.2.5.2 - NUMERICAL MODELS

Numerical simulations of the rear impacted occupant were first reported in 1969. Tarriere and Sapin [29] and Martinez and Garcia [41] produced simple head and neck models using a single rotary degree-of-freedom (DOF) to simulate head and neck rotation. Martinez added a shear DOF between the head and neck to improve the model. A better simulation of whiplash impacts was later presented by Williams and McKenzie [42], utilizing discrete modelling of the neck's vertebrae. These models used nonlinear joint properties to represent bending of the spine. Although Tarriere's model was developed to simulate the neck only, both Martinez and McKenzie's models incorporated the seatback into the occupant model, providing a means to study rear impact situations. Results of these two models showed that the occupants can experience acceleration levels higher than that exhibited by the car. In addition, the stiffness properties of the seat have a significant effect on the occupant's response. Damped seats tended to lower the occupant's accelerations, but excessive elastic deflections will increase the stresses in the occupant's neck. Because the seatback and occupant back are lumped together as one item, both models are deficient in simulating the headrest and occupant position relative to the seatback.

Prasad et al [43] developed a significant rear impact simulator. The occupant's head, spine, and pelvis were modelled as flexible links interacting with the seatback. Stiffness properties of the seatback could be varied to study the effect of stiffness and plastic collapse. This approach was useful in observing the back's movements during a collision. Unfortunately, the authors omitted the seatbelt in the simulation and experimental components in the study. The occupant experienced significant ramping up the seatback and extreme variations in spinal curvature during a collision. Because of high seatbelt usage rates of British Columbians (70-80%), the pelvic movements of these occupants are restricted by the lap belt, resulting in a different impact response.

The most recent neck models utilize the same approach as Mintes [37] attempting to directly model the major structures of the neck (muscles, vertebrae, ligaments, etc) from the head to the shoulder joint. The first model, by Reber [44], utilized a two dimensional lumped mass approach. The nonlinear behaviour of the soft tissues were simulated with springs and dampers. This simulation provided results very similar to volunteer testing done by the Navy [30]. The other model, from Merrill [45], employed finite difference techniques to model the head and neck, using essentially the same model construction. Merrill also extended the simulation to three dimensions, modelling the lateral stiffness. Again, the model appeared to adequately simulate the extension motion when referenced to the limited volunteer response data available. An illustration of this approach is given in Figure 2.10.

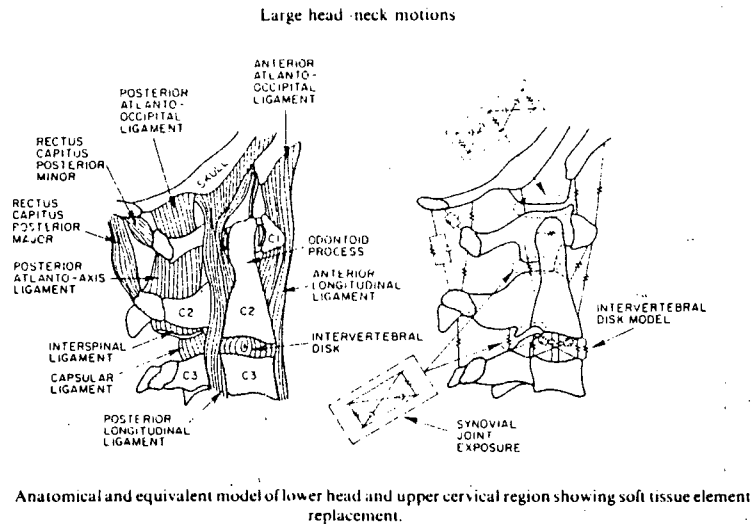


Figure 2.10: Discrete Anatomical Modelling used by Goldsmith *et al*
(from [47])

Limitations with this approach arises from the focus on the head and neck only, with the loading applied to the base of the neck. The drawback of this loading scheme is the requirement

of a known shoulder load before simulation. This value is part of the whiplash response, since the shoulder is being loaded by the seatback. Using shoulder displacements post hoc precludes the possibility of modelling the seatback's influence on whiplash injuries.

Again, a lack of actual volunteer response data limits the application of all these models (mechanical and numerical) to the analysis of trends. The models which have the best features for rear impact simulation are still deficient in a few areas. It is significant that none of the papers reviewed addressed the influence of a head restraint. Although most of these models were developed in the early 1970's, the government standards required head restraints in all vehicles after 1968. The reason for this omission was not explained by any author. In addition, the influence of neuro-muscular effects on the occupant response described by both Foust [31] and Seeman [28] are yet to be properly incorporated into a model. Neck simulation may be the preferred mode of current biomechanical study, since human volunteers are limited to non injurious tests, but full verification of any model has yet to be achieved.

2.3 - VEHICLE SIMULATIONS

The risk of occupant injury is dependent on the vehicle's performance during a collision. Other than full scale crash testing, numerical modelling of the vehicle's structures is a popular technique to predict vehicle deformation and absorption of impact energy. Vehicle simulation has not been significantly attempted through scaled physical models. The earlier numerical simulations employed lumped masses to represent the vehicle's large structural components with nonlinear springs linking the masses which were deforming. As the Finite Element Method (FEM) became more widely accepted, later researchers used its capabilities to discretize the structure and provide a more geometric representation of the models. The strengths and limitation of these two methods are discussed in the following sections.

2.3.1 - LUMPED MASS MODELS

The various lumped mass systems reviewed (Lin [46], Greene [47], Tomassoni [48], Kurimoto et al [49], Okamoto [50] and Arima [51]) all rely on lumped masses connected by nonlinear springs to represent the vehicle. These springs are not the classic elastic spring, but are based on the plastic deformation of the vehicle structures. These spring characteristics are usually determined by quasi-static crushing of the automotive components in question and are then corrected for dynamic effects using empirically based approximations. For modelling a frontal impact, the common mass components selected are the motor, shock tower, firewall, passenger compartment, and passengers. The springs that link these masses represent the connecting structures that deform during deceleration (frame rails, fenders, etc). A "gap" condition is used if there is an initial separation between components which closes when contact with another spring or mass has occurred (the front bumper being pushed into the engine, for example). It should be noted that all the models below have never been used for a nondamaging (or elastic) analysis. Restitution effects are small when significant plastic yielding takes place and are neglected in most of these models.

Of the models reviewed, only those of Lin, Arima, and Okamoto deal with the rear structure's response. The lumped mass model for a rear impact by Lin is displayed in Figure 2.11. Its capabilities include fixed or moving barrier impact, friction forces under the vehicle and barrier, strain hardening and elastic loading/unloading material behaviour. This last feature is important if rebound effects are considered.

Results of the simulation appear good for the single verification example given. The intent of this model was to monitor fuel system integrity, thus response of the structures surrounding the gas tank were important. Several parameters were analyzed, allowing several rear frame

design options to be studied and evaluated. Additionally, the effect of friction, impact mass, and the dynamic characteristics of the loading were evaluated independently. The parametric study employed in this research highlights the strengths of numerical simulation.

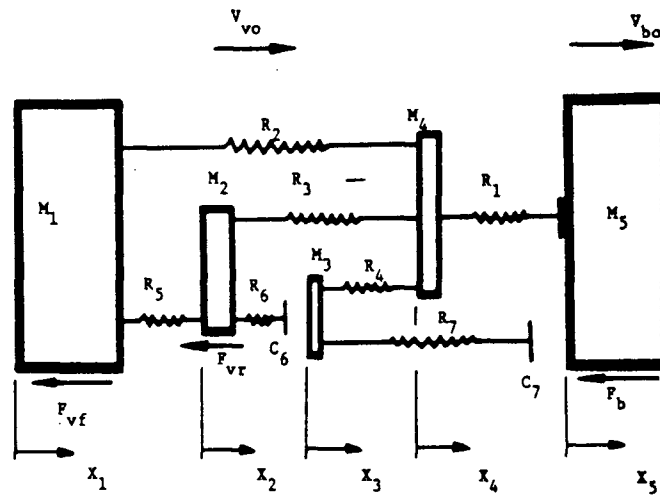


Figure 2.11: Lumped Mass Model for Rear Impacts
(from [46])

The study by Okamoto et al [53] also discretized the rear frame of the automobile to observe the energy absorption of different components. The model, shown in Figure 2.12, provided more two dimensional information regarding component interaction. Empirical methods were used to define the nonlinear springs needed to predict deformation characteristics. This model utilized a similar type of lumped mass representation as Lin; again looking at the fuel tank interaction within a crushing rear end.

Both of these models have potential application to the study of occupant safety since the passenger compartment loading can be determined from the model's simulated impact. To use these present models for low speed impact simulation, accurate formulation of the bumper response is required. Unfortunately, these models assume one dimensional vehicle

displacements only. Expanding the model to include two dimensional response would allow the researcher to also investigate the vehicle's suspension effects on occupant loading and vehicle response.

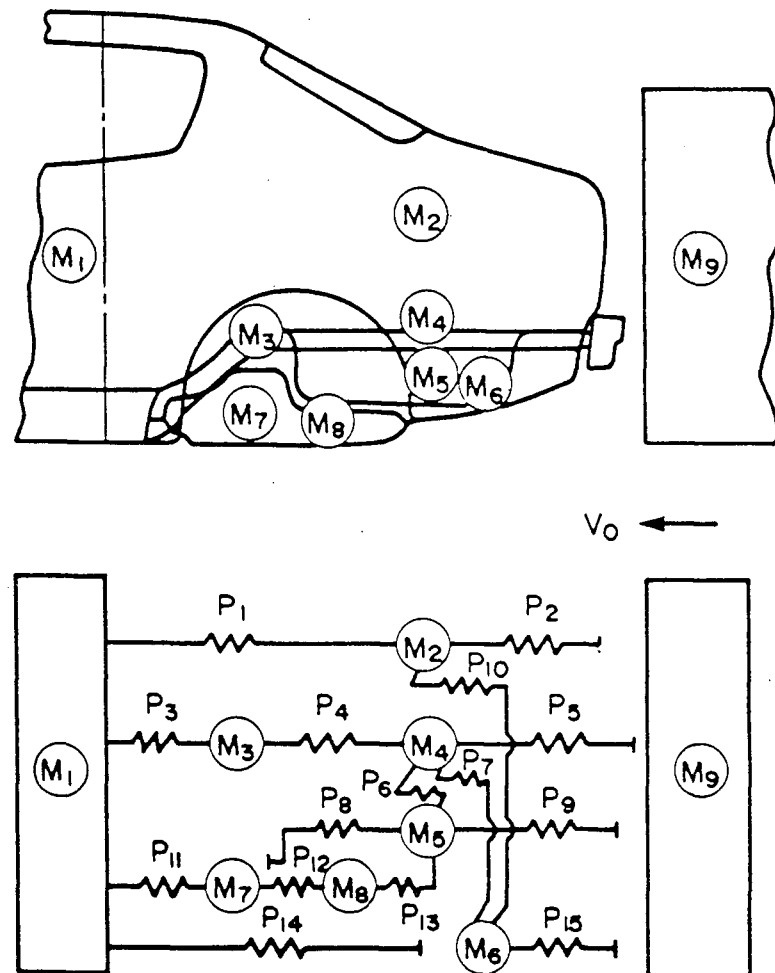


Figure 2.12; Rear Structure with Corresponding Lumped Mass Model
(from [50])

Unfortunately, dependence of a lumped mass model on empirical stiffness values may restrict simulation to specific vehicle models. Thus, modelling a new vehicle may require more compression tests to obtain the unknown spring properties. Since this requires the construction

of a partial prototype, the research can become expensive. However, this cost may be offset since the effects of several known component combinations can be studied quickly once the material behaviour is known. This eliminates the requirement to construct a prototype for every configuration studied.

To eliminate some of the testing required, approaches like that of Tani et al [52] combine theoretical and empirical stiffness formulations to predict the response of new structural members. Special interest has been placed on establishing predictive techniques to account for geometric effects including channels, angles, bending and weld locations on a structures response. In addition, buckling and wall collapse are under investigation to include their effects.

The correction from static to dynamic loading is also under further investigation. Tomassoni [51] noted the influence of different strain rate corrections showing that a static crush value could be suitably corrected with a linear relationship between stiffness and crush rate. However, his results also suggested that simulations using this type of strain rate correction are very sensitive to small errors in the transformation.

The benefit of lumped mass models is the speed in which they can be solved with computers, however, their simplicity also limits the information available from them. The use of single springs to model complex structures excludes the deformation mechanisms taking place. They have applications in whiplash research if specifics of the structural response are not necessary. The vehicle could be treated as a "black box" with predetermined stiffness characteristics allowing the resulting passenger compartment accelerations to be computed.

2.3.2 - FINITE ELEMENT METHODS

The first application of a finite element analysis to vehicle design was the simulation of static loading by Peterson [53]. He modelled a Pinto's body structure to observe the response of a vehicle to twisting and bending loads. Later work by Borowski et al [54] exploited the finite

element method (FEM) to determine vibration mode shapes of a car frame. However, the first application of FEM to occupant safety was not until 1974, when Kirioka [55] modelled seatbelt anchorages using FEM techniques and confirmed the results using full scale testing.

Unfortunately during this pioneering work, computing facilities which allowed time dependent or impact load simulations were not available or were not employed.

Most of the recent finite element modelling efforts have been directed towards producing element definitions for various structural components (Ishiyama [56], Yanoaka [57]). Most of this research has been directed at modelling the behaviour of both open and closed sections. The purpose of this work has been to establish numerical approximations for the response of typical automotive structures. As described in the section on lumped mass models, the prediction of vehicle deformation usually requires extensive testing to determine a given component's performance characteristics. The element definitions developed to date have been compared to empirical results; simulating the response of simple structures with reasonable accuracy. Unfortunately, this review did not uncover attempts to extend these element definitions in more complex configurations to simulate a partial or full car frame. The main applications of finite elements, described in the literature, have incorporated the beam and spar elements commonly used in structural engineering analysis to build lumped mass models as described below.

Arima et al [58] used a finite element approach to predict failure of a vehicle's rear frame rails during a rear end collision. In this study, deformation modes were analyzed to ascertain the risk of fuel tank rupture. The advantage of using FEM over lumped mass approaches is apparent in a comparison of this study to that of Lin or Okamoto. Finite element formulations provided geometric, two dimensional deformation predictions instead of the one dimensional crush measurement produced in lumped mass models. Arima utilized the study to optimize the rear

frame design by strengthening the areas most susceptible to yielding. The paper lists results of the simulation including floor accelerations in the occupant compartment, however, the authors did not scale the plots to indicate the magnitude of the loading.

A combined finite element - lumped mass approach was also used in the design of the Delorean sports car (Winter et al [59]). In this study, plate and beam elements were used to model conceptual designs while nonlinear springs representing the known response of standard components were incorporated in the design. The combined model was then used to evaluate the crush performance of the design. Only the front half of the car, up to and including the passenger compartment, was used to model the vehicle for the 50 km/h barrier test required for compliance. The initial design produced undesirable crash results when simulated so a prototype was not constructed for full scale testing, leaving the simulation without verification.

As shown, the use of finite elements has been limited in the past. A moderate size problem requires substantial computer time and memory. Historically, the power of the computer available controlled the size of the analysis. With the memory and speed of computers improving, more emphasis is being placed on the finite element approach. Its usefulness is evident in the more detailed results which can be obtained. The trade-off for this detail is computing expenses, but the savings in prototyping and static crush tests may offset this. The flexibility of the finite element approach in performing parametric studies is another attractive feature. The sensitivity of a model's response to various parameters (frame rail width and height, length of span, wall thickness etc.) can be obtained with less pre-simulation preparation than lumped mass techniques. It is interesting to note that FEM is also being heavily exploited in the design and simulation of airbags (Prasad and Chou [60]). Elaborate finite element models for simulating vehicles and occupants during a collision are just now being reported.

2.3.3 - HYBRID SYSTEM

In order to incorporate the best features of these two simulation techniques, Nakamura and Yashuom [61] proposed a hybrid FEM-Lumped Mass technique to simulate the crash response of vehicles. This technique begins with an analysis of the material and geometry of the components with FEM to produce the nonlinear spring and mass approximations used in the simulation. The FEM analysis accounts for vibration, buckling, wall collapse, bending, and axial loads. A lumped mass simulation for the transient component significantly reduces the computing time of the analysis. While this approach produces results faster, the benefits of using FEM (i.e. monitoring of individual components) is lost during the crash event.

The previously discussed models of vehicle crash dynamics all share the requirement of permanent structural deformations to predict response. Attempts to simulate low speed impacts, where elastic behaviour dominates the response, have not been documented. Since government standards do not address low speed-low damage vehicle behaviour, modelling attempts have not been directed at this area. Almost all the vehicle testing that has been performed involves vehicle damage (described later). Thus, without a government requirement, or experimental results for comparison, there has been no reason to apply these models to low speed impact analysis.

2.4 - SAFETY EQUIPMENT

An increased requirement for occupant safety has led researchers to investigate new or improved safety systems. The head restraint was the first device that was effective in reducing the severity of whiplash injuries in rear end impacts. However, they have only been responsible for a 20% reduction in whiplash claims [21]. Continued reports of injuries, even with the high-backed (integral headrest) seats suggests that an analysis of the seatback itself is required. Another protective mechanism is the crush response of the vehicle during high speed collisions.

Properly designed, this can reduce the vehicle accelerations to tolerable levels within the passenger compartment. However, the previous sections showed how little is known about energy dissipation in low speed applications. For low speed, non damaging collisions, the bumper and its isolator assembly are the only other source of protection for passengers.

2.4.1 - SEATBACKS AND HEAD RESTRAINTS

The first experimental documentation of seatback performance came from Severy et al [62] in 1968. Vehicle to vehicle (rear end) tests were conducted using new Ford four door sedans. Anthropometric test dummies were placed in the four window seats in order to observe the influence of seating position and seat back characteristics on occupant response. The Sierra test dummies employed were fitted with a special "whiplash" neck which is similar to the Hybrid III neck shown in Section 2.2.5.1. In this study, the standard front seats were replaced with bucket seats so that various combinations of seatback height and stiffness could be studied. In addition, different offsets between the occupant's head and the head restraint were explored. Impact speeds studied were set at five levels: 16,30,50,65,and 90 km/h.

Several important results were obtained from these tests. In general, higher seatbacks were the most effective in reducing rearward head deflections. A 71 cm seatback was deemed the most effective based on occupant response and the driver's rear visibility. The authors qualified this with the recommendation that the head restraint be integral with the seatback and of equal strength. The more rigid seatbacks tested were found to reduce the forward rebound into the instrument panel. Plastic yield of the front seats also provided effective occupant protection by reducing acceleration loading, as long as its deflection did not expose rear seat occupants to dangerous conditions (i.e. contact with the front seat structure or contact with other occupants). They observed that elastic rebound of the occupant was mostly due to the seatback structure; the

contribution of the padding material and seat springs were negligible in terms of energy storage when compared to the seat frame. The stiff seats tested produced little permanent yielding for impacts under 50 km/h.

The initial occupant posture was shown to have a significant influence on the impact loading experienced. Whiplash potential was found to increase with higher head offset distances as a result of increased occupant movement prior to impact with the seat. For example, a 30 cm head offset of the rear seat passenger doubled the chest accelerations when compared to the 0 cm offset case. Another finding was low seatbelt loads, none exceeding 450 N, for impacts below 50 km/h. These low belt loads were attributed to vehicle deformation and vertical movements of the dummies. Both processes allowed the belts to move forward, away from the dummies. Severy recommended attaching the seatbelt anchorages to the seat instead of the vehicle frame. This would reduce belt movement relative to the occupant, since there is less passenger movement relative to the seat. Severy reported other seatback research [63],[64]. Again, this work involved rigid seatbacks and high impact speeds essentially duplicating the results outlined above.

The main criticism of Severy's work is that very few tests were done with standard seat backs. As a result, his test results do not truly reflect production seat response. As mentioned by Strother and James [65], in their review of seat characteristics, the rigid seatback is not practical. Size and weight restrictions cannot accommodate the requirements for a rigid seat. Proposed rigid seat designs, the Cox Safety Seat (1963), Liberty Mutual Capsule Seat (1967), and the HSRI Integrated Safety Seat (1971) are all heavy, bulky and provide little for passenger comfort. Thus, a compliant and lightweight seat has been retained by manufacturers. In one paper [64], Severy promoted the concept of tying the top of the seatback to the roof with seatbelt type webbing. An additional roof anchorage would remove the cantilevered seatback arrangement presently employed, providing a stronger structure.

Another problem with Severy's results is the lack of biofidelity of the Sierra test dummy. Without reference to human neck performance, the reader has no indication of the relative performance between human and dummy. Another weakness with Severy's procedures is the pre-impact occupant posture. For the offset distances studied, only the largest, 30 cm, had the shoulders out of contact with the seatback. This may not be a true reflection of occupant postures, since many people may be seen slightly forward of the seat.

Similar seatback testing was carried out by Berton [66] who conducted sled testing of ATD's belted in rigid seats. He supplemented this information with full scale vehicle impacts containing the dummies in production seats. Like Severy, he used the Sierra 50th percentile male dummies for the testing - again no biomechanical relationship is given between these mannequins and humans. The seatback height was adjusted between 55 and 70 cm and some tests were conducted without a head restraint. The initial dummy head offsets from the seatback ranged from 2 to 10 cm. In this study, different seat cushions were used to change the seatback stiffness characteristics and the seat was sometimes braced to provide a more rigid structure. Impact speeds for both testing series were in the same range studied by Severy.

Bertons's results agreed with Severy's claim that increasing seatback height decreased neck extension and a more rigid seatback reduced forward rebound of the occupant. He also found a head offset tended to increase the neck extension as offset distance increased. Berton's cushions highlighted the differential rebound of the head and torso when thick materials would store elastic energy. The subsequent release of spring forces would catapult the torso first, increasing the neck extension. For higher speed impacts, the plastic collapse of the seatback would mitigate the head and neck accelerations, although this may expose the occupant to other injury mechanisms as discussed earlier. One interesting result for low speed impacts is the relationship between neck extension and impact speed, shown in Figure 2.13. Here the neck extension is shown to be higher at low speed (where little plastic collapse of the car and seat

structure is occurring) than at high speeds. Even with the head restraint, a 16 km/h (10 mph) impact is shown to be as severe as a 65 km/h (40 mph) impact, with respect to maximum neck extension. This result was not explored further by Berton and has never been investigated by other researchers.

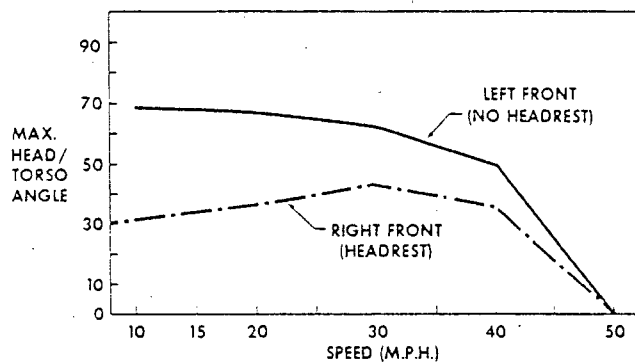


Figure 2.13: Influence of Impact Speed on Maximum Neck Extension
(from [66])

One final test technique employed to observe seat characteristics was reported by Hu et al [67] in 1978. A vehicle mock-up representing the passenger compartment was placed on the end of a pendulum, dummy and cadaver occupants were placed in the seats, and the entire assembly was swung into a barrier. The study observed the influence of seatback stiffness on the loading of the neck in rear impacts during low speed impacts. Unfortunately, the heads were not restrained by a headrest limiting the number of vehicles that results can be applied to. Contrary to Severy's and Berton's conclusions, Hu found that deflecting seatbacks would reduce neck loadings. However, testing was only carried out on four cadavers and two dummies, providing a small sample size.

2.4.1.1 - DEPLOYABLE HEAD RESTRAINTS

The largest complaint against head restraints is their obstruction of rear visibility. This and a lack of public awareness on the correct location for a head restraint manifests itself in improper head restraint adjustment. Studies by McKay [68] and States et al [20] show that 70-90% of adjustable head restraints were found in the lowest position in vehicles surveyed. To overcome this obstacle, head restraints that only act during a collision were proposed by Melvin et al [69],[70] who experimented with the deployable head restraint. Two different systems to deploy the head restraint from the top of the seatback were studied: a rigid restraint that is mechanically positioned, and a bag that is inflated. The HSRI Safety Seat (preceding section) was used as the seat structure into which the head restraints were incorporated. Computer simulation with an occupant simulator was used to determine the decision (go/no-go) and deployment time that provided the best protection. Results of this computer analysis indicated that a 40 ms window was available for deployment. Prototypes were then tested on the sled for 15, 50, and 65 km/h impacts using the Sierra test dummies (95th percentile male or 5th percentile female) as the occupant.

The results indicated that these head restraints performed better than standard production systems. A deployable head restraint adjusts its position or increases its size to reduce the initial head offset distance, but does not compromise rear visibility under normal driving conditions. As noted by the work of Severy and Berton, smaller head offsets reduce head extension and acceleration values experienced by the occupant. The rigid nature of the test seat may have also enhanced performance, but an increase in performance should be expected for production seats outfitted with this system.

2.4.2 - BUMPERS

An important piece of safety equipment is the bumper system. Its main function in low speed impacts is to absorb some impact energy and to reduce collision severity by damping the input accelerations. Commonly used systems are air/hydraulic isolators, foam core bumpers, or deforming bumper mounts. An alternative was introduced by Shibabuma et al [71] who proposed wood cutting as a energy dissipation mechanism. Wooden dowels were mounted such that bumper compression would force them through cutting surfaces. The wood was pre-shaped to produce any time dependent dissipation curve desired. A vehicle mock-up was fabricated to test these bumpers for 50 km/h impact speeds. Additional occupant protection was achieved in these tests by modifying the seat mounting. The seat was connected to the frame by a similar energy absorbing-wood cutting system. This design places two energy dissipaters between the occupant and the impact source, an approach not previously attempted by other researchers. Although not discussed in this research, this technology can be applied to low speed impact (below 20 km/h) protection systems.

Although bumper design is one of the first areas that can be explored as an impact protection mechanism, is not widely addressed in the literature. Shieh's [72] paper was the only other paper found describing bumper behaviour, but he described the bending deflections arising from a central pole impact on the bumper, not a typically reported whiplash related accident.

In summary, safety systems for rear end impacts include occupant restraint (seat, head restraint, and belt restraint) and energy management within the vehicle structure (bumper and frame). Published research using production seats and head restraints in conjunction with a biomechanically referenced test dummy is not readily available. The influence of the system variables on occupant response trends can be determined from the presented articles, but extending the analysis to predicting injuries is not possible with the existing information. Unfortunately, the government has not legislated effective compliance regulations given

Severy's [62] recommendation of a stiff seat with a 70 cm height (minimum). Presently, the government requires less than 1/2 of the stiffness proposed by Severy. His statement that the focus on airbag research in the 70's has left the fundamentals of seat design ignored, appears valid. In addition, the design of safe, low speed bumpers is a relatively unexplored area with only two papers addressing bumper performance.

2.5 - FULL SCALE TESTING

The last experimental technique to determine occupant response during a collision is the full scale vehicle to vehicle impact. As mentioned earlier, this technique was used by Severy et al [9],[62],[63] and Berton [66] in their seat evaluations. For completeness, this section will be used to describe some of the full scale test procedures and results.

The first rear impact testing involved a 1949 Oldsmobile striking the rear of a 1947 Oldsmobile. Six tests are reported for speeds ranging from 10 to 30 km/h where the rear vehicle was guided by a human driver in all tests with the struck vehicle being occupied alternately by a dummy and a human. The maximum impact speed with a person in the struck car was 14 km/h. For these tests, the doors were removed to allow high speed cameras to record the occupant motion during the tests, while accelerometers were placed on the dummy and vehicle to compliment photographic data.

These tests provided a basis for subsequent research into rear impacts. One of the first important results presented by Severy is the influence of vehicle crush on the acceleration of the vehicle frame as presented in Figure 2.14. The presence of vehicle crush tends to decrease the rate of acceleration onset (Run 5 compared to Runs 3 and 4) and delay the acceleration pulse.

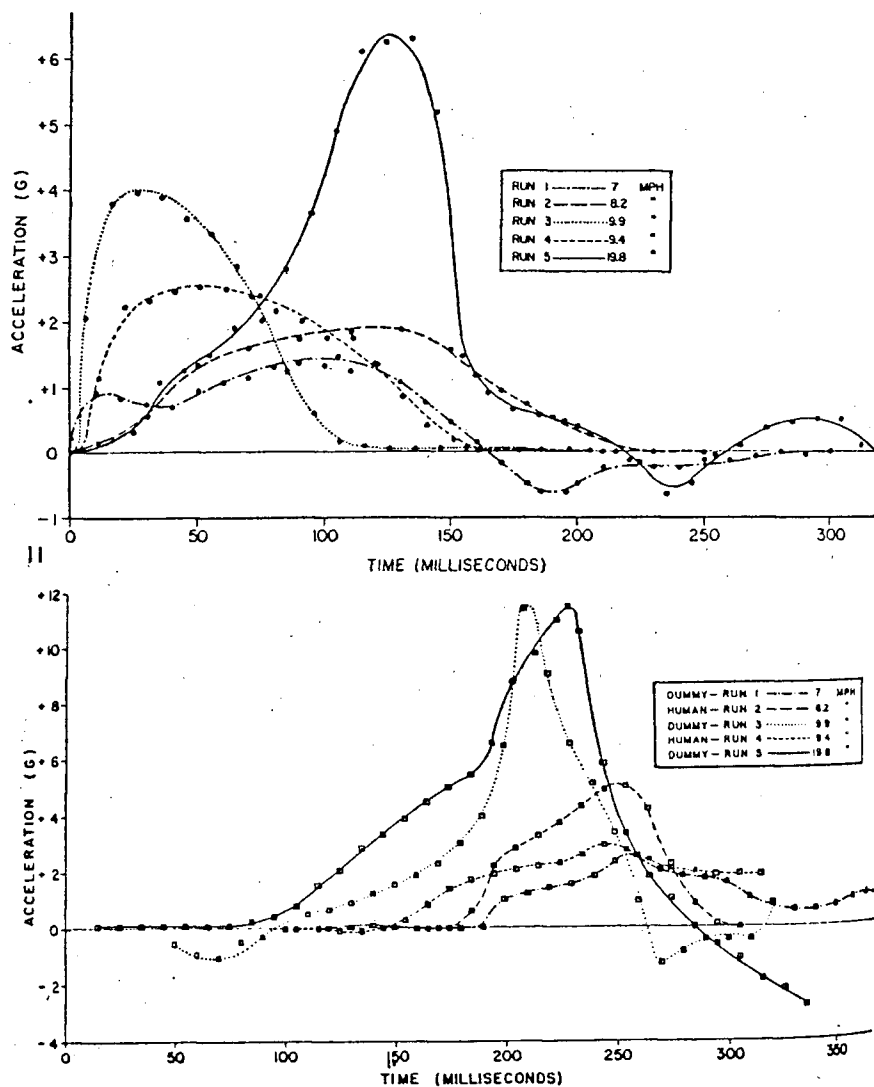
Severy stated that the accelerations of the head were reduced with increasing seatback deflection for higher impact speeds. This arises from the greater deflections over which the loading occurs. What Severy did not consider was the influence of this deflection on the necks

extension during rebound. As mentioned earlier, McKenzie and Williams [42] found that injury potential was increased with increased elastic deflection. The tests did show that occupant's shoulders rebound before the head has completed its deceleration and it is the relative motion between the head and torso which produces the neck loading during impact.

The film records of the volunteer tests indicated that the occupant had a higher level of muscular activity in the second impact than in the first. Severy claims this is a newly developed reflex mechanism resulting from exposure to impact in the first test. Care should be taken when describing "reflexes". The occupant may have tensed before the impact, using audio or visual clues to anticipate the second impact, or a neuro-muscular reflex may arise from exposure to dynamic loading. The experience of the previous test may have stimulated the nervous system of the volunteer to the point where he could not fully relax. Each of these possible sources of muscle activity are unique and may have different influences on an occupant's injury potential.

The geometry of the rear bumper of the struck vehicle also had some bearing on the occupant loading. The struck vehicle in Severy's tests tended to sink lower on impact due to a downward force being exerted on its bumper. The resulting downward deflection of the frame pulled the seat away from the occupant. This combined with ramping of the occupant (up the seatback) to produce an 8 cm separation between the passenger and seat cushion in one of the tests.

Rear impact tests were not reported again by Severy until 1968 [65] (described in Section 2.3). In 1971, [73] he published test results for higher speed rear impacts. In these subsequent tests, Severy did not place occupants inside the striking vehicle, but four occupants were seated in the struck vehicle. A monorail system was built on the test track to guide the striking vehicle at impact speeds ranging from 15 to 90 km/h. Information from these tests verified his earlier results on seat backs, described in Section 2.4.1.



Front car acceleration patterns.

Head acceleration patterns for subjects in front car.

Figure 2.14: Effect of Impact Speed on Vehicle and Occupant Acceleration
 (from [9])

Emori and Horiguchi are the only current authors of low speed impacts. The neck they developed for low speed testing (Section 2.1.5.1) was subsequently used in vehicle collisions below 5 km/h. They used a 1980 Toyota Celica (1180 kg) to strike a 1978 Nissan Van (926 kg). Production bumpers on the vehicles were replaced with rigid units faced with a cushioning material to approximate original bumper performance so that a "new" bumper was available for each test. To record the event, accelerometers were placed in the dummy and both vehicles.

The results showed that without a head restraint, the dummy experienced 60° neck extensions for impacts as low as 2.5 km/h. This value was reduced to 20° when a head restraint was in place. An additional parameter studied was the braking force of the struck vehicle, moderated by the emergency brake of the struck car. They found that braking force had little influence on neck response in extension, however neck flexion increased when vehicle braking was present. The braking also had little influence on the maximum acceleration levels. The struck vehicle was slower to respond when the brakes were applied, but peak post-impact velocity was encountered (in the braking or non-braking scenarios) at the same time after contact (Figure 2.15). For equivalent impact speeds, peak acceleration values are thus similar, regardless of the braking forces of the struck vehicle. However, the duration of peak acceleration is shorter when the brakes were applied.

Weak points in this paper were mostly related to his dummy's response. As described in Section 2.1.2, verification of the model's biofidelity is lacking, as well as their approach to modelling a "relaxed" neck (i.e. they assumed no restorative forces were developed in the neck during impact). However, their findings on vehicle response, particularly that of braking effects, are noteworthy. The influence of braking on the dummy's flexion response may be significant. If persistent problems are associated with injuries to the posterior neck tissues, the flexion experienced by the occupant may be an important component of the injury mechanism.

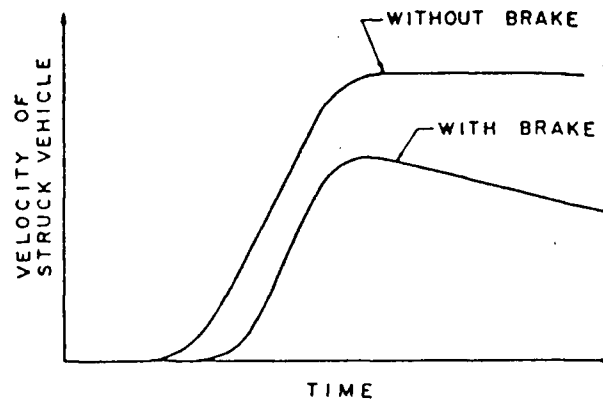


Figure 2.15: Test Results of Emori and Horiguchi
(from [11])

Reported work on other low speed impacts, of any orientation, are limited in the current literature. Aside from Severy and Emori, the only paper discovered in the literature for impact speeds below 20 km/h was presented by Naab [74] who observed the performance of vehicles striking barriers and poles at low speed. The speeds were not in excess of 12 km/h but were limited to frontal impacts with unrestrained occupants. The Insurance Institute of Highway Safety continually releases bumper testing data from 5 to 15 km/h, but the repair cost is the only information recorded and no occupants are placed in the vehicle.

The most alarming trait of information available for vehicle and occupant impact response is the lack of data for impact speeds below 20 km/h. Previous research has focused on speeds from 20-90 km/h with particular emphasis on the 50 km/h impact. This limits the understanding of low speed impacts, and particularly restricts the validity of simulations used for occupant response and injury mechanisms. Without the reference to the accident severity, understanding the injuries that may arise in a collision is impossible.

2.6 - SUMMARY

This review of the literature highlights not only a deficiency in low speed-rear impact information, but also a weakness in the whiplash literature. No one researcher has presented a comprehensive testing protocol that satisfactorily addresses the aspects of seatbacks, head restraints, occupant posture, vehicle characteristics, and the biofidelity of occupant response. Biofidelity is the only parameter that may defy further research, given the limited use of humans to provide this information. However, these other variables must be considered when attempting whiplash research.

The description of whiplash injuries differs between various authors and must also be addressed. There are several tissues that are referred to in neck injuries. Macnabb and also Severy speak of muscle traumas; McKenzie and Goldsmith isolate the ligaments while Clemens evaluated the intervertebral disc injuries. The criteria describing the onset of injury generally fall between two main parameters: 1) Mertz and Patricks' torque about the occipital condyles, or 2) hyperextension of the neck beyond the range of normal motion. All these descriptions of injury and criteria for its onset have been put forward individually. However, a well documented article evaluating these theories has yet to be presented. This is beyond the scope of the current project to be discussed, but should be considered when whiplash documentation is being assessed.

In review, very limited information on human response is available for true whiplash research. Cadaver and animal studies provide important, but limited, injury tolerance data. Occupant analogues have not been satisfactorily verified against actual human response because of the limited information available. Additionally, vehicle testing or simulation for low speed impacts is essentially non-existent. It is important to recognize that no modelling reference reviewed incorporated occupant and vehicle responses within the same modelling scheme. Historically, the occupant and vehicle have been modelled independently. Thus, occupant

studies employing sled testing or numerical approaches have not accounted for the vehicle performance during the simulated accident - correlation of injury and vehicle damage/accident severity is not possible within these tests. Full scale testing has been explored to a limited degree, but information derived from these studies is usually suspect due to modified hardware or impact speeds in the medium to high speed ranges.

Looking ahead to the experimental component of this program, it is obvious there is a need to document the vehicle and occupant response for low speed impacts. This is necessary to understand what loading environment is presented to the occupant during a rear-end impact, especially one that produces minimal or no damage to their vehicle. Once this is explored, numerical modelling can be attempted to highlight the influence of different vehicle components during the accident.

Chapter 3 EXPERIMENTAL TESTING

3.1 - LOW SPEED IMPACT TEST FACILITY

The main goal of this project is to experimentally determine low speed collision dynamics (speeds below 20 km/h) of an occupant and vehicle struck from behind. In order to provide this information, the pendulum style impact facility shown in Figure 3.1 was designed and constructed. Design specifications for this facility were based on providing impact energies up to the level controllable using the existing U.B.C. barrier facility. Speed control limitations of the crash barrier suggested that the facility should be capable of impact speeds up to 20 km/h. Within this speed range, the pendulum should simulate any particular striking passenger vehicle. This required the swung mass to be selectively variable from 500 to 2000 kg. A further design requirement was to ensure the pendulum impact facility could be recognized as a valid information source based on the Canadian Motor Vehicle Safety Standards (CMVSS 215) [20] and Society of Automotive Engineers (SAE J980a) [75] guidelines. Both call for a 3.3 m swing radius and a swung mass equivalent to that of the test vehicle. Pendulum impactor shapes prescribed in the guidelines were, however, modified to provide a surface profile more representative of a vehicle front end.

It must be pointed out that two bumper systems are interacting in a rear end accident. The front bumper of the striking vehicle will absorb energy and introduce geometry effects during the energy transfer. Because of the many combinations of bumper systems available, the variability of the striking vehicle has been eliminated from the experiment. This allows the bumper of the test vehicle to be studied under controlled conditions.

In the facility design, the pendulum mass and impactor plate are pivoted about a shaft mounted to a tubular steel, cable-stayed frame. The frame and cables are fastened to an auto-frame straightening fixture consisting of a series of symmetric steel channels set into a high

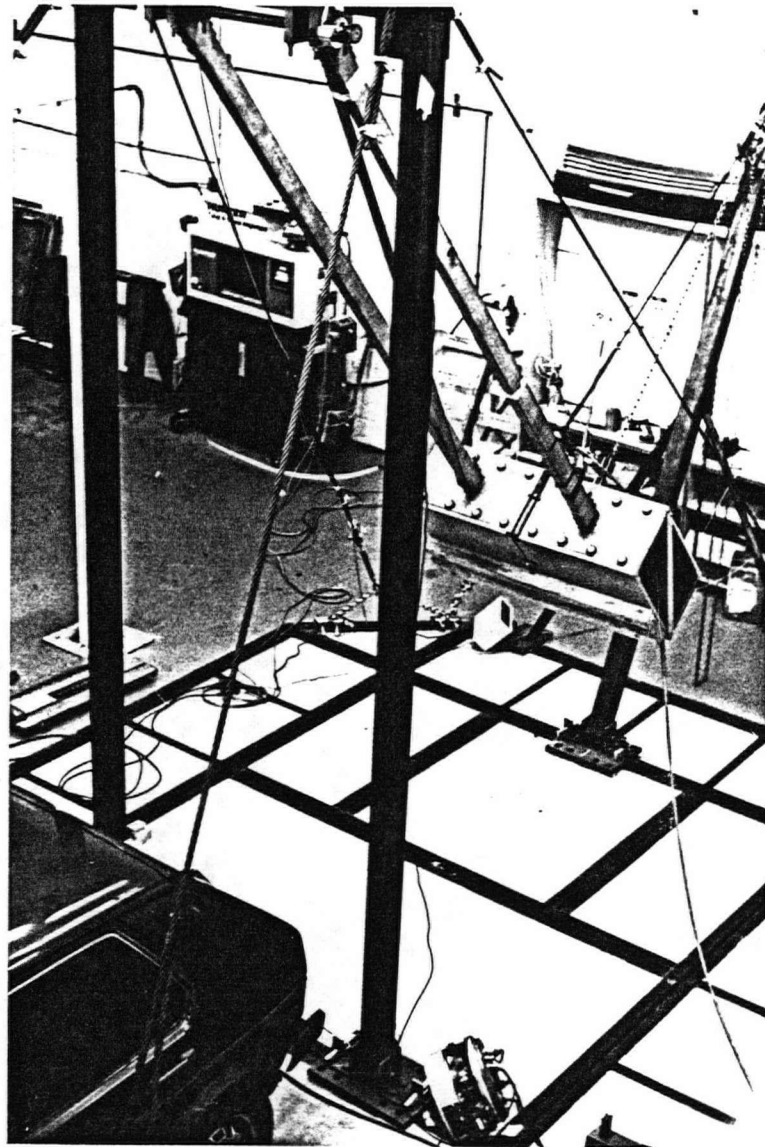


Figure 3.1: Pendulum Impact Facility

strength concrete floor at the I.C.B.C. Research and Training Center in Burnaby, B.C. As this fixture could not be permanently devoted to the pendulum facility, portability and relatively quick assembly/disassembly was provided in the design. A 50:1 ratio chain hoist is employed to

manually raise the pendulum into position prior to testing. Total cost for the test facility materials was approximately \$1300 for materials and fabrication required approximately six man-weeks of shop time.

The experimental program consisted of two separate testing segments. Series I tests were commissioning tests to monitor facility performance and provide preliminary, exploratory data. This learning experience was used to refine the facility and develop the Series II tests one year later. The instrumentation and test procedures for each test series are described separately in the following sections.

3.1.1 - INSTRUMENTATION

Data acquisition for the low speed impact tests required a system capable of recording the kinematics of the collision sequence. Specific motions of interest were those of the occupant, vehicle (translation and crush) and the pendulum. To observe different aspects of the system, Series I tests required a flexible recording system. The only method having these features was an optical recording system which was also found to be invaluable for detecting qualitative information beyond the recording capabilities of a sensor based system. A high speed video system was chosen to provide instant playback of the test results so that important trends could be immediately recognized and focused upon during subsequent tests. The video recording of the occupant and vehicle, both benchmarked with targets as in Figure 3.2, can be post-processed to provide a permanent record for further modelling and analysis work.

The specific video system utilized in the testing (Kodak Ekta-Pro 1000) was chosen as it was the only system capable of a 1000 frame/sec recording speed. Since the most important segment of the impact occurred within the first 200 milliseconds, a sampling rate of less than 1000 frames/sec would not provide sufficient data for subsequent analysis. The Kodak system provided an elapsed time counter such that velocities and accelerations could be readily and

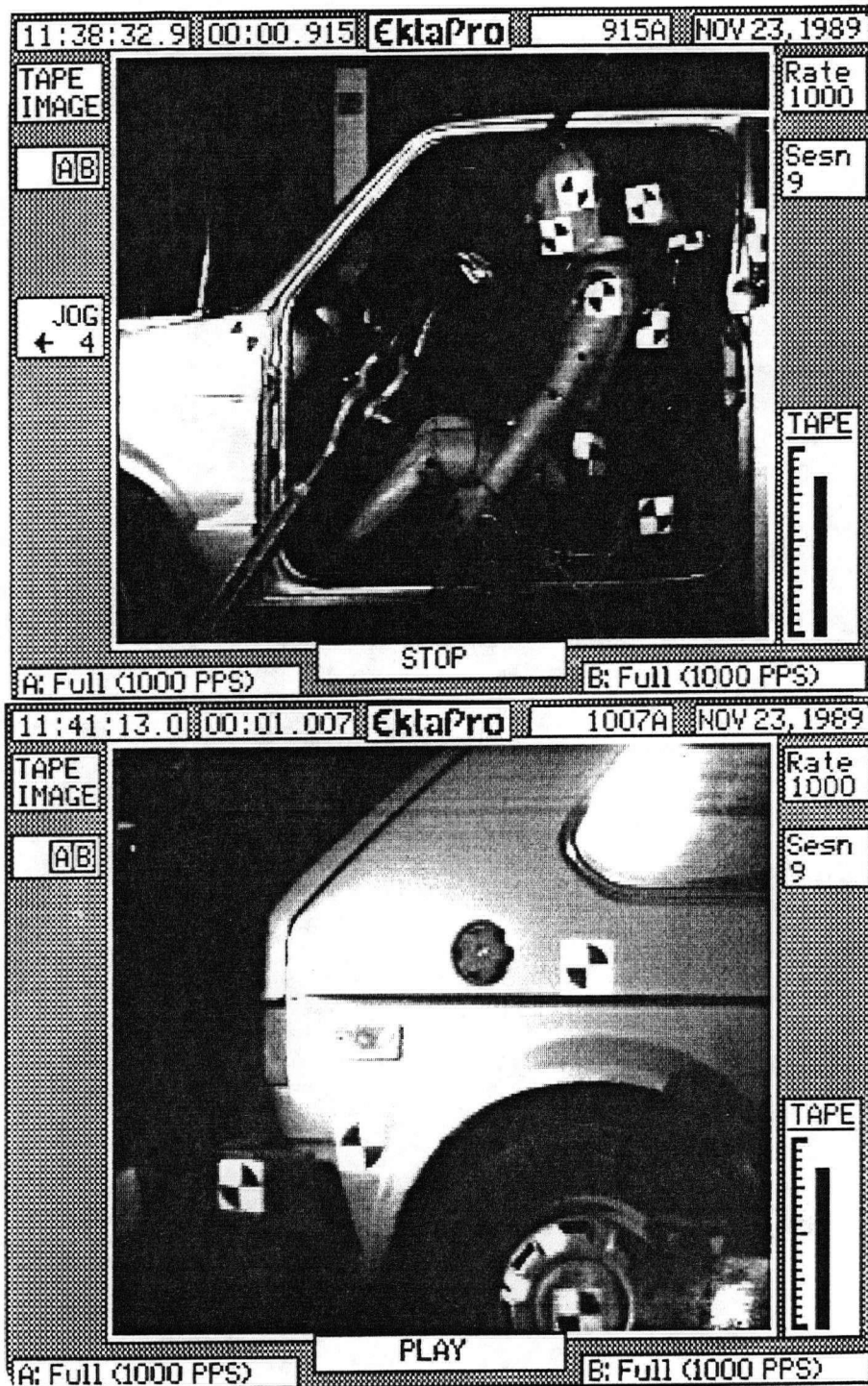
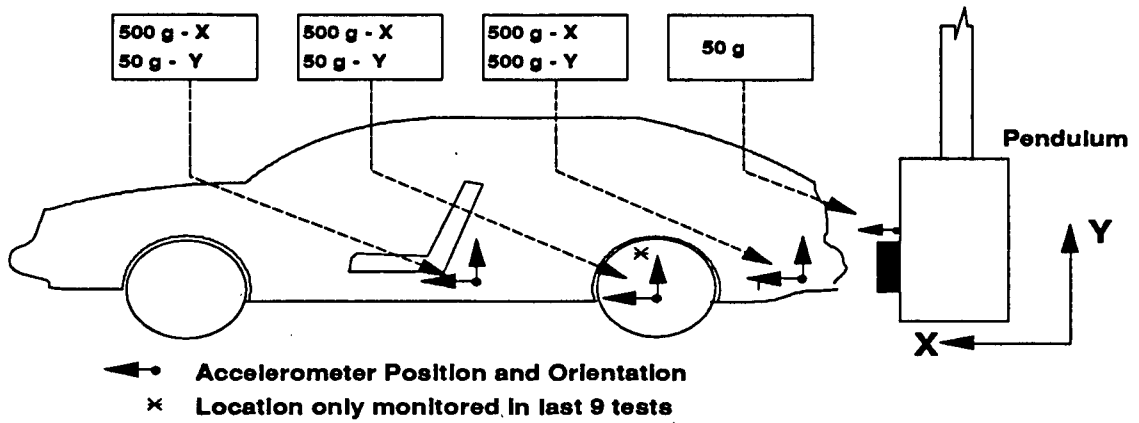


Figure 3.2: Typical Video Images

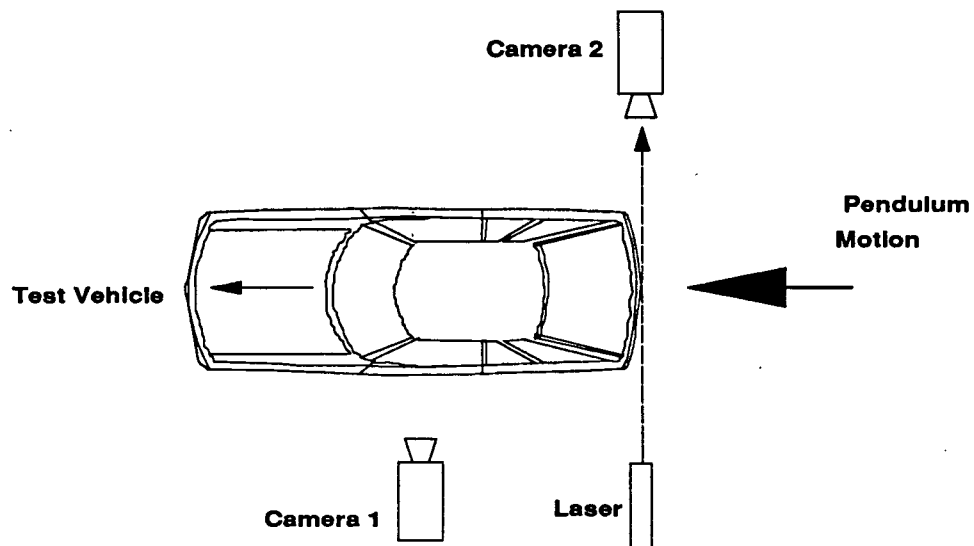
accurately determined from the displacement data recorded. The system's operation required a pre-event trigger of approximately 2 seconds and sequencing of the test was performed manually. To record the time of initial pendulum/bumper impact, a laser was aimed along the bumper and reflected back to the video imager such that contact of the pendulum with the vehicle interrupted the beam.

Series II testing again utilized the high speed video system, but with an additional imager to allow simultaneous recording of the bumper and occupant movements. Accelerometers were also used to supplement the video information. The accelerometers employed were piezotron 50 and 500 g range models (supplied by Kistler). These accelerometers require a voltage coupler to energize the piezoelectric amplifiers and separate the output signal from the DC voltage. The information was recorded by a data acquisition board installed in a microcomputer host and provided sampling rates up to 100 kHz. Figures 3.3 and 3.4 provides information on the transducer locations.

Pendulum velocity was measured slightly prior to impact using a speed trap. The initial speed trap system consisted of three equidistant mechanical switches mounted such that the last switch would be closed about 3 cm from the pendulum resting position. A storage oscilloscope was used to record the time between the switch closures caused by the passing pendulum. An improved pendulum speed recorder was used in the Series II tests. An optical shaft encoder (Figure 3.5) was mounted on the pivot, replacing the first system. This mechanism allowed the velocity profile for the pendulum to be recorded.



a) Accelerometers



b) High Speed Video

Figure 3.3: Instrumentation and Transducer Locations

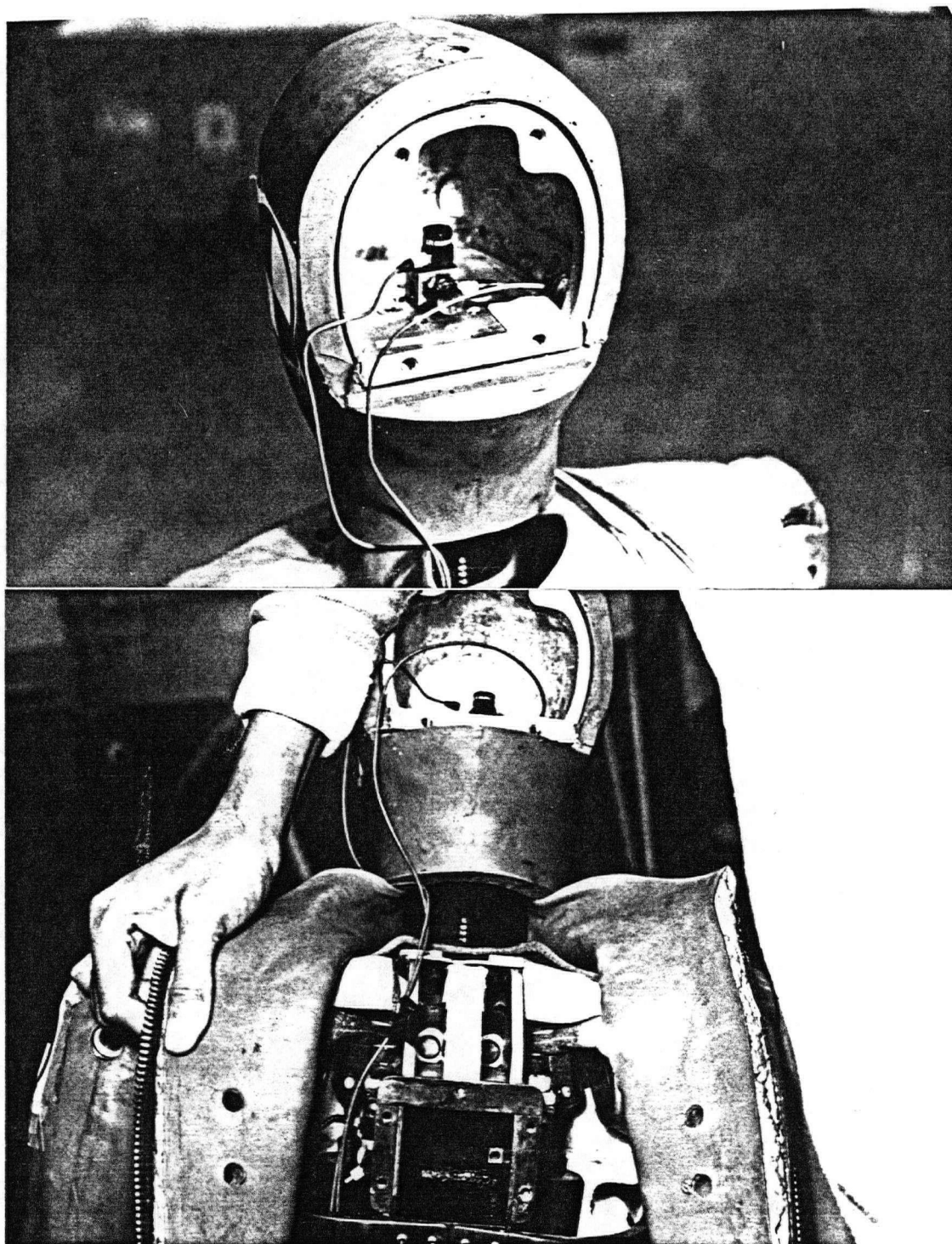


Figure 3.4: Occupant Instrumentation

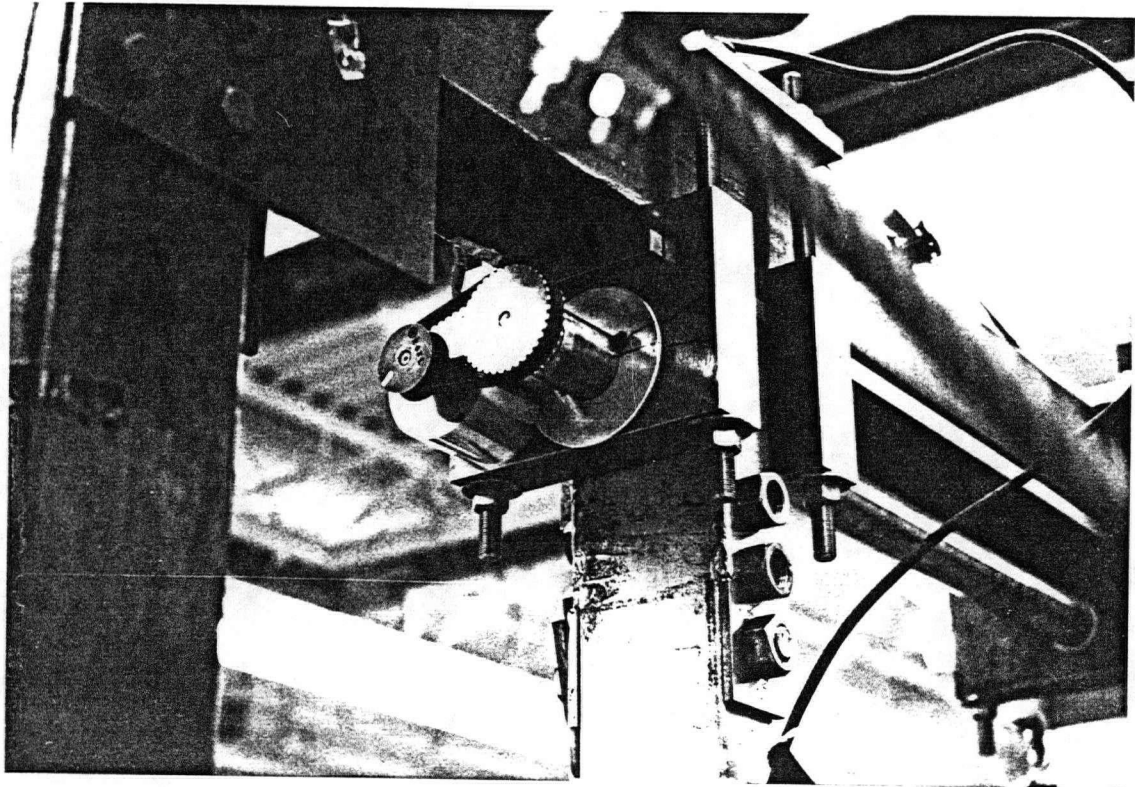


Figure 3.5: Optical Shaft Encoder for Speed Trap

3.1.2 - TEST MATERIALS

A Hybrid II anthropomorphic dummy was used to represent the occupant in the collision and was kindly made available by the Transport Canada Test Centre in Blainville, P.Q. This dummy has limited use in whiplash testing because of an overly stiff neck arrangement, as described in Section 2.2.5.1. The stiffness, compared to the performance suggested by Mertz and Patrick in Figure 2.7, provides a reference relative to volunteer data. These results indicate that this structure is typically 2.5 times the stiffness of a human neck.

The Hybrid II is only designed to meet CMVSS and FMVSS dummy criteria for a frontal impact, however, this dummy still can be used in rear impact testing. The repeatability of the dummy does provide an advantage over volunteer testing, especially when parametric studies are being performed. As mentioned in Chapter 2, there are many variables associated with human response which include: muscle activity, age, sex and physical condition. Removing these variables and only analyzing relative movements of the neck is a better gauge of performance for preliminary investigations.

The vehicles tested in this project were two and four-door Volkswagen Rabbit hatchbacks. These particular models were chosen because they were deemed to be representative of compact cars currently on the road, and have been extensively tested by the University of British Columbia Accident Research Team in previous research studies. All of the tested vehicles were insurance 'write-offs' supplied through I.C.B.C. The cars were free of damage in the rear portion of the vehicle and capable of free rolling. This was necessary to ensure that the test vehicles were representative of functional cars.

3.2 - PROCEDURES: SERIES I

Preparation of the test vehicle was the first step in the impact testing procedure. The vehicle mass was determined and recorded so the pendulum mass could be adjusted to match the

vehicle. Test vehicle specifications (model, year, seatback type, occupant safety system, etc.) and information related to the initial damage present was logged. The vehicle was then positioned and aligned to obtain bumper contact perpendicular to the impactor plate at the lowest point of the pendulum arc. This was aided by the use of a laser which was positioned to mark the pendulum bottom-dead-center. A reference for vehicle positioning was then available after the pendulum was raised slightly out of the way.

Direct rear end impacts were investigated for two reasons. While it is recognized that few rear impacts are truly straight on, the sensitivity of the longitudinal impact forces for small changes in the impact angle (± 10 degrees) is less than 2.5%. Direct impacts also provide full utilization of the vehicle's safety system as designed by the manufacturer. This makes comparisons between different vehicle types more appropriate since each is given similar attention in the design. Research on whiplash has been historically treated in this manner.

Safety chains were fastened loosely between the vehicle frame and the floor to prevent excessive movement (more than 75 cm) after the test. The parking brake was engaged and the vehicle was placed in gear. The purpose of locking the wheels was to simulate the case of a car stopped in traffic and thus provide the lower limit of occupant loading. The crash dummy was positioned in the seat in accordance to posture requirements of the test. As various occupant postures were studied, Figure 3.6 shows the extremes that were employed in the tests. The dummy and car were fitted with optical targets and their locations were recorded (Figure 3.2). The bumper position relative to the frame was also measured, such that a value for residual crush could be obtained after the test. The laser, aligned along the rear bumper, was reflected back to the video imager to show the time of impact.

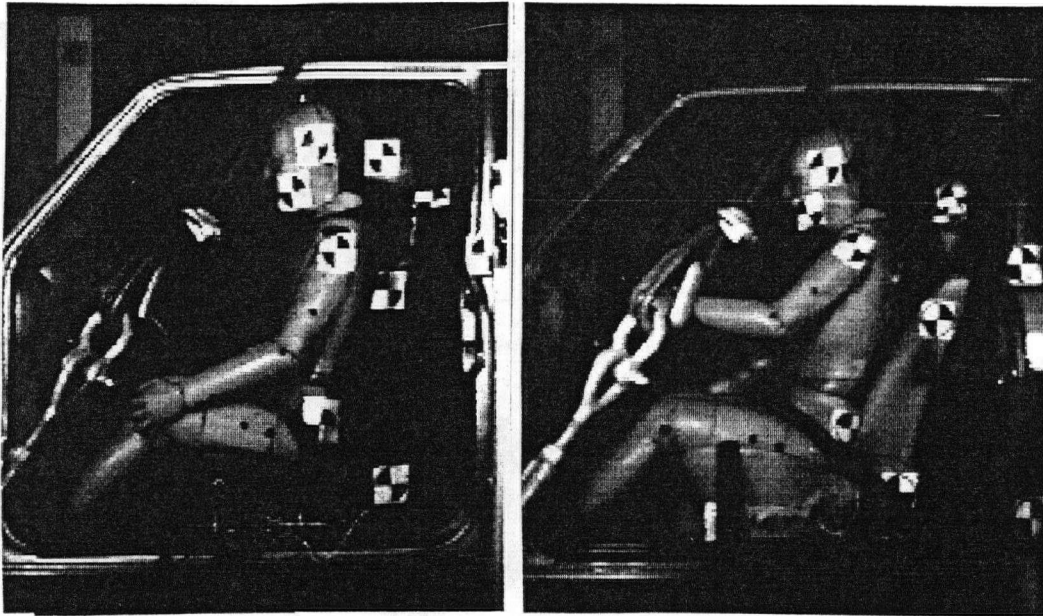


Figure 3.6: Occupant Positions Studied

Positioning and measuring the anthropomorphic dummy prior to a test is documented by Backaitis [2],[3]. His recommendations - place the dummy in the seat, allow it to achieve its equilibrium position as close to the desired position, and then measure the markers - were adopted in this project.

For safety reasons, the pendulum was raised into position just prior to impact. The change in vertical height was determined from the center of gravity of the swinging structure and its angle from vertical. The impact velocity was found to be reliably estimated from the basic equation of motion for a pendulum, ignoring frictional losses.

An anchor shackle, connecting the chain to the pendulum, was utilized as the release mechanism in the Series I tests. The test was initiated by driving the shackle bolt out of this assembly using an air impactor.

Triggering of the camera preceded the release of the pendulum by about 2 seconds to provide the necessary lead time for the video recording system. Problems were occasionally encountered with the original release mechanism at the high pendulum positions as a result of the increased bearing load on the release bolt.

After each test, a general inspection was carried out to locate and record measurements of any vehicle damage resulting from the impact. The assistance of the staff at I.C.B.C. was invaluable during this inspection due to their significant experience in vehicle accident damage assessment. Areas that were particularly susceptible to damage (eg. bumper, isolator mounts, rear panels, floor pan, etc.) were the main focus of these inspections. The dummy was also examined for final position, signs of interior contact, etc. Information from the speed traps was recorded and compared with the video data to verify the measured pendulum impact velocity.

3.3 - PROCEDURES: SERIES II

The second series of tests were conducted using the same procedures as the initial experiments with the following modifications:

- 1) addition of accelerometers to the pendulum, vehicle and occupant
- 2) use of two high speed video cameras allowing simultaneous recording of the occupant and rear bumper
- 3) use of a constant pendulum mass of 929 kg (2044 lbs) for all tests
- 4) removal of the driver's door to improve visibility
- 5) utilization of an improved pendulum release mechanism
- 6) use of an improved speed trap

Biaxial accelerometer clusters were installed in the dummy and the vehicle with a single axis accelerometer placed on the pendulum. The dummy was instrumented (as in Figure 3.4) so that the relative head and shoulder movements could be obtained, providing an estimate of neck loading. In each vehicle, the accelerometers were placed such that the loading difference

between the bumper mounting brackets and the seat could be recorded. All the accelerometers were energized and connected to the data acquisition board just prior to raising the pendulum. The pendulum angle was measured with the new speed trap and verified using the protractor.

With the new pneumatic release mechanism, shown in Figure 3.7, the camera was activated just before the air line was pressurized. Switches were mounted just prior to impact to trigger the accelerometer based data acquisition system and a photographic flash unit. This flash was used to mark the data acquisition trigger recording on the video tape and allow cross referencing between the two data acquisition systems. Post impact inspections were carried out as described in Series I.

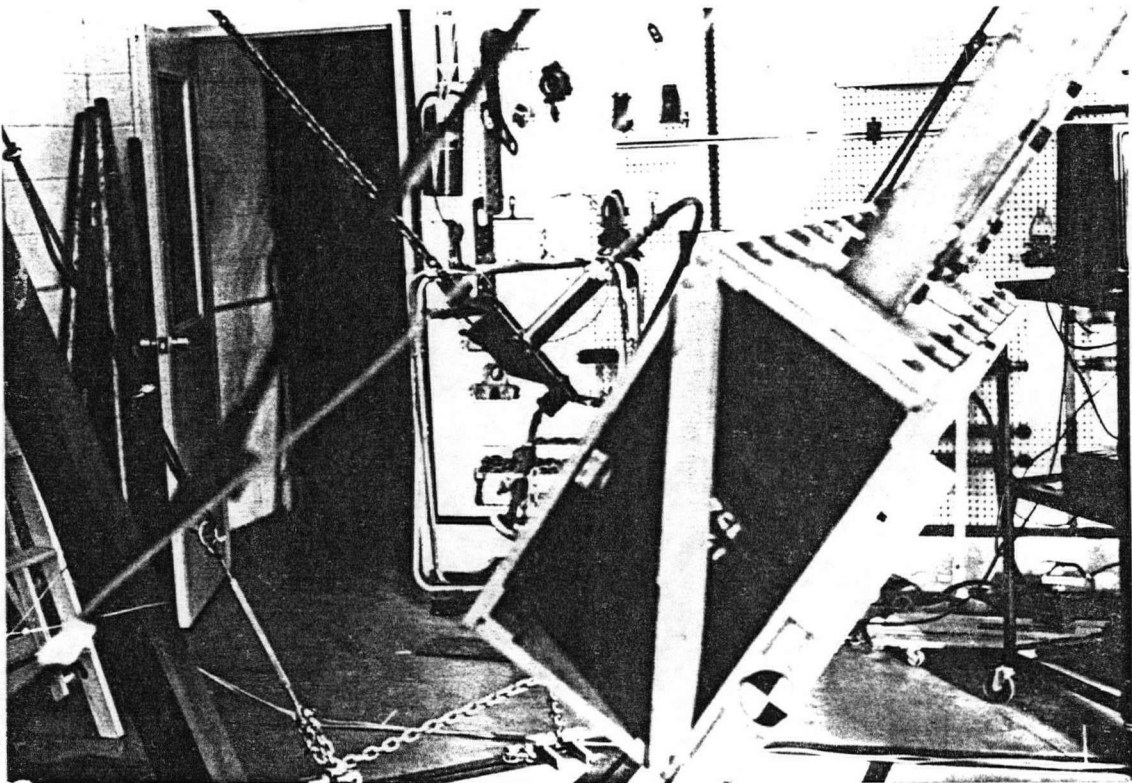


Figure 3.7: Pneumatic Pendulum Release Mechanism

3.4 - TESTING SCHEDULE

The number of vehicles available for testing was limited, thus it was necessary to utilize the vehicles in the most effective manner. The philosophy employed was to hit the vehicle three or four times. In the first series most of the vehicles were impacted at speeds between 8 and 12 km/h, which produced no structural damage to the vehicle, and then at a final speed ranging from 15 to 20 km/h. These tests generally employed the dummy located in the typical driving posture, however, two vehicles were utilized to study the effect of variation in the initial occupant posture (i.e. forward leaning angle) and the head restraint position on the occupant dynamic response. During these tests, each of the vehicles were impacted at approximately 8 km/h with the dummy position varied systematically. Note that some of the tests were conducted after structural damage was observed (notably tests 4 and 12). These tests were for observation only and not intended to represent an undamaged vehicle impact.

In Series I, limitations in the field of view of the video equipment did not allow images of both the occupant and the rear bumper to be obtained simultaneously, thus only one area was focused upon for any specific impact. The first three tests were used to observe the bumper/pendulum interaction. For these tests, the video imager was focused only on the rear bumper region. However, the remainder of the tests were carried out with the video imager focused on the occupant compartment where the occupant and vehicle frame translation could be recorded.

Series II tests took a similar approach, but a second imager allowed the bumper performance to be simultaneously recorded. Twenty-four impacts were performed on 10 cars. The number of impacts experienced by each car was dependent on the damage visible on the vehicle after each test. The first car went through two initial non-damaging impacts at 8 km/h. After these tests, the speed of the first impact was increased for each vehicle. This was used to

determine if the prior impacts at low speed influenced the later impact at higher speed. The test cars were paired such that test conditions were identical for headrest up and headrest down conditions. The conditions for both testing series are given in Tables 1 and 2.

Table 3.1: Matrix of Series I Testing 1988

TEST No.	VEHICLE No.	IMPACT SPEED [km/h]	HEAD RESTRAINT POSITION	OCCUPANT POSITION
1	1	8.0	*	*
2	1	10.1	*	*
3	1	14.4	*	*
4	1	22.4	down	upright
5	2	8.0	down	upright
6	2	8.0	up	upright
7	2	11.3	up	reclined
8	2	18.1	up	reclined
9	3	8.7	down	reclined
10	3	10.8	down	reclined
11	3	15.1	down	reclined
12	3	21.5	down	reclined
13	4	8.7	down	upright
14	4	11.2	down	forward
15	4	13.0	down	forward
16	4	13.3	down	forward
17	5	11.5	fixed	upright
18	6	9.1	down	upright
19	6	9.1	down	forward
20	6	8.0	none	forward
21	6	8.7	none	forward
22	7	8.7	fixed	forward
23	7	11.2	fixed	forward
24	8	18.7	down	upright
25	9	8.7	down	upright
26	9	8.7	down	forward
27	9	8.7	none	forward
28	9	8.7	down	forward
29	9	8.7	down	forward
30	9	11.5	down	forward
31	9	11.5	down	forward
32	4	13.0	down	forward

* camera on bumper - no occupant data

Table 3.2: Matrix of Series II Testing (1989)

TEST No.	VEHICLE No.	IMPACT SPEED [km/h]	HEAD RESTRAINT POSITION	OCCUPANT POSITION
1	1	8.2	UP	BACK
2	1	8.2	UP	BACK
3	1	10.1	UP	BACK
4	1	15.5	UP	BACK
5	2	21.0	INTEGRAL	BACK
6	3	8.2	DOWN	BACK
7	3	10.1	DOWN	FORWARD
8	3	13.7	DOWN	FORWARD
9	4	10.1	DOWN	FORWARD
10	4	12.3	DOWN	FORWARD
11	4	16.5	DOWN	FORWARD
12	4	20.8	DOWN	FORWARD
13	5	10.3	DOWN	BACK
14	5	12.4	UP	BACK
15	5	15.1	UP	FORWARD
16	6	10.9	UP	FORWARD
17	6	13.7	UP	FORWARD
18	6	11.5	UP	FORWARD
19	7	13.7	DOWN	FORWARD
20	7	13.6	DOWN	FORWARD
21	8	15.7	DOWN	BACK
22	9	14.1	DOWN	BACK
23	10	12.7	DOWN	FORWARD
24	10	14.7	DOWN	FORWARD

3.5 - DATA FORMATS AND PROCESSING

In general, data acquisition and signal processing tasks can be divided into 3 basic procedures. A digitizing or analog to digital (A/D) conversion process is needed to convert the measured parameters into a computer readable format. The information is then sorted and scaled to represent the measurements' magnitude and system of units (ie. acceleration - m/s^2 or g's, displacement - m). The last step is usually a smoothing operation to assist in the interpretation of the data. Curve fitting routines or digital filters are used to remove noise from the signal.

The two data collection systems used in this project have unique processing requirements. Accelerometer readings were processed readily using the existing facilities available in the Mechanical Engineering Department and through the development and use of additional

software. However, the processing of video recordings require more sophisticated equipment for proper handling. Two different approaches were utilized for the video analysis with each method explained in the following sections.

3.5.1 - SERIES I

The first processed results of this project were obtained from the high speed video records of Series I. Since this was the first attempt within the Mechanical Engineering Department to obtain motion analysis from video records, equipment suitable for this process was not available. Industrial applications of video processing utilize a frame grabber board connected to a host computer. The image is scanned by the hardware and converted to an array where each image pixel is represented by an array element. This array can then be manipulated and processed as desired. Without this equipment, an alternative method had to be developed. The Series I analysis equipment consisted of a projection television, video cassette recorder (VCR), digitizing table, and a microcomputer. With this apparatus, the image was projected onto the tablet and the benchmarks selected with the mouse. Communication software transferred the digitizer output to the computer files for later processing.

The procedure for digitizing the images began with positioning the projector to produce an image square to the tablet. The corners of the video image were digitized to record the view size. The tape was then positioned to the point one millisecond prior to impact (indicated by presence of the laser image). The benchmarks on the image were all selected to provide the initial positions required in the scaling from image to full physical size. The digitizing that follows required the picking of reference points in each image. The order of point selection was maintained to allow for later sorting of points corresponding to each reference marker.

Most VCR's are limited to working in the "Pause" mode for only five minutes. After this time the VCR automatically switches off. To compensate for these interruptions, the marker on the stationary (ground) position was selected to provide a relative position common to each data block.

The data was sorted into time/displacement histories for each marker using the relative position of each optical marker in the data record. After this collation, the points had to be corrected for distortion as the image had a trapezoidal appearance when projected. Deviation along the length of the edges was small enough to permit approximation by straight lines. To appropriately map the image into the appropriate area, the data was first adjusted horizontally, based on the vertical coordinate of the point. Subsequently, the vertical position was shifted according to its horizontal location. The aspect ratio of the corrected image was then verified against the original image.

The relationship between the video and full size image was based on the pre-impact position of the benchmarks. This transformation was based on the ratio of the full size measurements to the digitized coordinates. This scaling factor is different for each benchmark since each has a different plane of motion. The different distances between the focal plane and these planes of motion were factored into the respective scaling factors.

Errors in the scaling factor were a function of the initial benchmark measurements and the target selection during digitization. Errors in the full size measurements were in the order of 1 part in 50 but digitizing errors were smaller, estimated at 1 part in 150. The author was responsible for all the measurement and digitizing duties and this processing by a single operator maintained the consistency of data between tests.

The original form of the data, after processing to yield the actual motion of the car and occupant, contained a significant scatter component about the actual signal. The first set of tests

employed curve fitting routines to smooth the data for subsequent analysis. Least squares routines ("DOLSF and DOLNT" on the MTS computer system at U.B.C.) were employed. Their ability to provide first derivatives of the fitted coordinates was used to calculate the speed and acceleration curves from the displacement data. One drawback of the least squares method was the high curvature introduced at the end-points by the polynomial's attempt to satisfy boundary conditions. This required hand editing of these sections of the data, displayed in Sections 4.1 and 4.2.

3.5.2 - SERIES II

3.5.2.1 - VIDEO PROCESSING

Processing of images obtained in the Series II tests was improved with the assistance of the Institute of Advanced Research in Computer Science. A frame grabber, in the Laboratory for Computational Vision was made available for the Series II analysis. Their video "frame grabbing" system is accessible through computer workstations where the images were viewed. Software was developed to project the image on the monitor, select the points in the frame, attach a time value to each frame and write the information to an ASCII file. To increase the number of frames captured and stored into RAM, the number of grey levels in the image was reduced from 16 to 2. The size of the image was also reduced by capturing the central image and time windows, ignoring the data borders around the image.

The procedure for digitizing video with this equipment began with grabbing the video frames to be analyzed. The memory capacity of the file server to which the frame grabber was attached allowed several tests (of about 250 images per test) to be captured and stored as image files on the disk. These files were recalled through software and displayed on the monitor. The time from the image's clock was entered and the benchmarks on the first image were selected and stored to the data file with the time value. The software retained the locations of the

benchmarks such that the cursor would advance to the previous position of each marker. Thus, only minor cursor adjustments accommodated the movements of the markers between frames. This allowed the order of benchmark digitization to be retained and streamlined the process.

As in the Series I processing, a calibration of the video system was required for the transformation from video pixel values to full scale dimensions. The Series II calibration utilized a reference grid photographed at various distances. This represented the position of the markers relative to the camera. Using the digitizing method described above, transformation constants could be established between the known grid coordinates and the corresponding digitized values for different object-camera distances. This transformation was based on the Eight-Parameter Method commonly used in photogrammetry, briefly described in Appendix E. Since this transformation was based on a large grid (25 x 25 cm spacing - 70% of the available video image), errors in measurement did not influence the transformation precision as much as encountered in Series I. As described in the previous section, Series I transformations were based on smaller areas (both in actual and displayed size) containing fewer reference points.

This second digitizing method was subject to errors introduced from the small image size displayed on the monitor. With only a 10 x 15 cm image displayed on the Sun workstation, a slight error in target selection had a significant effect on the total processing error because scaling function amplifies the error. This error was not as pronounced in the Series I processing where a larger (8 times) display image was used to select the targets. As the image size increases, the amplification caused by the scaling function is reduced. A review of the total processing error introduced by these two methods suggests that the Series II procedures provided more consistent results. The projection method of Series I could only be carried out in the dark making the operator uncomfortable and thus consistent processing difficult. Direct display on a monitor for Series II processing eliminated the lighting and distortion problems introduced by projection encountered in Series I digitizing.

Scaling was followed by a least-squares curve fitting routine and a sixth order Butterworth digital low pass filter to smooth the data. Comparison of the two techniques suggested that the low pass filter was better suited for this analysis. It was found that the displacement data presented a step input when introduced to the digital filter. This was especially apparent in the case of a pendulum which was moving at the beginning of the data logging sequence. This step input into the filter resulted in an initial lag in the output data, and is described in the discussion of Series II results (Section 4.4). This lag also presented problems in the calculation of velocities and accelerations using the 5-point Taylor-Series expansion described in [78]. The initial discrepancy in the filtered displacement signal produced inappropriate velocity and acceleration data. Fortunately, this was limited to the first few milliseconds of the pendulum data and did not affect the important segments of the data. To provide a comparison between the video and speed trap estimates of impact speed, the pre-filtered video data was used to calculate impact speed. Of the two sources listed, the speed trap was found to be more accurate.

3.5.2.2 - ACCELEROMETER PROCESSING

The accelerometer output signals were processed more directly than the video information. The voltage levels acquired were converted to accelerations using the calibration values supplied for each accelerometer. Verification of these values was accomplished using a ± 1 g accelerometer calibrator. The recording frequency (approximately 10 kHz per channel) produced data files which were too large for convenient analysis. The files were digitally filtered with a low pass filter to a value below 1 kHz and then reduced by editing out 90% of the values. Comparison of pre- and post- compression plots showed that there was no loss of information. The edited file was then further filtered, based on the highest frequency of interest within the test. Fortran software (ACCEL.FOR described in Appendix C) was used for this signal conversion and filtering.

The edited file was then further filtered, based on the highest frequency of interest within the test. Fortran software (ACCEL.FOR described in Appendix C) was used for this signal conversion and filtering.

Output signals from the occupant accelerometers required little filtering. The natural damping inherent to this type of dummy movement reduced any spurious noise in the signals. However, the vehicle mounted accelerometers were extremely susceptible to the natural frequencies of the vehicle's metal components. These vibrations corrupted the signals to the point that interpretation was not possible without filtering. The typical cutoff frequency employed was 25 Hz for vehicle mounted transducers. The SAE J211 [75] procedure recommends that filters on vehicle mounted accelerometers should have a cut-off frequency of 180 Hz. Filtering at this level did not provide informative plots, since vehicle vibrations were still evident. The lower filtering frequencies were chosen because they brought out the translational acceleration pulse. Extensive use of digital filtering will decrease the precision of signals, but consistent processing of the data allows comparison of the acceleration levels between the tests. The video results were subsequently compared to the accelerometer output to determine the validity of the test results.

Chapter 4 DATA ANALYSIS AND RESULTS

4.1 - SERIES I TESTING: VEHICLE PERFORMANCE

The most significant observation obtained during the 32 impacts conducted during Series I (see Section 3.4) testing was the impact speed at which structural crush began on the vehicle. For the Volkswagen Rabbit, limited damage to the vehicle was found for speeds below 15 km/h. Only a 5 mm movement of the bumper isolator mounting bolt within its adjustment slot was detected. An impact speed between 14 and 15 km/h was found to be the threshold speed where crush began to develop in the rear fenders and trunk area floor panels. For impact velocities below this threshold, only cosmetic damage to the bumper itself was found. A slight curvature initially present in the bumper design was straightened as a result of the impacts, however, the amount of energy absorbed during this process was minimal compared to the total impact energy. Some fluid leakage from the bumper isolators also occurred, but did not have a significant effect on the isolator performance during subsequent higher speed impacts. The full stroke length of the isolators appeared consistent around 5.7 cm which is consistent with the Volkswagen test results which range from 5.6 - 5.9 cm.

Figure 4.1 shows the impact pendulum, bumper and rear axle displacements versus time for a 14.7 km/h impact. The area between the bumper and rear axle displacements is representative of the energy absorbed by the bumper system. Information supplied by Volkswagen on the isolator response indicate that the bumper will absorb between 1400 - 1700 J when struck with a 950 kg mass at impact speeds between 7.3 and 8.3 km/h.

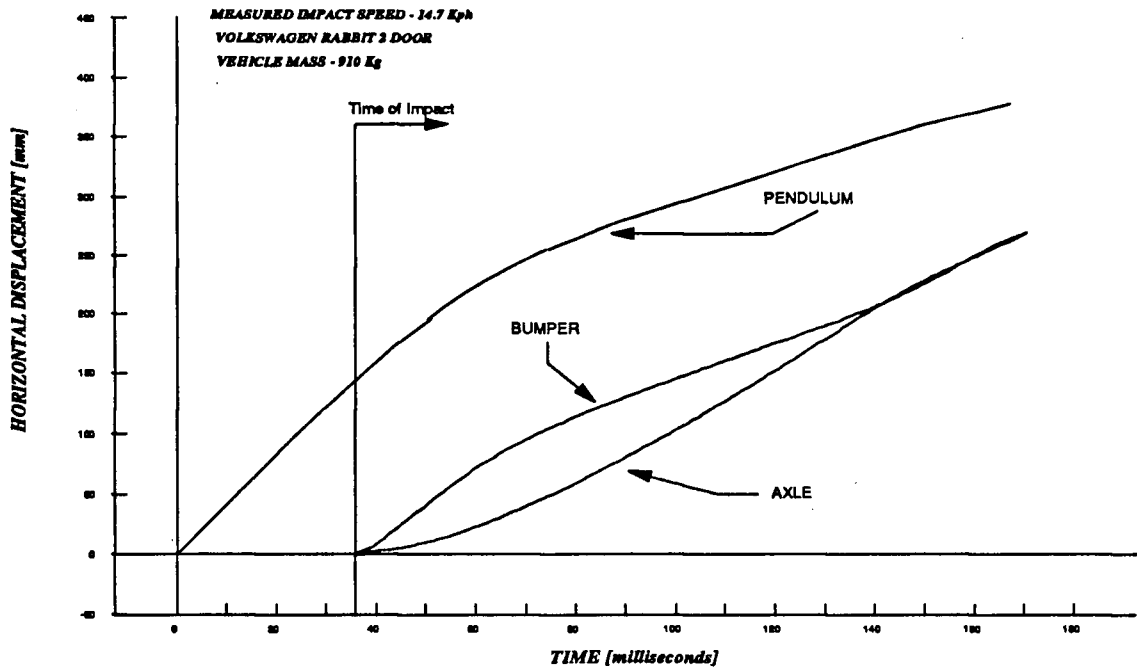


Figure 4.1: Pendulum and Bumper Displacements

The wheels were locked for these tests, thus the energy dissipated in sliding friction can be derived from:

$$E_{friction} = \mu m g d$$

where:

μ = coefficient of sliding friction

m = mass of the vehicle

g = gravity

d = distance moved

Based on conservation of energy, the kinetic energy of the pendulum just prior to vehicle contact should be equivalent to the kinetic energy of the vehicle and pendulum just after contact is lost plus the energy dissipated by the bumper and tire friction.

$$KE_{pend}^{init} = KE_{pend}^{final} + KE_{car} + E_{bumper} + E_{fric}$$

Table 4.1 shows the results of this calculation for the first three tests compared to information from Volkswagen [5] (described in Appendix D). Figure 4.2 shows the bumper isolator construction. Its operation is based on the metering of oil through an orifice. As the oil passes into the second chamber, a piston is driven back, compressing the gas behind it. This compression acts as a spring which subsequently expands against the piston, driving the oil out through the orifice.

The orifice controlling oil flow is spring controlled so that a predetermined load on the bumper will open the valve, increasing the orifice size. Expansion of the isolators causes the valve to close, restricting the orifice size and slowing the return flow of oil. These characteristics are depicted in the performance curves listed in Appendix D.

Table 4.1: Bumper Performance in Series I Testing

Impact Speed [km/h]	Input Energy [J]	Absorbed Energy [J]	% Absorbed	Absorbed Energy* [J]
8.1	2174	808	37.2%	1636
10.5	3392	2020	59.6%	2152
14.7	7034	4316	61.4%	3054

* from Volkswagen Tests - Appendix D

It is important to recognize that these impacts only involve the bumper system of the struck vehicle. If the bumper of the striking vehicle was included, we would expect energy to be dissipated within both structures. Thus, a higher vehicle-vehicle impact speed would be required

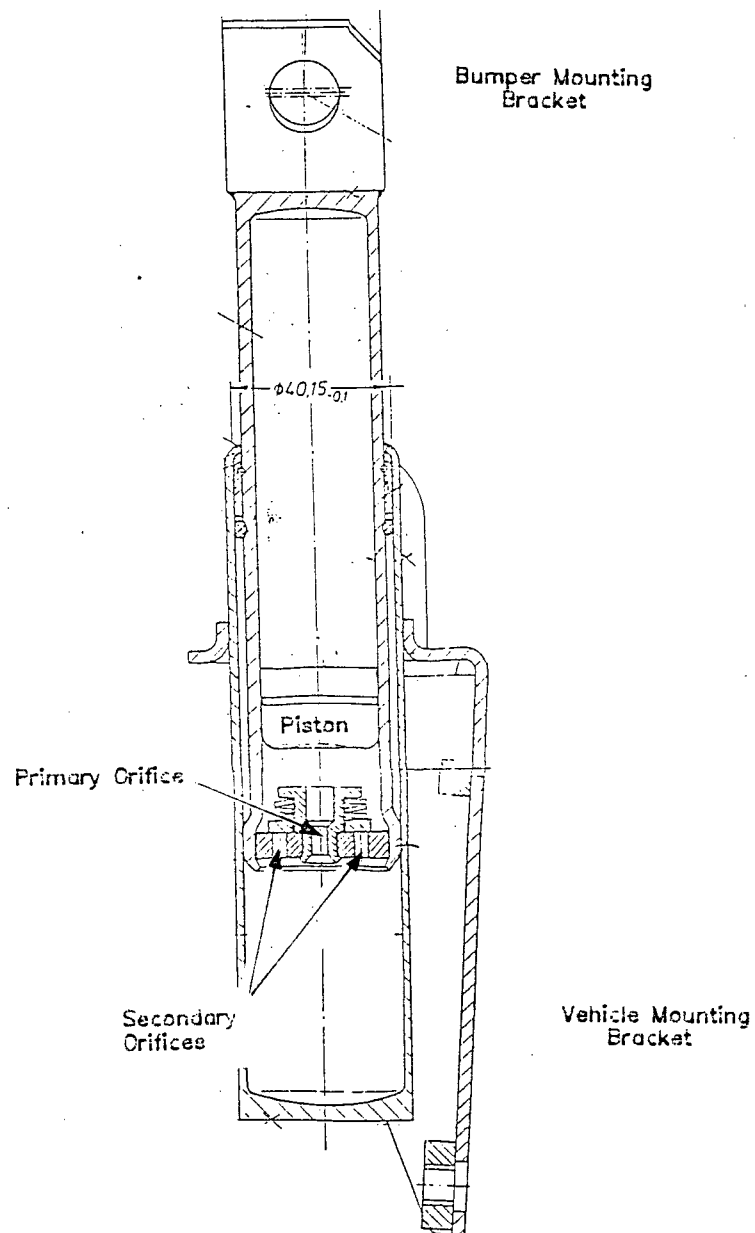


Figure 4.2: Bumper Isolator Construction
(from [79])

to duplicate the energy levels recorded. However, these impacts may introduce other loads if, for example, one bumper over-rides the other. It is because of these complicating factors that the striking vehicle is assumed to be rigid in this parametric study.

4.2 - SERIES I TESTING: OCCUPANT RESPONSE

Figures 4.3 and 4.4 show a typical set of vehicle and occupant response curves for 18.4 and 8.1 km/h impacts respectively, as derived from the digitized video images. This data clearly indicates that a substantial time lag, on the order of 50 ms, exists between the detection of initial vehicle and occupant motion. This time lag is significant as the vehicle achieves its final velocity before the occupant begins to move. Dynamic loading of the seat structure by the occupant results in significant seatback deflections. The rebound from the seatback then causes the occupant to be accelerated forward to a velocity higher than the car velocity. As a result, the occupants encounter higher accelerations than the vehicle as they attempt to "catch up" with the

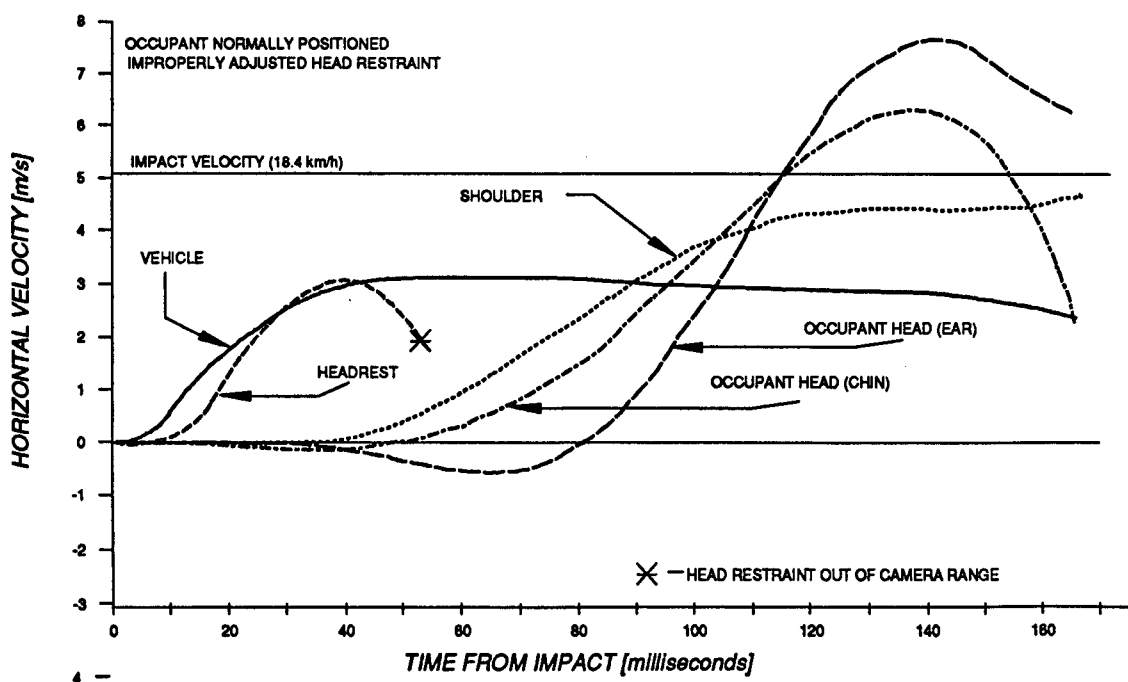


Figure 4.3: Vehicle and Occupant Response for 18.4 km/h Impact

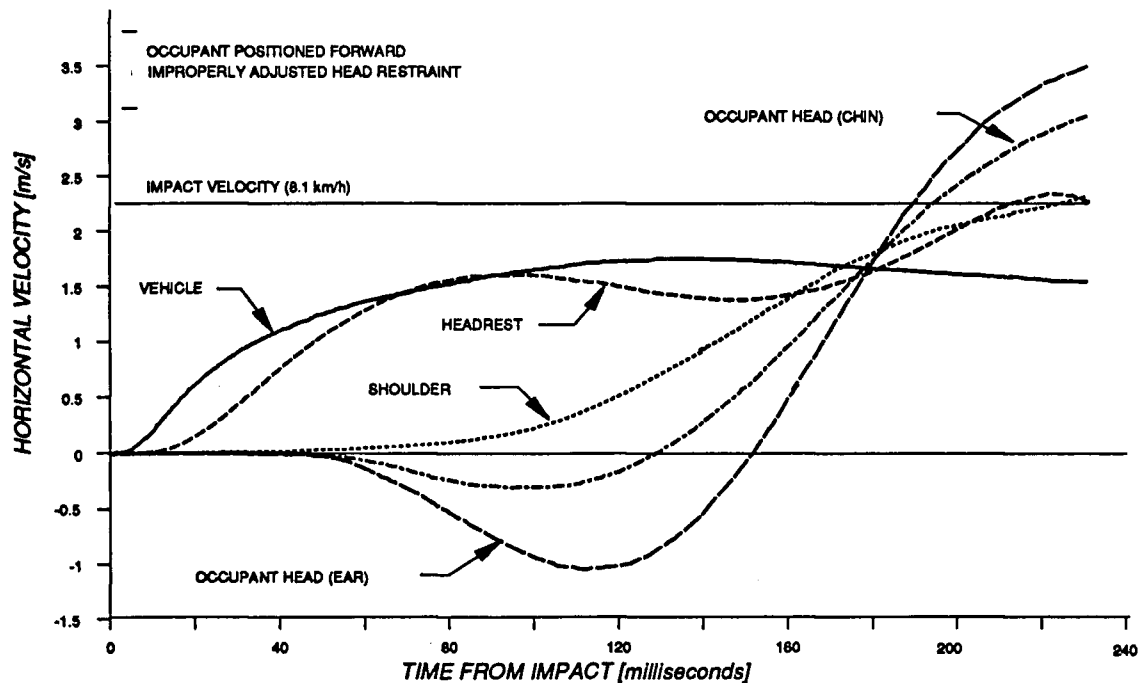


Figure 4.4: Vehicle and Occupant Response for 8.1 km/h Impact

car. It is also important to recognize from these figures that the shoulder is rebounding before the head. This relative movement of the head to the shoulder during the rebound is the likely cause of neck injuries as this is the point at which dynamic loading of the neck will be a maximum.

The mechanism by which the occupant responds is depicted in the series of images in Figure 4.5. Initially (image 1) the body of the car and occupant are at rest. The impact force on the rear bumper acts over some period of time (approximately 50 ms) because of the damping and deflection of the bumper system. As the force is transmitted to the frame, the vehicle begins to move and loads the passenger through the seat, image 2 and 3. The specific response of the occupant will be a function of the loading parameters, seat characteristics, occupant behaviour, and the position of the occupant relative to the seat. The inertia of the head and neck cause them

to remain motionless until forward movement of the lower body causes them to rotate backwards, as shown in image 4. This rearward motion is compounded with the added articulation of the head/neck system. The occupant's shoulders load the seatback and begin to rebound (images 5 and 6) as the head continues backward in combined translation and rotation. This instant is the point of maximum loading on the neck. The free body diagram of the head and neck at this point, Figure 4.6, schematically illustrates this loading.

The head then rebounds off the headrest (image 7). The rebound induced motion is superimposed upon the vehicle's motion resulting in the head achieving speeds in the order of twice the vehicle's post impact speed. The rebound is finally arrested by the body's contact with the seatbelt. Unfortunately, the head's inertia maintains its forward movement past the torso, placing the neck into flexion (image 8).

Whiplash or hyper-extension is often related to the rearward deflection of the head relative to the body. Figure 4.7 shows the relative displacement and acceleration of the head's center of gravity, relative to the shoulder. The results shown were produced by a 9.2 km/h impact. As indicated, the maximum horizontal deflection and accelerations occur at approximately 120 ms. The rotational deflections of the head, Figure 4.8, also reach maximum values at this time. The positive rotation and velocity in this diagram signify the extension movement (head rotating rearwards). It is also evident from these figures that the head continues to move rearward while the shoulders rebound off the seat (shown at 108 ms on Figures 4.7 and 4.8). This differential motion between the head and shoulders results in increased neck loading especially as the inertial forces developed by the head grow larger at higher collision speeds. The occurrence of whiplash in cars with head restraints was recognized by States [20] noting that differential rebounds, from the seatback and head restraint, may produce increased rearward deflections of the head relative to the shoulder. The shoulder was found to rebound before the head in all of the tests analyzed in this study. To further investigate this effect, the acceleration

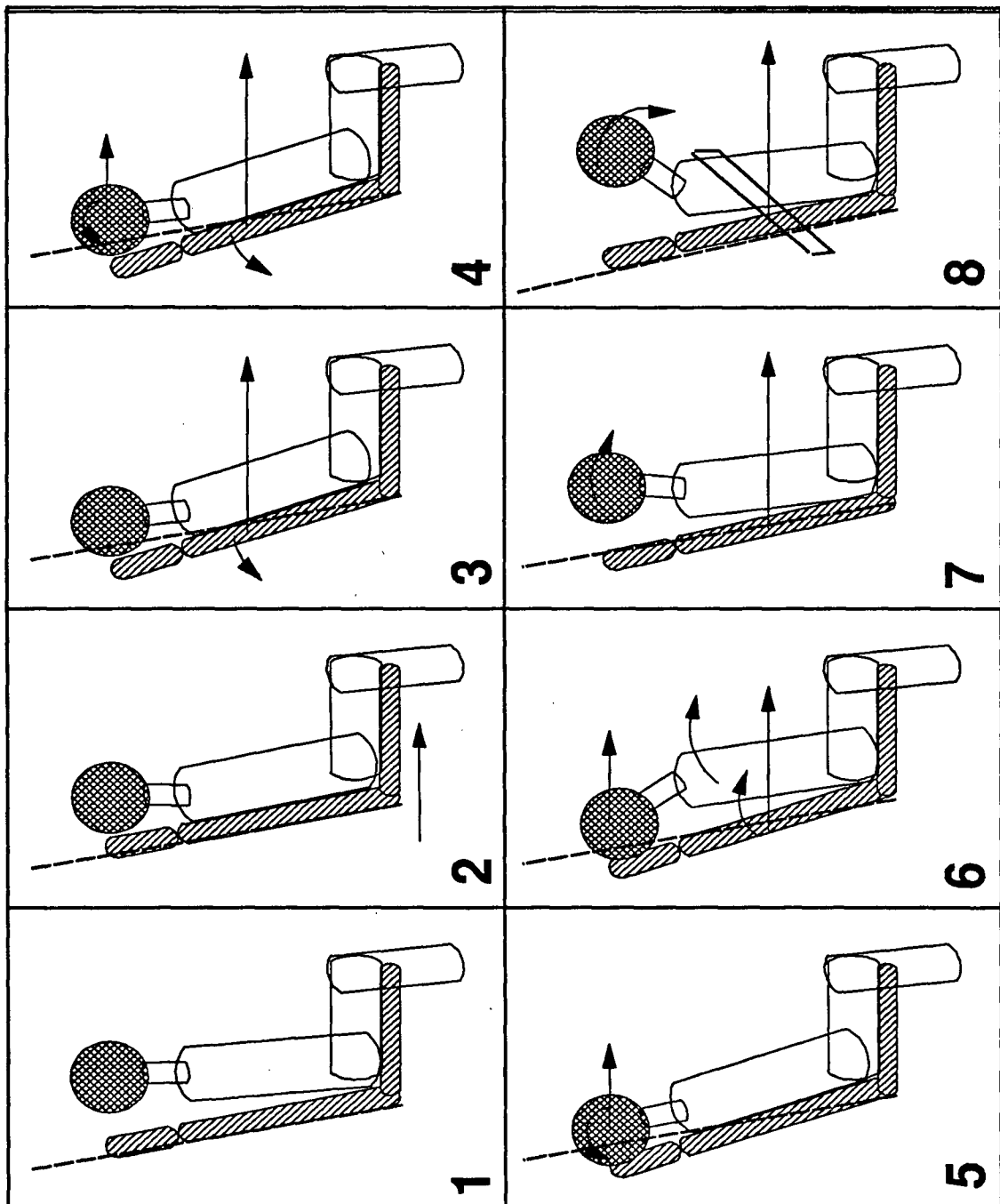


Figure 4.5: Typical Occupant Movement

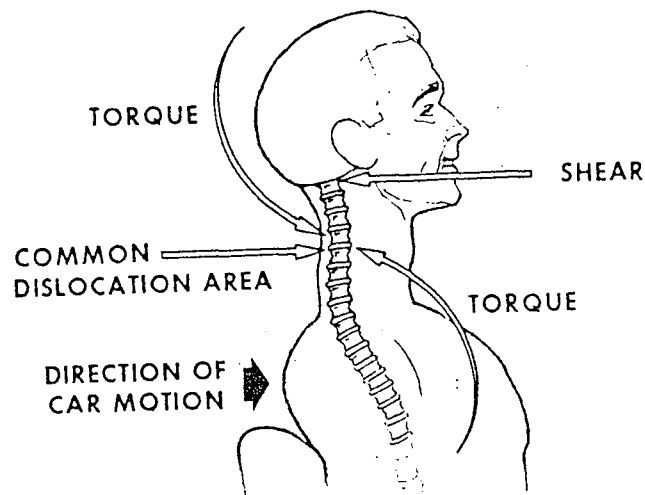


Figure 4.6: Loadings of the Occupant's Head and Neck
(from [66])

and displacements (relative to the car) for the shoulder and head are compared in Figure 4.9 for cases with and without head restraint. These plots are the results of 8 km/h pendulum impacts. The vehicle is used as the frame of reference to indicate the occupant load on the seat. It also indicates the rotations of the occupant's head and shoulders relative to their pelvis (at distances 76 and 53 cm respectively), since the lower body can be assumed to move with the vehicle. The curves clearly show that the shoulder moves through a smaller range of motion than the head. As a rigid body, the head and shoulder accelerations would be in the ratio of 76/53 (1.4:1) but the accelerations and deflections of Figure 4.9 clearly indicate that this is not the case. States' suggestion for a tuned seating system stiffness may require a similar "stiffness" approach to properly match the seatback and head restraint response.

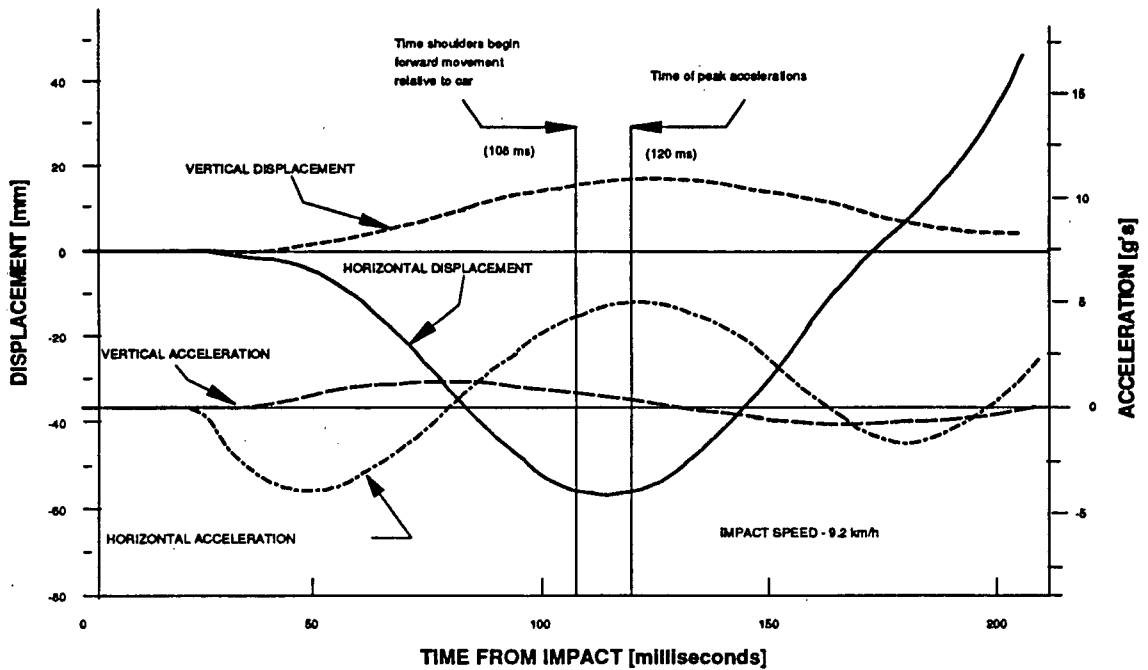


Figure 4.7: Occupant Head Deflections and Acceleration

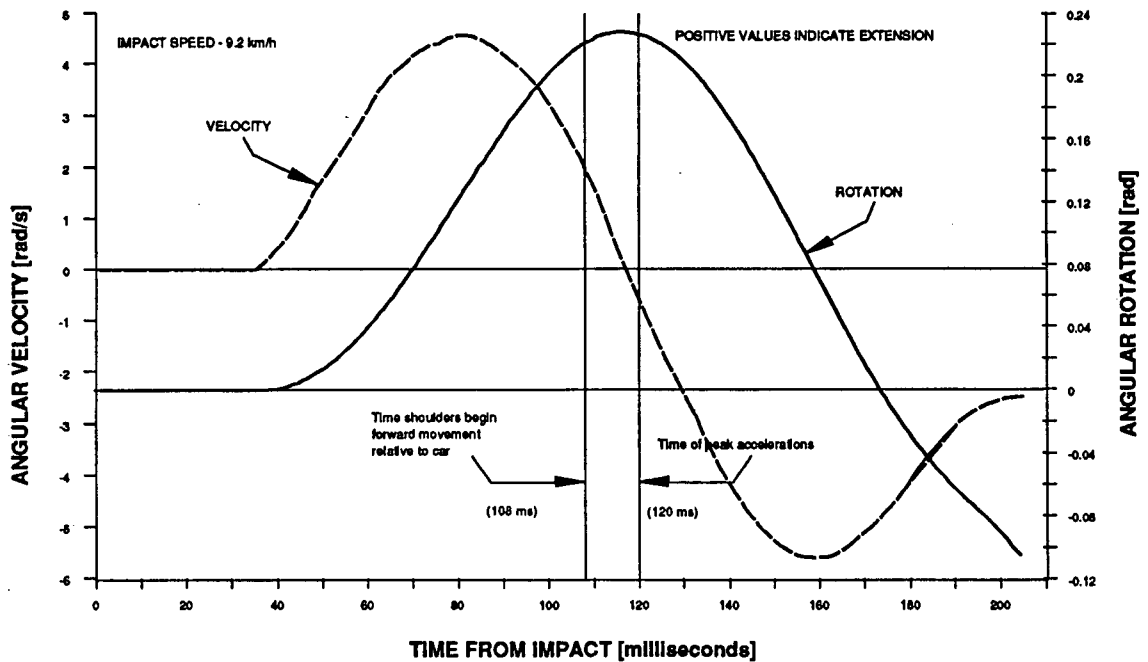


Figure 4.8: Head Rotation

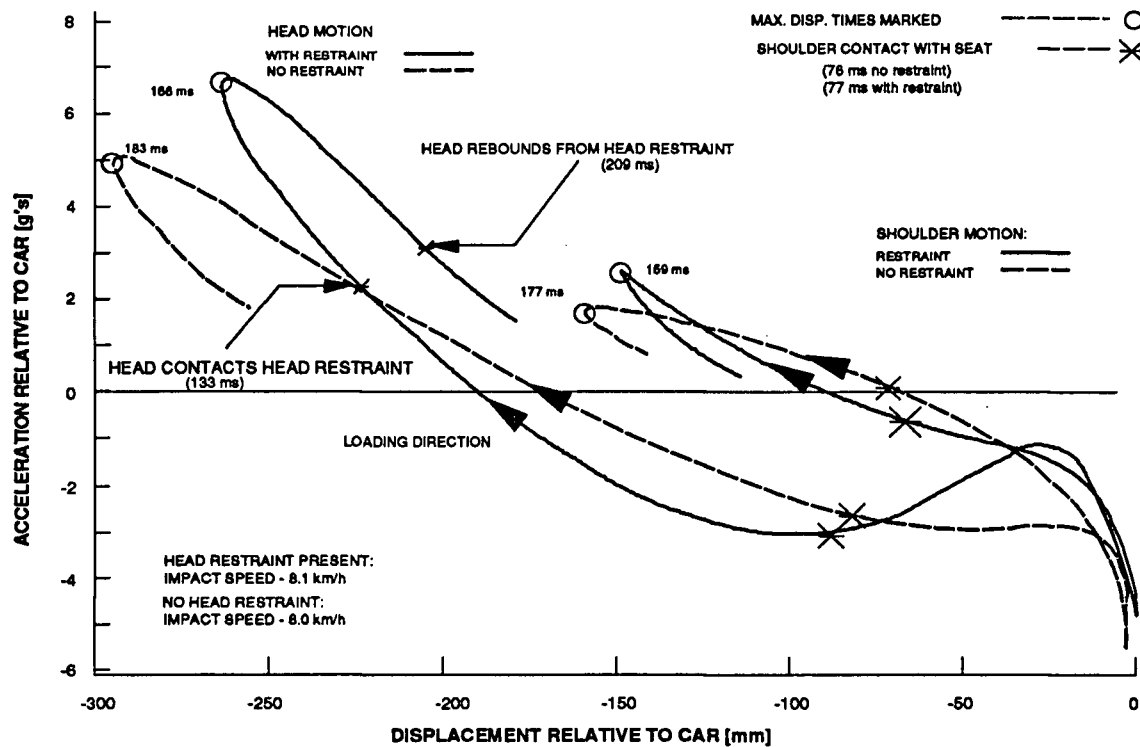


Figure 4.9: Occupant Acceleration Relative to the Vehicle

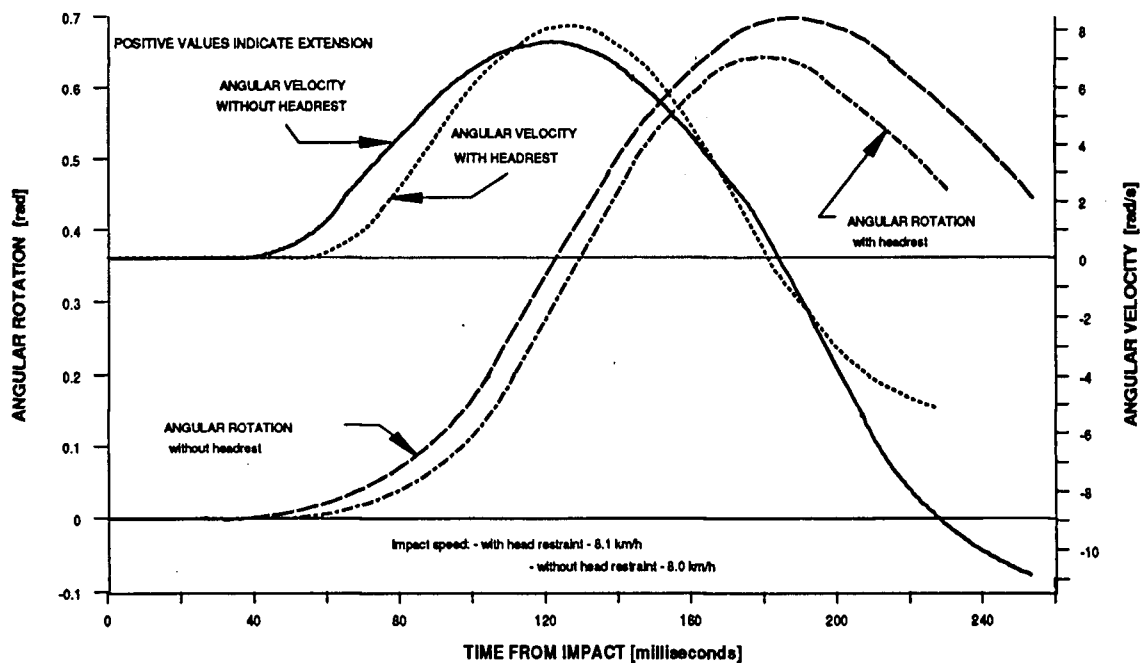


Figure 4.10: Effect of Head Restraint on Head Rotation

From Figure 4.9, one can see that the shoulders exhibit smaller deflections with higher accelerations in the presence of a head restraint than without a head restraint. For the head, higher accelerations are encountered after rebound than before headrest contact (for the same displacement) because of the spring effect of the restraint. The converse is true without the headrest because there is no reloading of the neck from the seat structure. These trends also appear in the angular motion plots of the head depicted in Figure 4.10 for the same test. A higher peak angular velocity is experienced with smaller rearward rotations of the head with the use of a headrest compared with lower peak angular velocity and larger rearward rotations without the use of a headrest. This resulted in an increase of approximately 25% in positive differential acceleration of the head with the introduction of an improperly adjusted head restraint. Since whiplash injuries are still reported in the presence of head restraints, these trends suggests that injury severity may be a function of both displacement and dynamic loading.

Figures 4.3 and 4.4 can also be used to observe the influence of initial occupant posture. Note that for the data shown in Figure 4.3, the dummy was positioned in an upright position before the 18.4 km/h impact, while the test data in Figure 4.4 was obtained by employing a 20 degree (approximately) forward leaning dummy posture for an impact at 8.1 km/h. Comparison of these curves show that the initial rearward velocity of the head taken at the ear for the properly positioned dummy at the higher impact speed is approximately 30% less than that found for a leaning dummy at half the collision speed. This occurs because the head has less time to rotate rearward before contacting the head restraint and indicates that small changes in head position can significantly affect head velocity experienced during an impact. Figure 4.11 shows the relative displacement between the head and the shoulder for these two tests. The displacements are of the same magnitude, indicating that a forward leaning occupant could increase their chance of injury to levels found by normally positioned occupants at much higher impact speeds.

As noted on the diagrams, again the shoulder rebounds to a forward velocity relative to the car before the head. The corresponding occupant head deflections at 9.2 km/h (Figure 4.7) show that a normally placed dummy moves less than the forward leaning occupant shown in Figure 4.4,

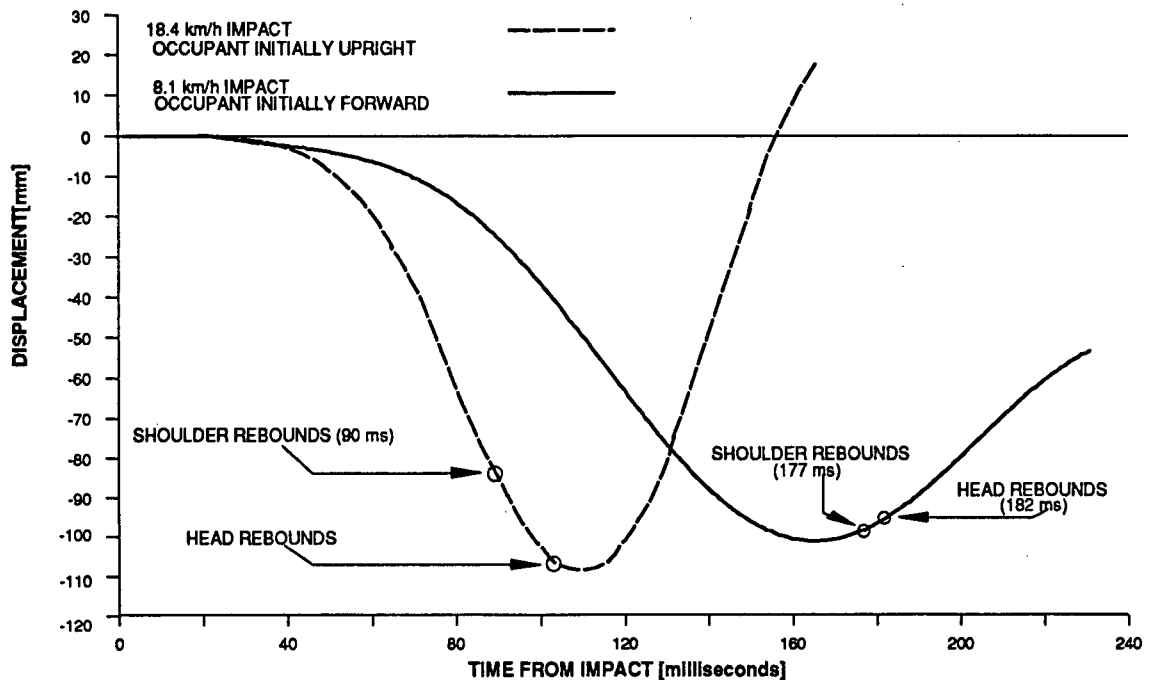


Figure 4.11: Posture Effects on Occupant Displacement

even though the latter experienced a slightly lower impact speed. All the of impacts recorded suggest that the elastic effects of the seat allow the vehicle to almost reach its maximum forward speed as the occupant's head reaches its maximum rearward speed. This increases the rearward displacements encountered and thus the propensity for a whiplash injury. Decreasing the rearward deflection of the head would reduce this velocity disparity and the associated neck loadings.

4.3 - SERIES I TESTING: DISCUSSION

The developed pendulum impact facility performed reliably, providing controlled and repeatable impacts throughout the initial testing phase of this project. The video recording

system employed in these tests provided useful information for understanding the collision kinematics of both the vehicle and occupant. Of interest to researchers is the lack of, or minimal, structural damage resulting from impact speeds below 15 km/h, and the increase of personal injury claims associated with these impacts. The absence of structural damage indicates that the bumper isolator system and retardation forces at the tire/ground interface are the predominant mechanisms of energy absorption by the vehicle during impact.

The difference between damaging and non-damaging vehicle response is best displayed by the vehicle velocity curves (Figures 4.3 and 4.4) and comparison of the vehicle velocity attained with the original impact velocity. This reduction is approximately 38% in Figure 4.3 where structural crush took place and 22% in Figure 4.4 where a greater portion of the energy was elastic and was translated to the occupant compartment. At lower speeds, losses through the sliding wheels and compliance of the bumper and suspension systems constitute 50-60% of the total energy put into the vehicle.

It was observed that the resulting deflection of the seatback with subsequent rebound, tends to pitch the occupant forward during the impact with the shoulder displacement leading the head's. This relative head-to-shoulder motion is the likely source of whiplash injury. The spring effects for the seatback and the head restraint have been quantified in Figure 4.9. Based on the higher stiffness of the Hybrid II neck, it is predicted that a human neck would allow a much greater relative displacement between the head and shoulders and thus a greater potential for injury than shown in these tests. It is also felt that the same trends can be expected in a human subject for the same conditions albeit at different magnitudes.

The effect of an improperly positioned head restraint and initial occupant posture were both shown to affect the maximum deflections of the head. The occupant experienced lower accelerations with increased deflections when the headrest was not present. The head also

experienced larger deflections relative to the shoulder when the occupant's initial posture was inclined forward in the seat. This latter effect was found to produce effects comparable to responses at twice the impact speeds with a normally seated occupant.

Visually noted from the video recording was the ramping displacement of the occupant up the seat back, even at the lower speeds (8 km/h). Also detected from the video was the slack which developed between the seatbelt and the dummy's chest at the higher impact speeds. This resulted from the inability of the retractor to spool up the free play of the seat belt. The loose seatbelt then allowed the occupant to bounce off the seat unrestrained, producing the high rebound velocities.

4.4 - SERIES II TESTING: VEHICLE RESPONSE

The results of the Series I tests isolated two vehicle performance characteristics that contribute to the potential for injury. The spring characteristics of the seatback and head restraint were shown to introduce undesirable occupant motions. Some of these characteristics have been mentioned by previous researchers, but have not been thoroughly investigated. However, a thorough documentation of seatback performance is beyond the scope of the current program. The main emphasis of the Series II tests was to further study the bumper and vehicle structure performance (see Section 3.4).

Ten Volkswagen Rabbits were impacted 24 times at speeds between 8 and 21 km/h in the second test series. They continued to exhibit structural damage only at impact speeds above the 14-15 km/h transition velocity previously identified. Only cosmetic bumper damage, and movement of the isolator mounting bolts were observed in impacts between 8 and 14 km/h. Estimators at the I.C.B.C. Research and Training Centre indicated that vehicles tested at speeds below 15 km/h typically required less than \$500 of repairs. In one test, (#6) an 8 km/h impact did not induce any observable damage to the vehicle. The only evidence of an impact was the

indication of isolator stroking. It was also found that the cosmetic damage due to a 14 km/h impact was comparable to those resulting from 8 and 10 km/h impact speeds. This suggests that estimates of the impact speed based on vehicle damage can be unreliable.

The Series II data was filtered and processed as described in Section 3.5. An example of the error introduced in the filtering process is shown in Figure 4.12. It can be seen that the initial step input of pendulum displacements is not followed accurately by the filtered data and is reflected in the velocity and acceleration curves presented later. However, the remainder of the data is unaffected and it can be seen that the smooth vehicle response presents no problem to the filter.

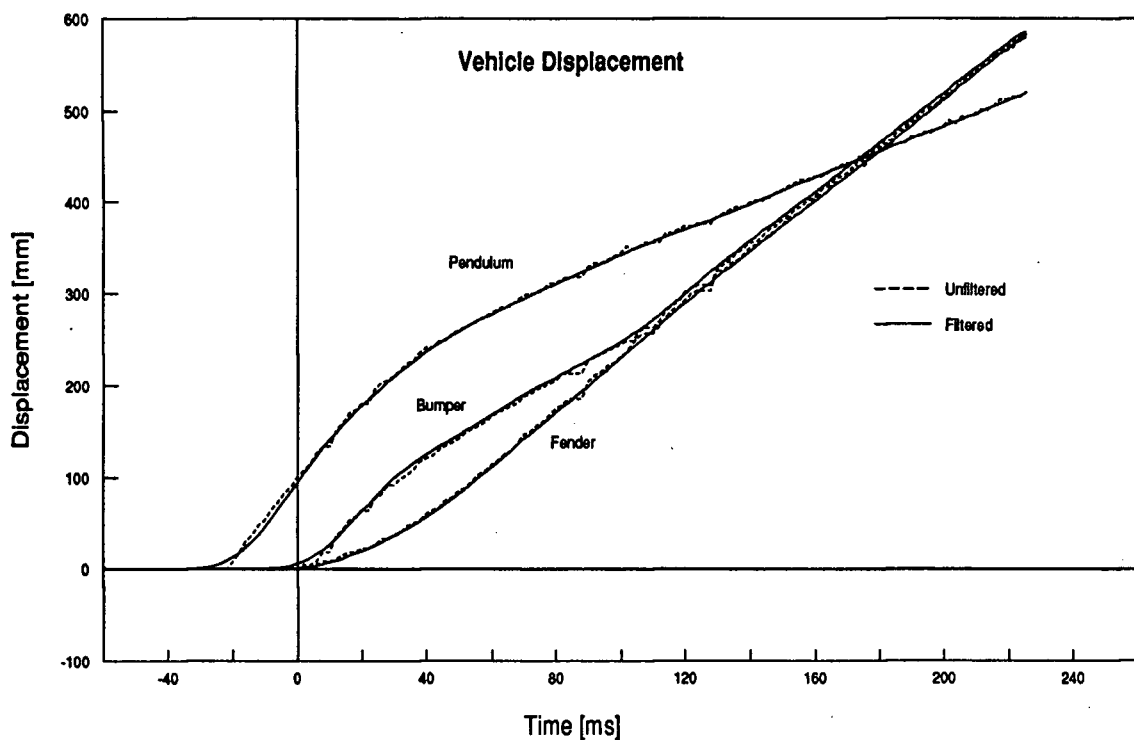


Figure 4.12: Errors in the Filtering Process

Figures 4.13-15 document the bumper, vehicle and pendulum response to impacts of approximately 8.2, 12.5, and 14.5 km/h, respectively. The limited data available for the axle in

these plots is due to its movement beyond the camera's view. As in the Series I data, the small vertical deflections recorded are significantly affected by the errors in the digitizing process. These errors are more noticeable in the differentiated data presented later.

These curves all exhibit similar horizontal displacement trends, where the difference in the bumper/vehicle data represents the length of isolator stroke. The downward vertical deflections of the rear of the car (in the initial stages of the collision) were found to increase with increasing impact speed. This is a result of the eccentric loading of the vehicle since the bumper height (typically 30 cm) is lower than the vehicles c.g. (50 cm). The moment created by this offset produces a pitching torque on the vehicle which causes the rear of the vehicle to drop. The vertical rise of the vehicle is a combination of the upswing of the pendulum, and the braking of the vehicle. After the vehicle starts moving, the braking action of the wheels produces the standard "nose-down" attitude assumed by a vehicle as it brakes. The maximum upward deflection of the bumper and rear fender was roughly 10% of the vehicles horizontal displacement at this time. This maximum value increases with impact speed and occurs after the bumper loses contact with the pendulum. Bumper performance for the Series II tests is also presented in Table 4.2.

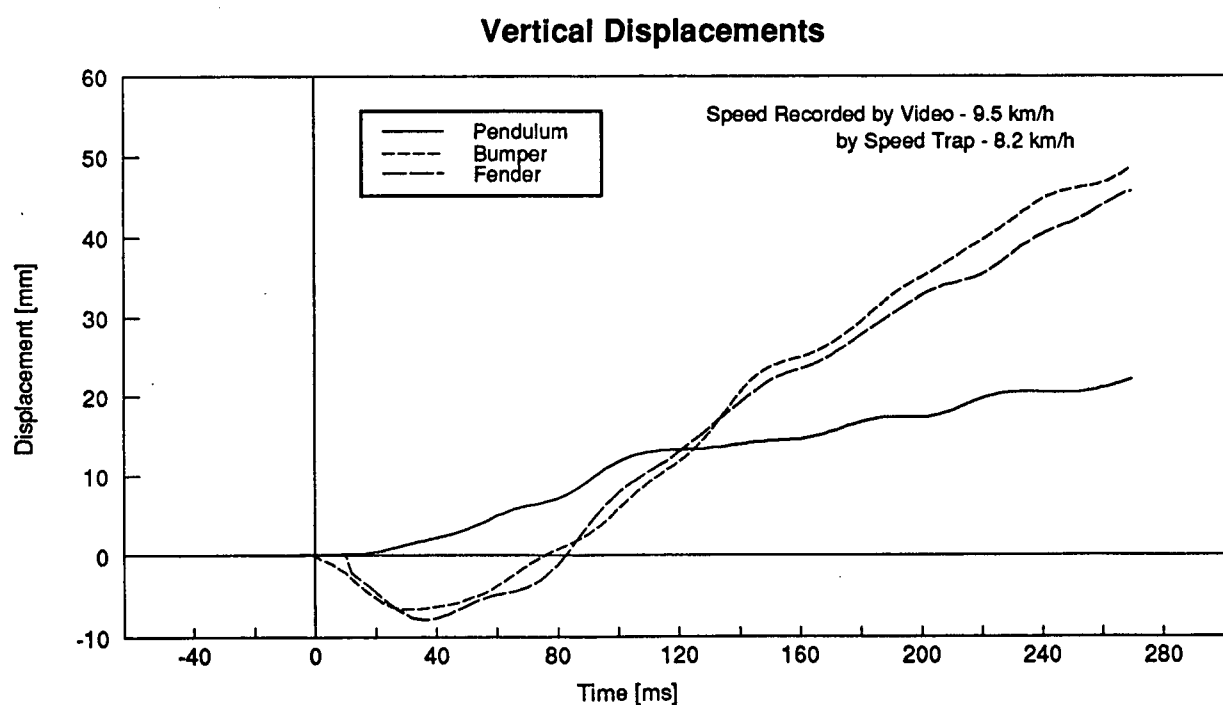
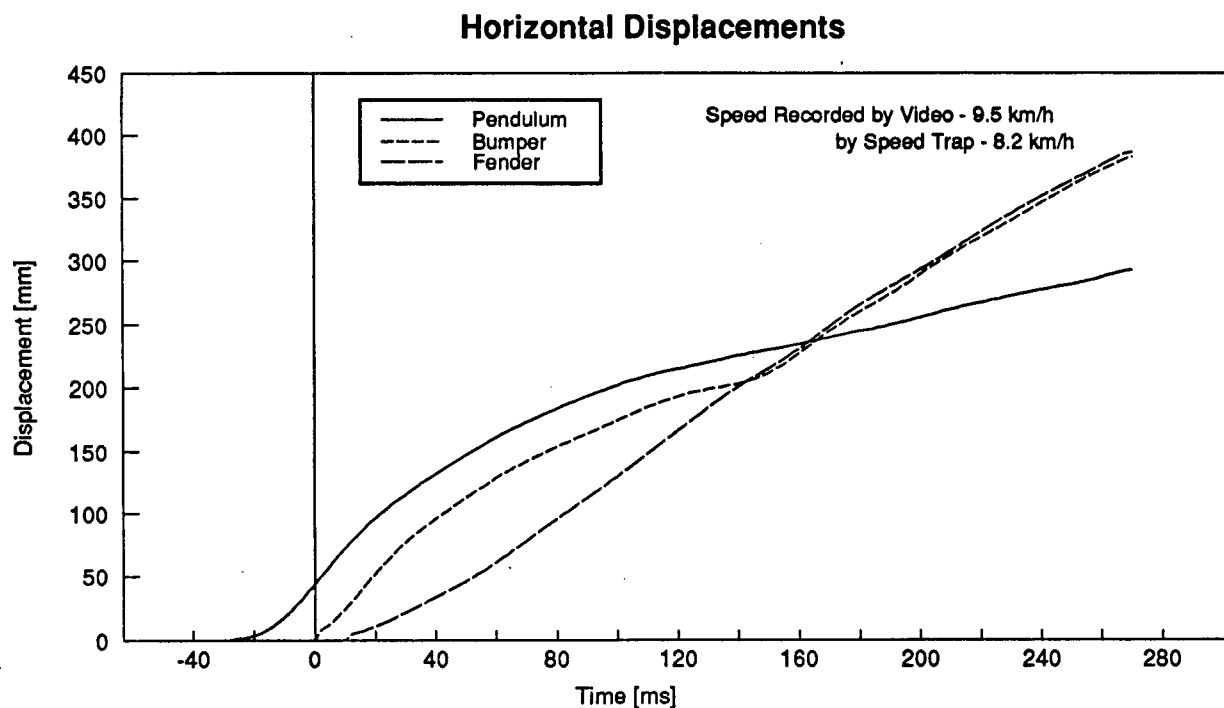


Figure 4.13: Bumper Response for an 8.2 km/h Impact

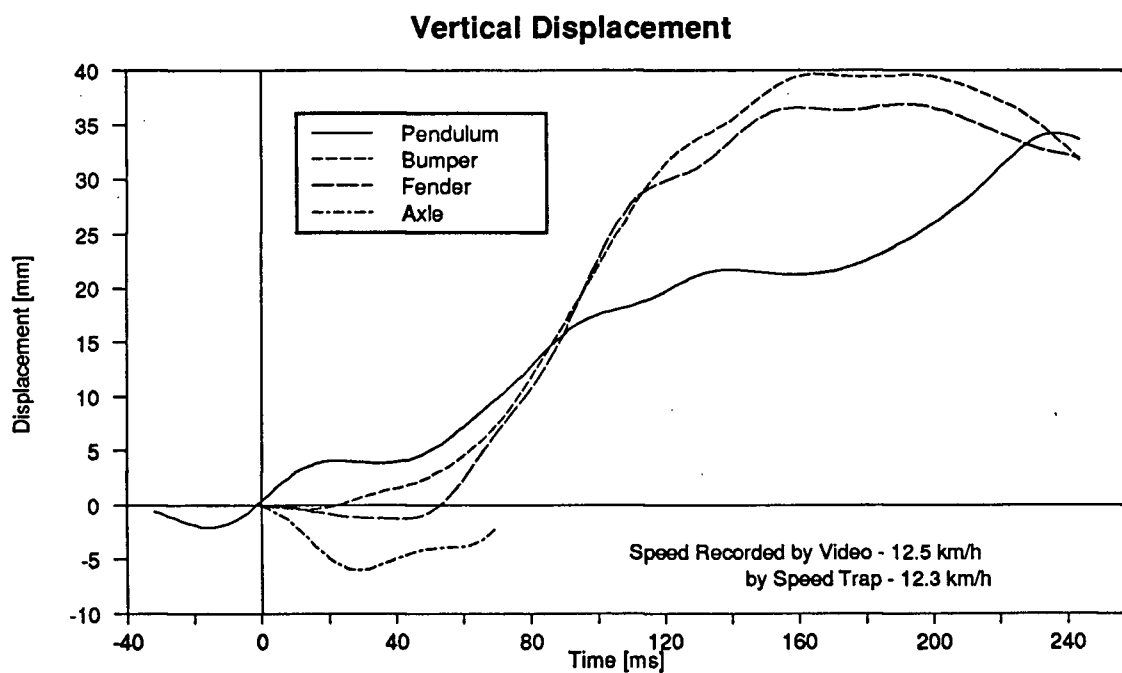
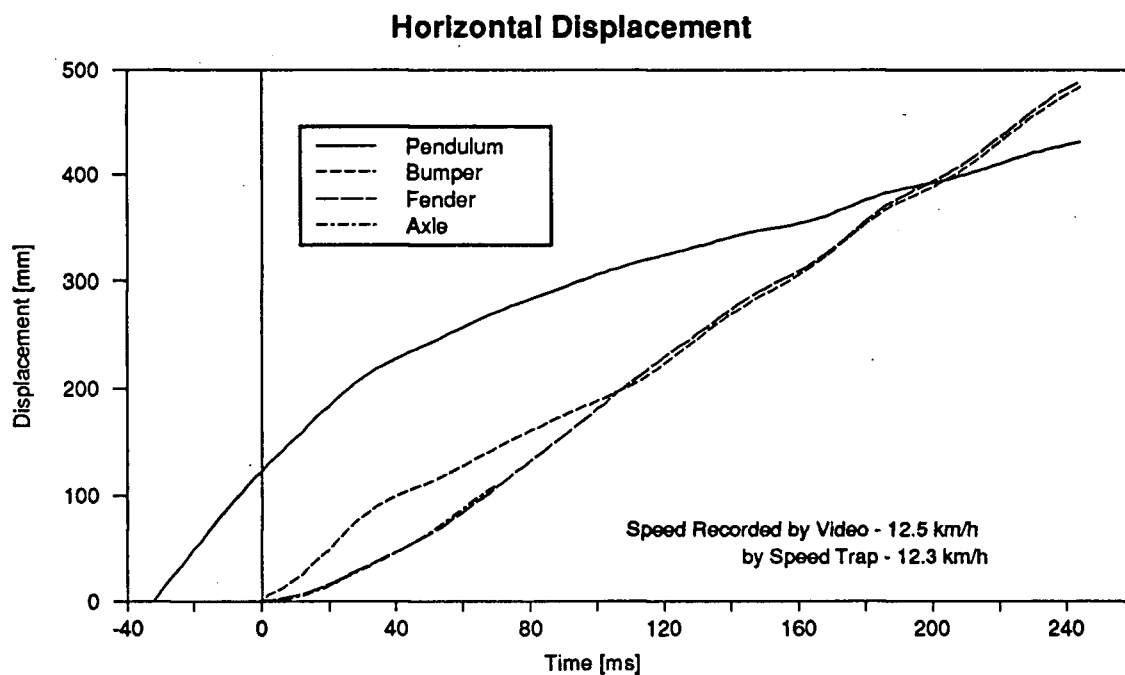


Figure 4.14: Bumper Response for a 12.3 km/h Impact

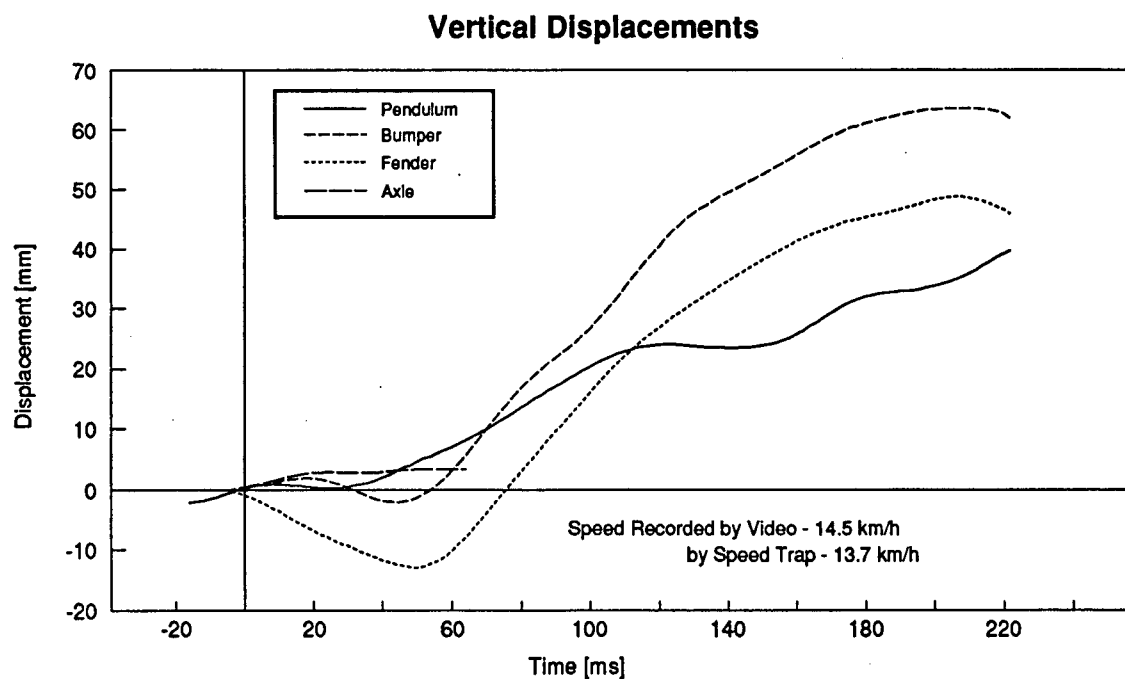
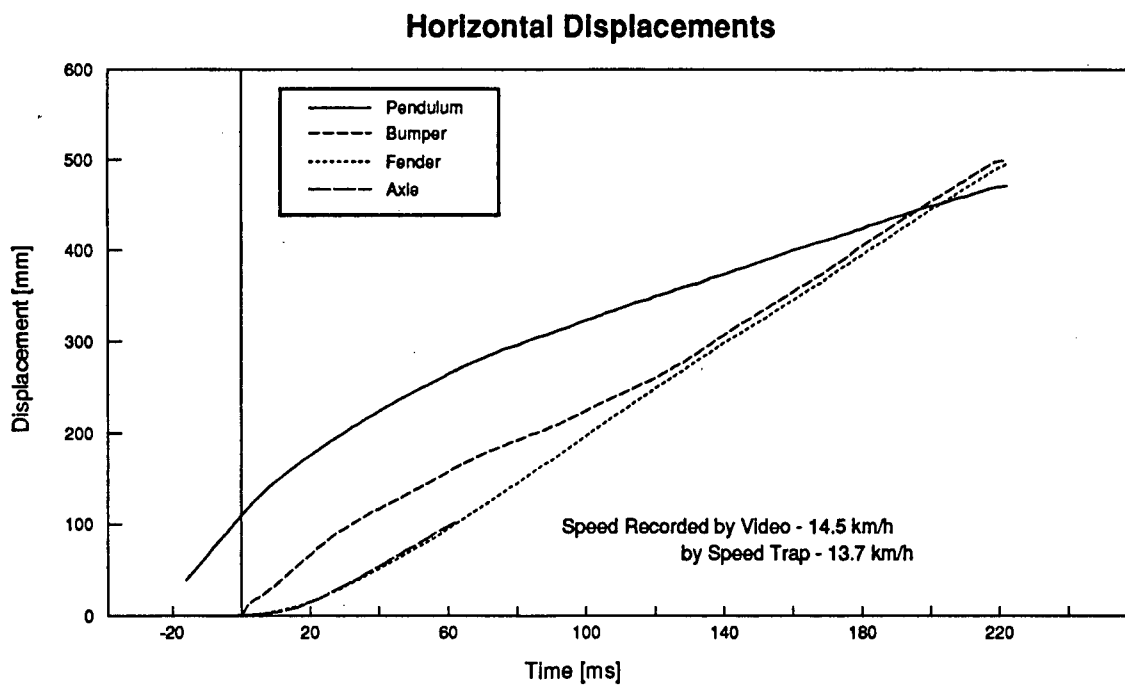


Figure 4.15: Bumper Response for a 13.7 km/h Impact

Table 4.2: Bumper Performance - Series II

Test	Impact Speed (Video) [km/h]	Impact Speed (Speed Trap) [km/h]	Input Energy [J]	Braking Energy [J]	Energy Dissipated within Vehicle [J]	Efficiency of Bumper [%]
1	*	8.2	*	*	*	*
2	9.5	8.2	3102	610	1667	46.5
3	9.6	10.1	2845	622	444	58.5
4	15.5	15.5	7372	858	3102	71.7
5	20.8	21.0	13507	1022	6270	81.7
6	*	8.2	*	*	*	*
7	9.5	10.1	2947	592	618	48.9
8	14.5	13.7	6744	732	2759	66.0
9	10.2	10.1	3600	535	1677	54.7
10	12.5	12.3	5210	598	2341	52.6
11	12.5	16.5	5210	598	2341	52.6
12	20.8	20.8	13117	687	6099	73.6
13	9.9	10.3	3090	403	525	7.4
14	12.2	12.4	4804	595	1748	51.8
15	15.7	15.1	7842	666	3381	47.0
16	10.9	10.9	3773	577	1642	52.1
17	14.2	13.7	6524	654	2897	55.9
18	10.9	11.5	4062	526	1878	59.3
19	13.2	13.7	5798	601	2591	51.4
20	13.2	13.6	5758	577	2052	56.4
21	15.5	15.7	7922	717	3889	63.0
22	14.0	14.1	6421	708	3162	55.6
23	11.6	12.7	4466	651	1718	68.1
24	14.3	14.7	6531	642	2364	56.9

* no video data

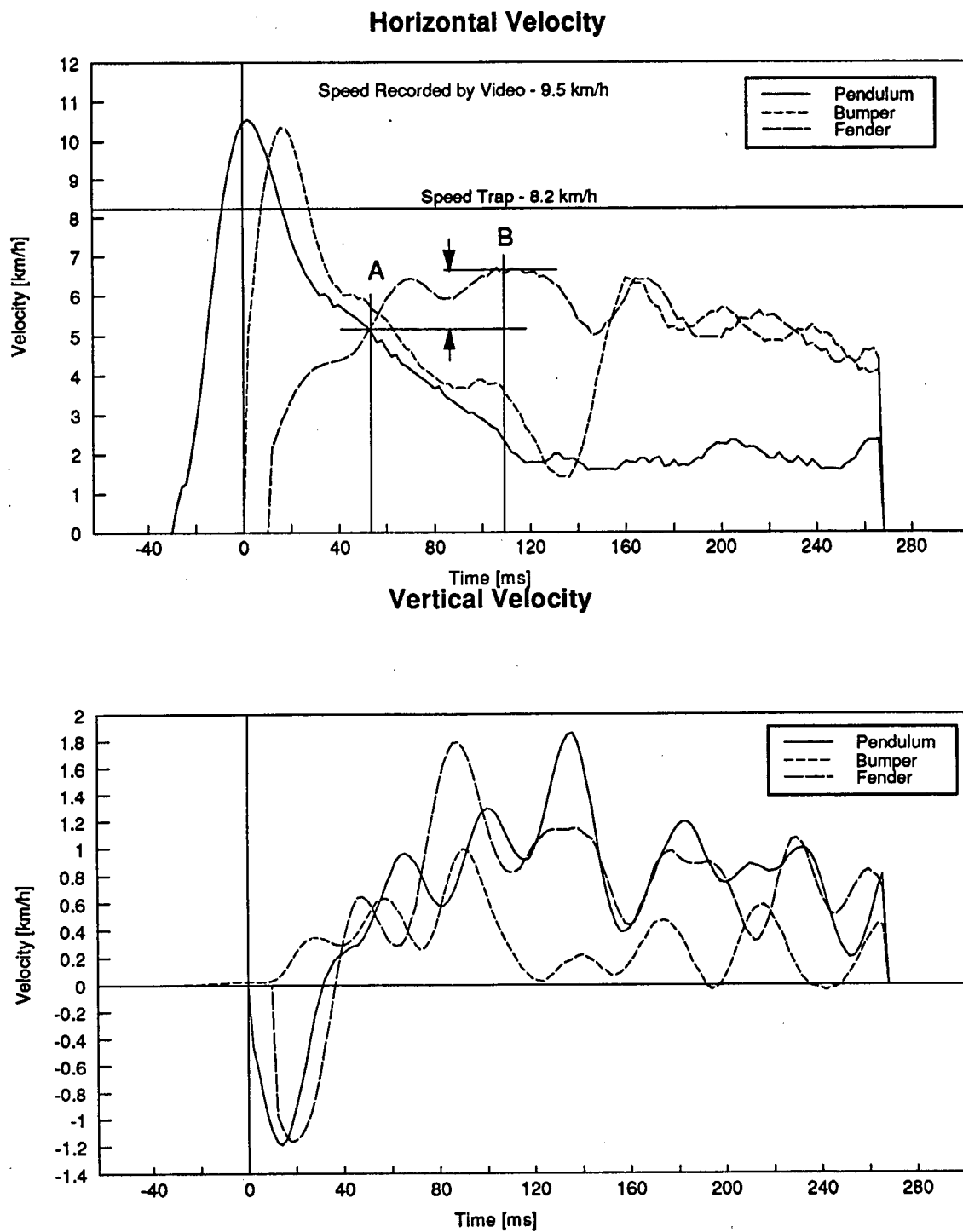
The velocity profiles of these same tests are shown in Figures 4.16-4.18. The initial overshoot of the filtering process due to the step input of the pendulum data is exhibited in the aberrant signal before impact. The dashed line indicates the speed recorded by the speed trap.

It can be seen that the bumper's horizontal velocity mimics the pendulum's (ignoring some of the processing noise in the results) until contact is lost. It is important to note in these figures that the vehicle continues to speed up after its velocity matches that of the pendulum. Point A in

Figure 4.16 denotes the point where the vehicle and pendulum have a common velocity, but the vehicle continues accelerating to the velocity marked by point B. This indicates that a significant amount of spring force is stored in the isolator since it pushes against the pendulum as the vehicle is pulling away. A review of the velocity profiles indicate that this spring force contributes an additional 3 or 4 km/h (representing approximately 320-570 J) to the vehicle and is independent of the impact speed. As the spring energy is only dependent on the spring constant and maximum deflection, this value would be expected to remain constant for all impact speeds which fully stroke the bumper.

The vehicle was found to attain speeds of 60 - 70% of the initial impact speed, quickly falling off due to braking forces. The velocity oscillations (particularly in the vertical motion data) as the vehicle slows down can be attributed to the small number of data points recorded and the degree of optical resolution. The pixels used to identify the markers represent about 1 cm in full size dimensions. This coarse resolution causes the data to take on a staircase appearance. This is further aggravated by the differentiation process, especially when the time interval is small (0.002 seconds in this case).

Finally, it is important to look at the accelerations exhibited by the vehicle and pendulum. For comparison, the data from the video records (Figures 4.19-4.21) and accelerometers (Figures 4.22-4.24) are presented for the previously discussed range of impacts. The video records exhibit a great deal of noise after performing two consecutive differentiations to calculate accelerations. Even with this noise, it is important to recognize that the peak values found in the video have a reasonable agreement with that of the accelerometers, providing reasonable validity for the data. The peak bumper mount accelerations of Figure 4.22-4.24 (accelerometer based) are identified in the video derived data for comparison. The fender marker used for the video processing has the same response as the accelerometer placed on the bumper isolator mount. The presence of acceleration levels before impact ($T = 0$) in Figure 4.20 is attributable to the



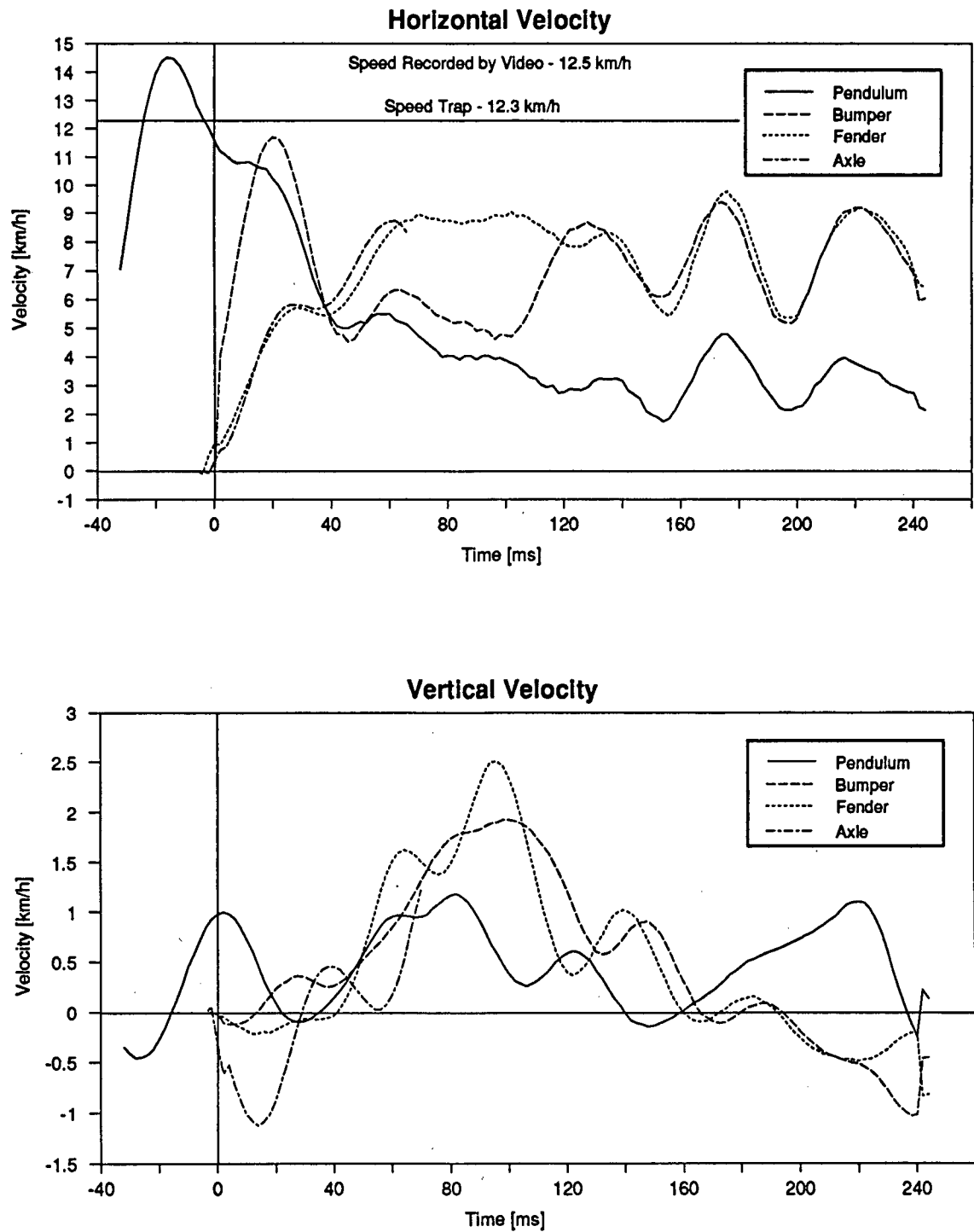


Figure 4.17: Vehicle and Pendulum Velocities for a 12.3 km/h Impact

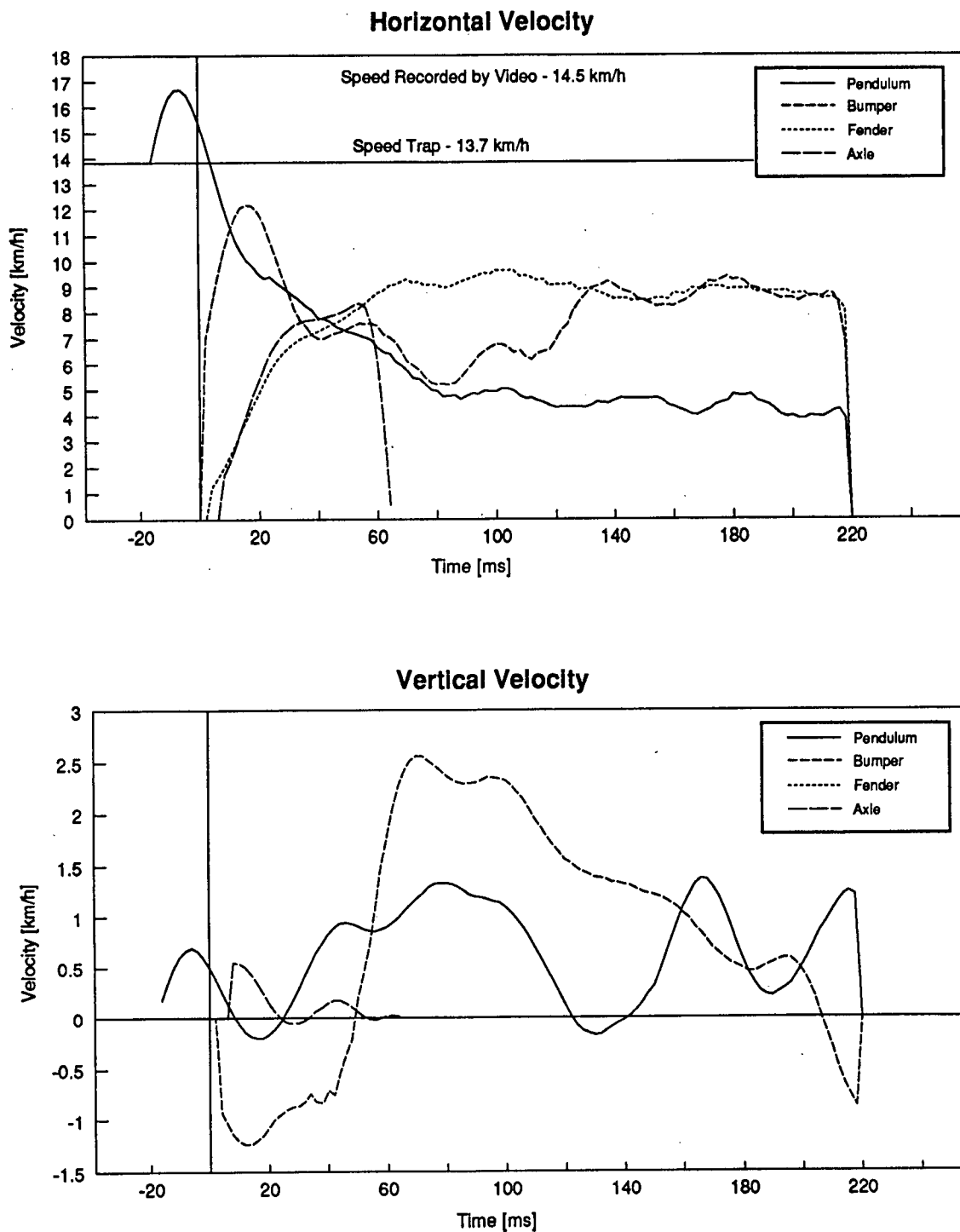


Figure 4.18: Vehicle and Pendulum Velocities for a 13.7 km/h Impact

signal noise. The impact time was selected using the displacement data. Noise present in this displacement data (prior to impact) was amplified during the differentiation process, producing the 'pre-impact' accelerations seen in Figure 4.20.

The acceleration pulse of the vehicle, recorded by the accelerometer, is typical of that shown in Figure 4.22. There is a smooth rise to the maximum value which occurs after the isolator has fully stroked. As the pulse drops to a zero value, there is a slight deviation. This variation arises from expansion of the bumper isolators pushing against the pendulum, also evidenced in the increase in vehicle velocity mentioned in the preceding discussion.

The accelerations of the vehicle frame at the bumper and seat mounts are also shown in Figures 4.23 - 4.24. The first point to note is that the pulse width is almost identical, starting and ending at the same time, for these two locations in the vehicle. This indicates that the frame is essentially responding as a rigid structure. The differences in magnitude represents some compression of the vehicle frame, but the short duration of these signals suggest that little time is available for deformation to take place. For impact speeds of 14 km/h and below, it was typical to find no damage to the vehicle frame, slight straightening of the bumper, and some localized deformation on the bumper around its attachment brackets. Thus, it can be inferred by these similar accelerations that the elastic deflections within the frame are minimal and a rigid frame is not an unreasonable approximation for low speed impact simulations. The timing of these acceleration pulses is also important. As seen in the Series I results, the occupant response lags the vehicle response by 50 ms. When the torso has come into full contact with the seatback, the vehicle velocity has peaked and has begun to drop, depending on the braking force. Thus, frame deflections are transparent to the occupant, only the level of energy absorbed has an influence on the passenger.

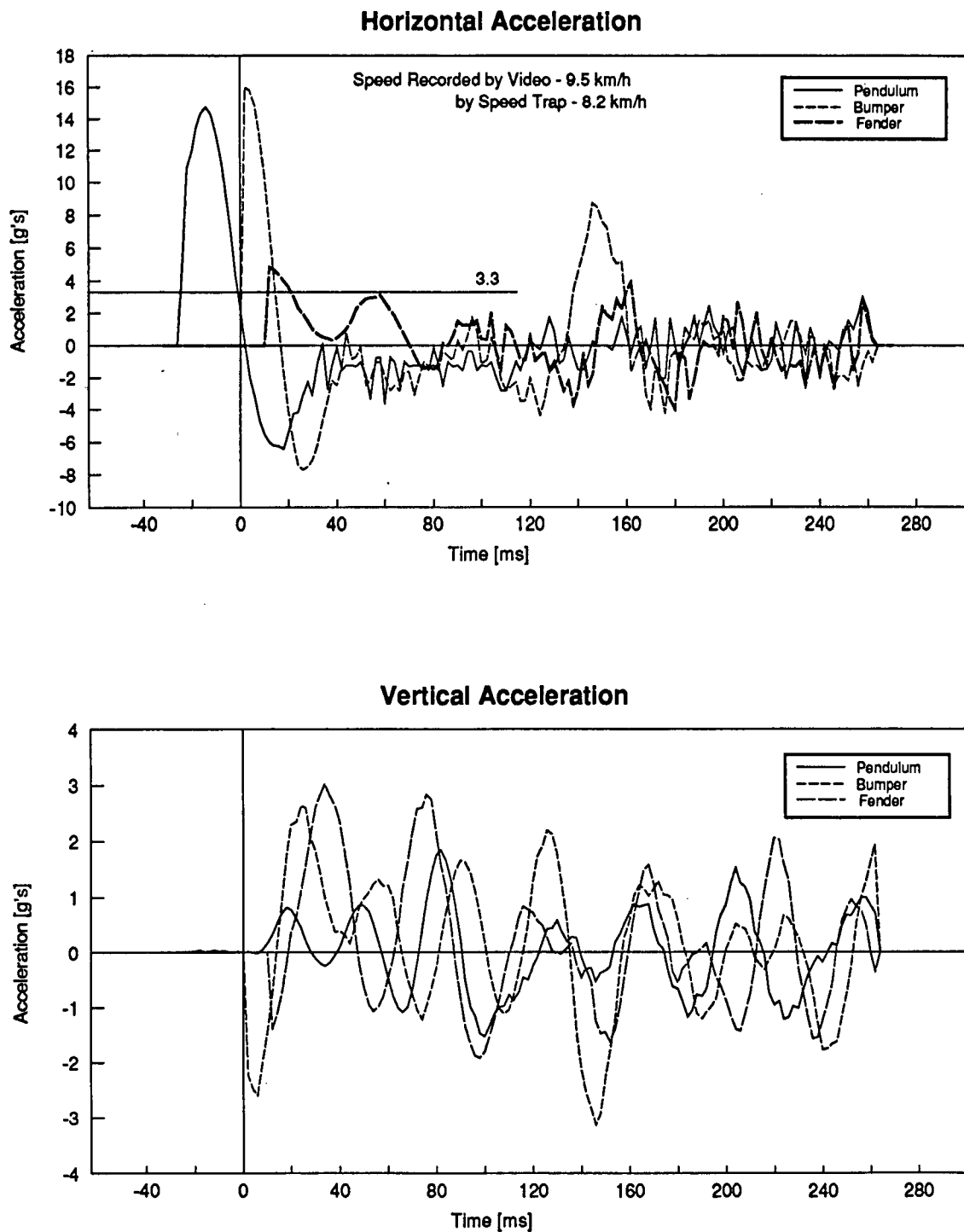


Figure 4.19: Accelerations of the Vehicle and Pendulum for an 8.2 km/h Impact

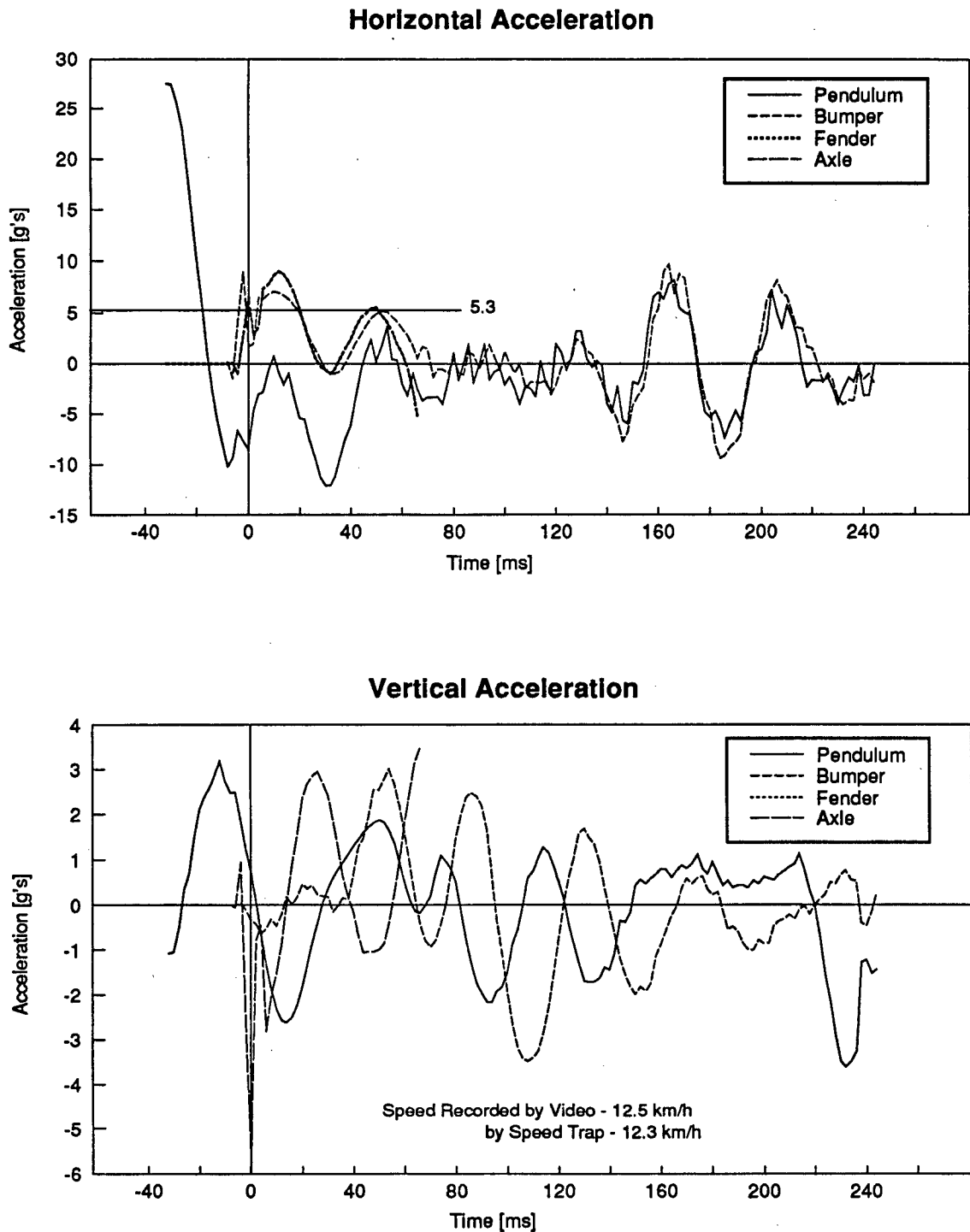


Figure 4.20: Accelerations of the Vehicle and Pendulum for a 12.3 km/h Impact

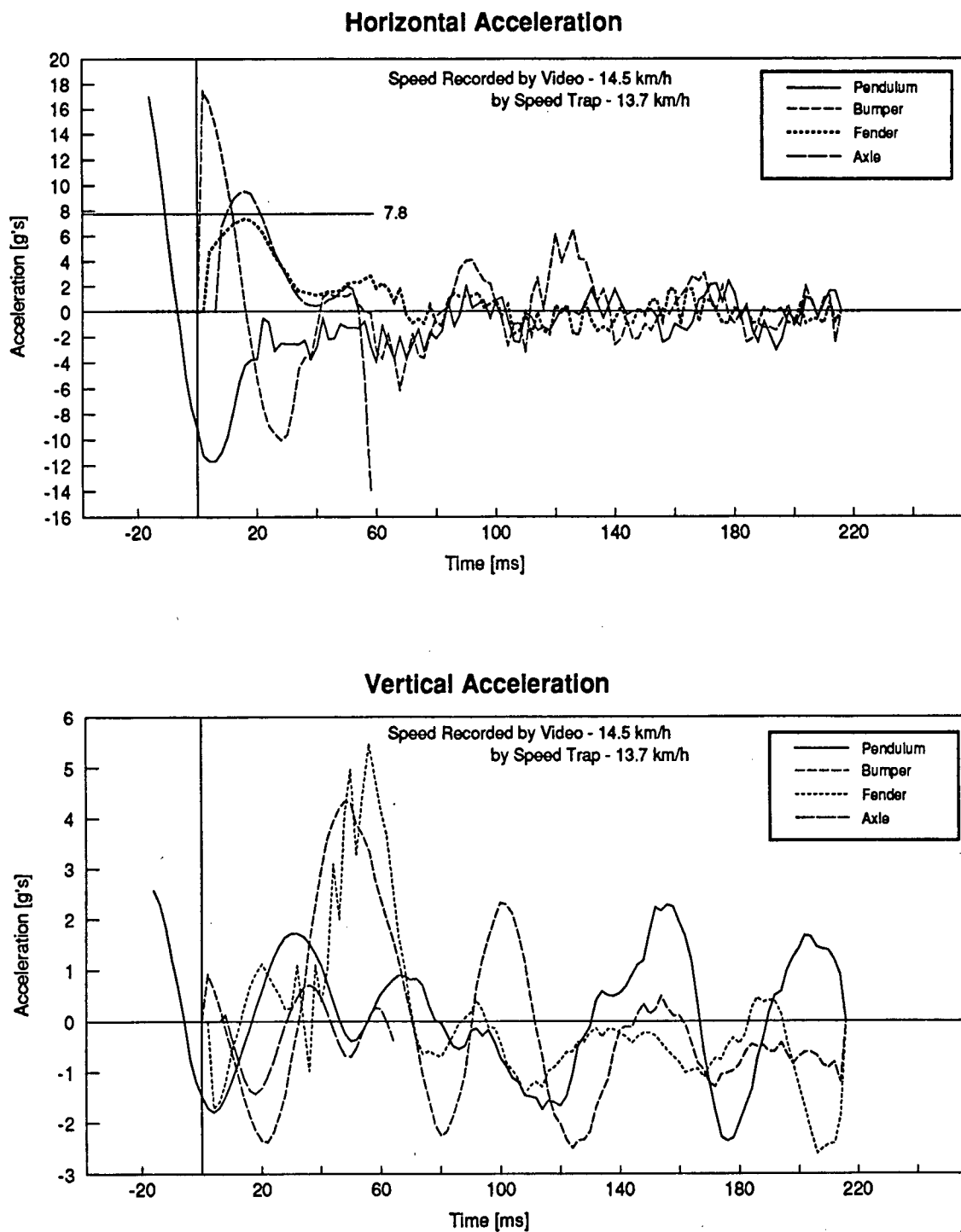


Figure 4.21: Accelerations of the Vehicle and Pendulum for a 13.7 km/h Impact

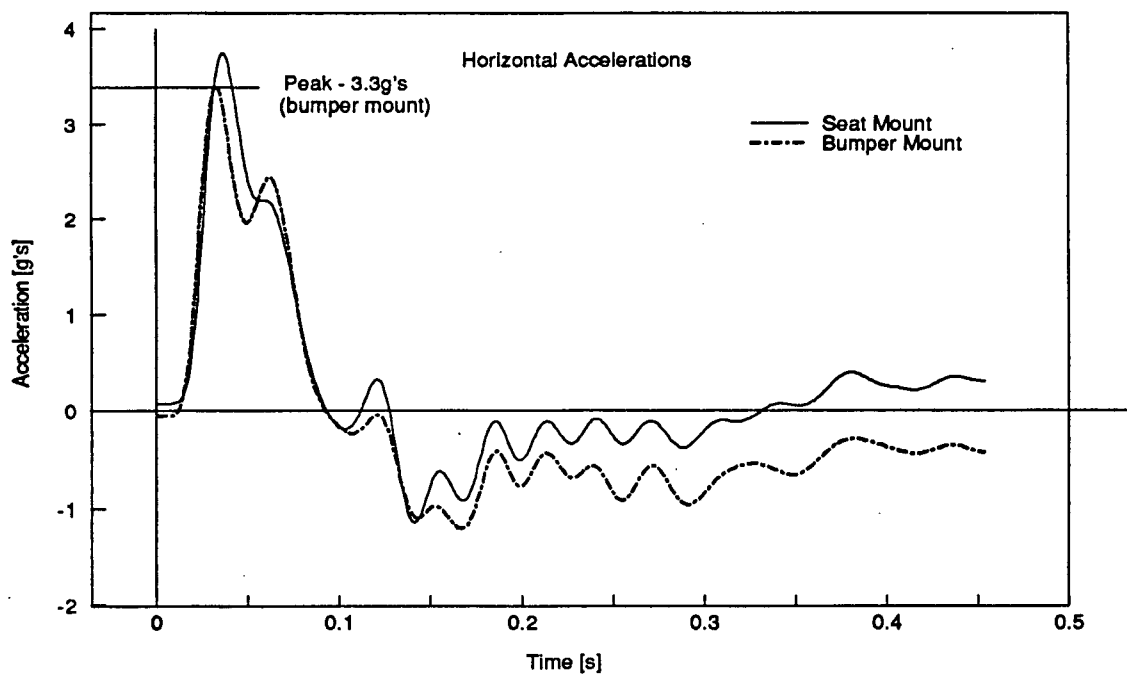


Figure 4.22: Accelerometer Results for an 8.2 km/h Impact

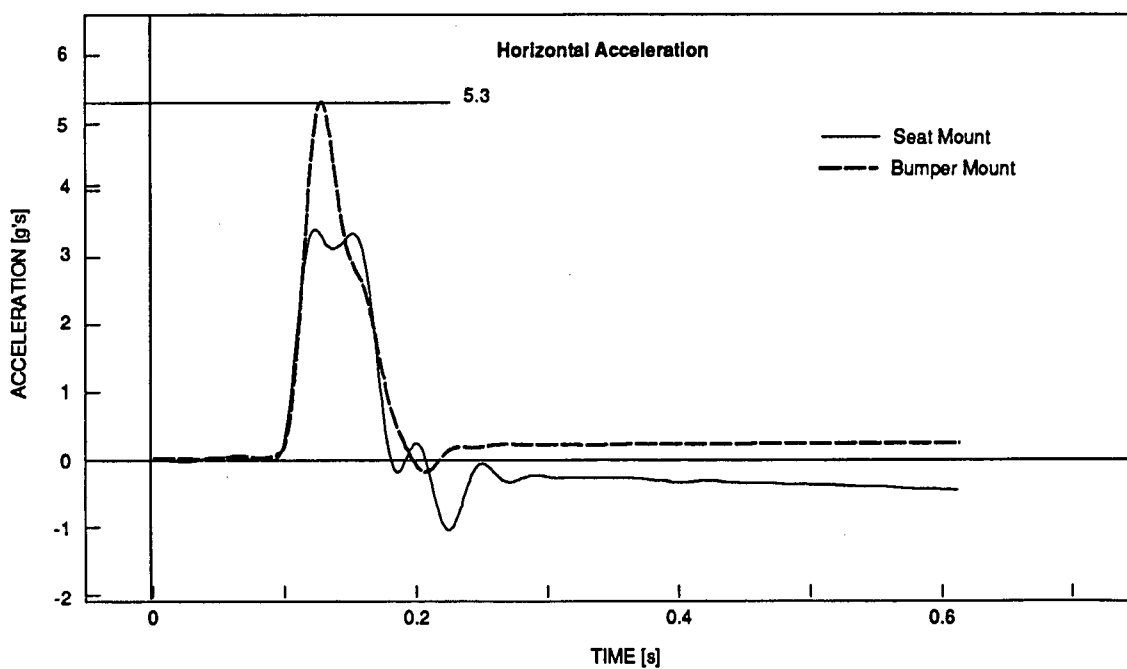


Figure 4.23: Accelerometer Results for a 12.3 km/h Impact

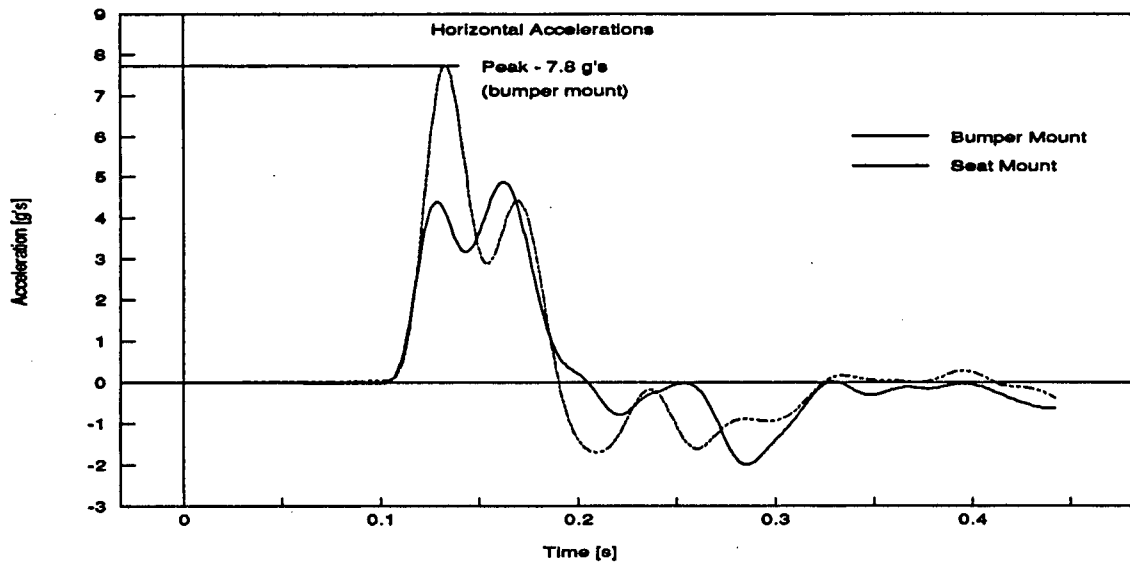


Figure 4.24: Accelerometer Results for a 13.7 km/h Impact

The vehicle's elastic behavior is also illustrated in Figure 4.25. The peak accelerations recorded at the seat in Series II are plotted against the impact speed. The trend (predicted by a linear regression), shows a direct relationship between the impact speed and vehicle loading to speeds around 15 km/h. This is the visual damage threshold (14-15 km/h) of the test vehicles for these tests.

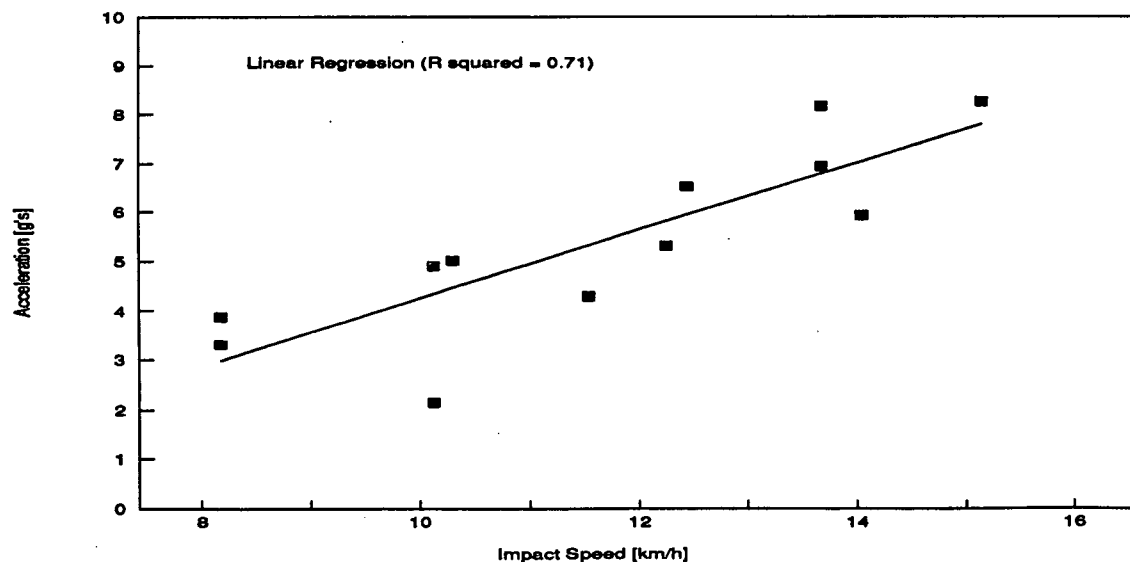


Figure 4.25: Influence of Impact Speed on Peak Seat Mount Accelerations

4.5 - SERIES II TESTING: OCCUPANT RESPONSE

The occupant kinematics reported here are only based on the accelerometer recordings of the Series II tests. Essentially, the trends exhibited in Series II testing support the observations reported in Series I. Differential rebound and resultant acceleration differences were observed in every test. For example, response of the occupant and vehicle experiencing a 13.7 km/h impact speed is shown in Figure 4.26. This behaviour was typical of the occupant kinematics recorded. The delay in occupant response is seen by comparing the shoulder and pendulum histories. The differential rebound of the head and shoulders off the seatback is seen by the different X peak acceleration times experienced. The rotation of the torso about the hips, along with rotations of the head, are evident in the different Y accelerations of the head and shoulder. The rotation of the head and neck about the shoulder produces a centripetal acceleration. This would be added to the shoulder's Y acceleration, yielding the higher value shown in Figure 4.26. The result of this loading is an axial tension on the neck which, when added to the differential X accelerations, exposes the occupant to relatively high dynamic loading during low speed impacts. The timing between the head and shoulder movements, coupled with the magnitude of the loading by both X and Y accelerations are the external injury mechanisms experienced by the occupant. The actual occurrence of a whiplash injury is a direct result of the occupant's physiological reaction to this loading mechanism and difficult to forecast.

Comparison of the occupant acceleration values in Figure 4.26 with the vehicle values in the same test (Figure 4.24) highlight the amplification of vehicle accelerations by the seat structure. In this particular test, the occupant experienced 80% higher peak values, and experienced these accelerations over a longer time span. The torso strike on the seat belt is displayed in speeds as low as 8 km/h as depicted in Figure 4.27. Review of both head and shoulder curves show that as the torso contacts the restraint system, it stops sharply. However, the head's momentum carries it past the torso creating the longer negative (directed towards the

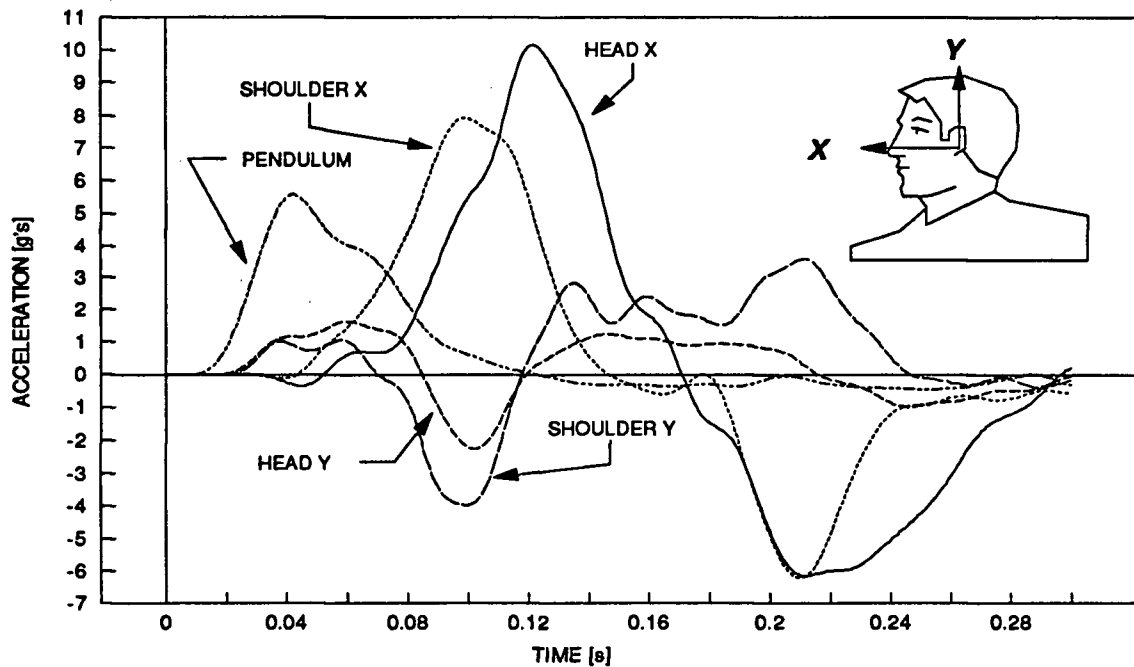


Figure 4.26: Occupant Response During a 13.7 km/h Impact

rear of the vehicle) acceleration pulse. This combination of acceleration and displacement loading experienced by the neck has not been clearly identified as non-injurious in previous research. This is especially disconcerting when the vehicle comes out of the same accident undamaged.

The general trend of peak occupant accelerations follows that of the vehicles, as illustrated in Figure 4.28. The shoulder's acceleration exhibits a linear relationship with impact speed up to 15 km/h. Similar behaviour is exhibited by the head, but at higher magnitudes. It is important to note the drop in the occupant response for the highest impact speed. This particular test involved a vehicle with a repaired rocker panel where body fill and welds were present under the driver's door. The one impact the vehicle was subjected to caused buckling within this rocker panel and the energy absorbed by this process resulted in a marked drop in occupant acceleration values. The effect of occupant posture on occupant loading for impact speeds up to 15 km/h is shown in Figure 4.29. Here the peak accelerations of the occupant tend to be higher in the cases where the

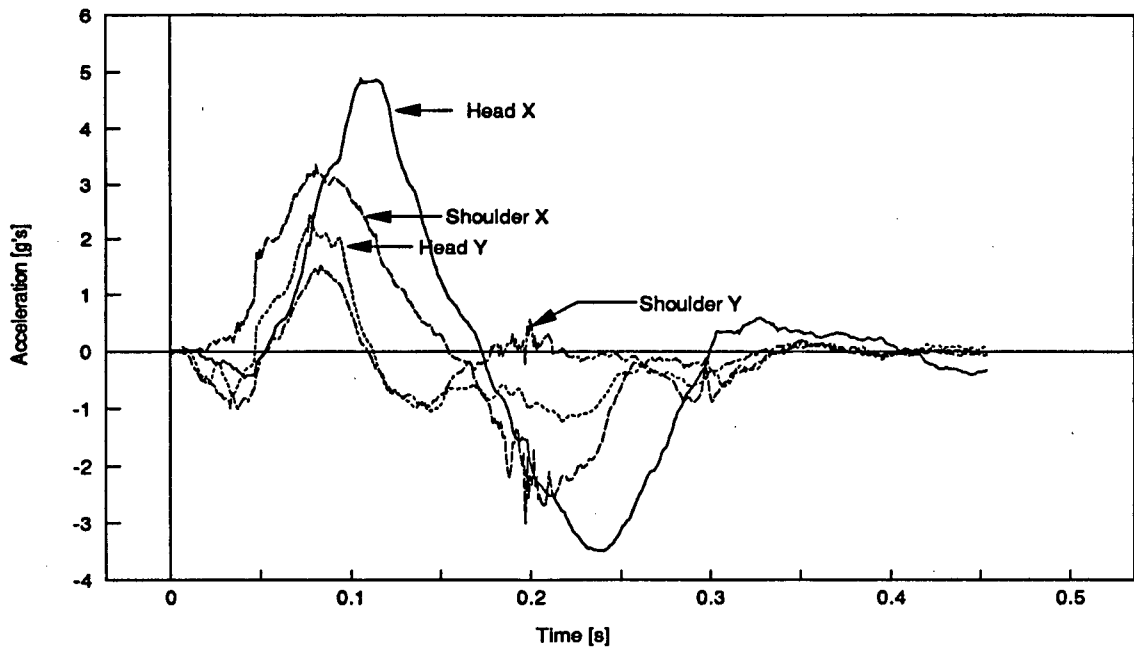


Figure 4.27: Occupant and Vehicle Response During an 8 km/h Impact

occupant is inclined forward, supporting the results of Series I tests. The inclined occupant response has a higher degree of variability due to the different amount of offset. It is difficult to reproduce the same offset distance test-to-test with anthropometric dummies.

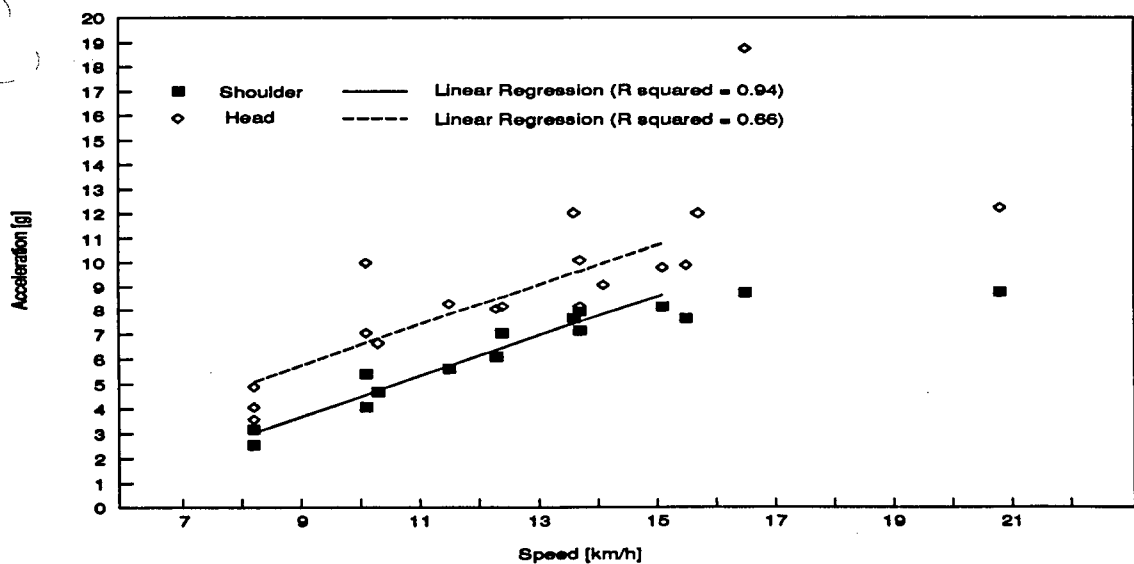


Figure 4.28: Influence of Impact Speed on Peak Occupant Accelerations

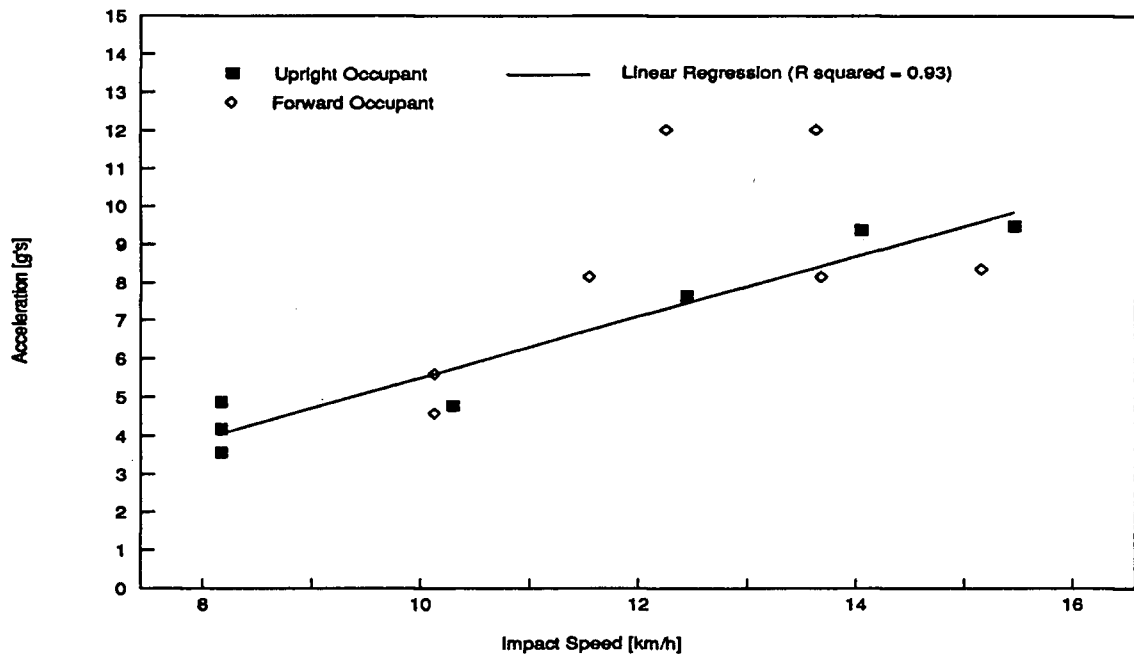


Figure 4.29: Influence of Initial Occupant Position on Shoulder Accelerations

4.6 - DISCUSSION (SERIES I AND II)

The results of both Series I and II testing show that the elastic response of both the vehicle frame, bumper, and seatback will expose the occupant to unnecessarily high dynamic loading during a rear impact. The differential accelerations between the head and torso could reach 8 g's during an impact below 15 km/h. As a first order analysis one can assume that 8 times the head's normal weight will act on the neck in shear. This appears to be a severe neck load but, as discussed in Chapter 2, there is no criteria to absolutely determine if this will or will not produce an injury. The elastic vehicle behaviour was shown to produce violent occupant motions for impact speeds as low as 8 km/h. Significant structural damage, however, began to develop for impact speeds between 14 and 15 km/h at which point repair costs were still estimated at less than \$500.

The occupant response is best summarized as a violent acceleration forward, catapulted by the seatback and quickly arrested by the seatbelt when thrown forward. The occupant's neck

undergoes combined dynamic loading as axial, torsional, and shearing accelerations (arising from differential head and shoulder rebounds) are encountered. The head and neck undergo extension and flexion motions, their severity is a function of seat loading and neuro-muscular activity (in human occupants). The occupant can also increase the level of dynamic loading by leaning forward relative to the seatback. The larger separation distance results in higher accelerations and associated deflections of the occupant. Support given by the head restraint prevents the head from rotating excessively over the top of the seat, however, a low head restraint offers little protection when the torso is allowed to slide up the seatback as witnessed in several tests. The video recording showed that a low headrest can begin to act as a fulcrum on the neck of average sized males.

Finally, the results from both test series show that current frame mounted seatbelt systems provide little protection from excessive movement during a rear impact. Since the occupant and seat deflect rearward, resulting slack in the seatbelt allows the torso to move freely during most of the impact sequence. The only protection offered by the seatbelt is to prevent an impact with the steering wheel or dashboard of the vehicle, violently snapping the passenger's head into flexion in the process. Fundamental changes in seatbelt systems are required before they can offer any protection for rear impacts.

Chapter 5 COMPUTER MODELLING OF THE VEHICLE

5.1 - INTRODUCTION

Section 1.3 outlined the three dynamic events that describe the rear impact accident:

- 1 The impact dynamics and energy transfer from the striking vehicle into the frame of the struck vehicle;
- 2 The mechanisms by which energy is transferred from the bumper, through the vehicle frame to the seat occupied by the passenger; and
- 3 The occupant interaction with the seatback / head restraint which leads to the injury.

The experimental data presented in the previous chapter addressed all of these areas, but even the large database presented previously does not fully describe the behaviour of the different vehicle systems. To better identify and document the vehicle performance, analytical modelling was also undertaken. This exercise increases the understanding of the event since the interacting components can be modified in a manner not conveniently accommodated in experimental studies.

Based on this initial simplified model, precise reproduction of the experimental results can not be expected, however, trends and the effects of altering various parameters can be expected. In this study, the initial stage of the model development is used to simplify the system to the point that a general description of the vehicle can be used to investigate vehicle rear impacts. Once the model is created, simulations are carried out to evaluate the model's effectiveness and verify the modelling approach. When this is accomplished, refinements to the analytical description can then be incorporated, achieving the desired model precision for available experimental data.

The three areas listed above are divided such that each can be studied in turn, independent of the other two. This feature was used to initiate modelling rear impacts starting with of the energy transfer from the striking vehicle into the struck vehicle. The purpose of this preliminary model was not to precisely reproduce the vehicle's response, but to develop a valid modelling approach that can be refined and expanded in subsequent projects. Once satisfactory vehicle simulations are accomplished, subsequent modelling projects on the second and third areas could be appended, allowing the entire impact event to be defined analytically.

The advantages of analytical modelling are obvious when the resources required to experimentally obtain data are considered. A model provides an efficient method to assess the relative significance of vehicle and impact parameter variations. The results of the full scale testing are still required to verify the capabilities of the developed model. However, changes in the structural stiffness, braking effects and bumper stroke (to name a few) can be tested and closely monitored under more controlled conditions.

The computational requirements for an analytical model of this complexity are substantial. It is obvious that non-linear systems like shock absorbers and bumper isolators require iterative solution techniques. To accommodate the necessary calculations, computer modelling software using the Finite Element Method (FEM) was used as the tool to conduct these impact simulations.

5.2 - VEHICLE MODEL CONSTRUCTION

The current modelling approach is based on observations from the full scale tests. With very little vehicle damage taking place, vehicle response during a low speed impact ($V_{imp} < 15$ km/h) is dominated by the compliance of the bumper and suspension, treating the vehicle frame as a rigid body. The proposed model is shown schematically in Figure 5.1 where springs and dashpots represent the flexible components. Based on the fact that the vehicle frame stiffness is

significantly large when compared to the more compliant components mentioned above, a worst case model can be created. Here a rigid vehicle frame directly translates impact energy at the bumper isolator mount to the seat support. A model of this simplicity can be used to evaluate the elastic effects of the bumper and suspension, without the complication of the frame deflections.

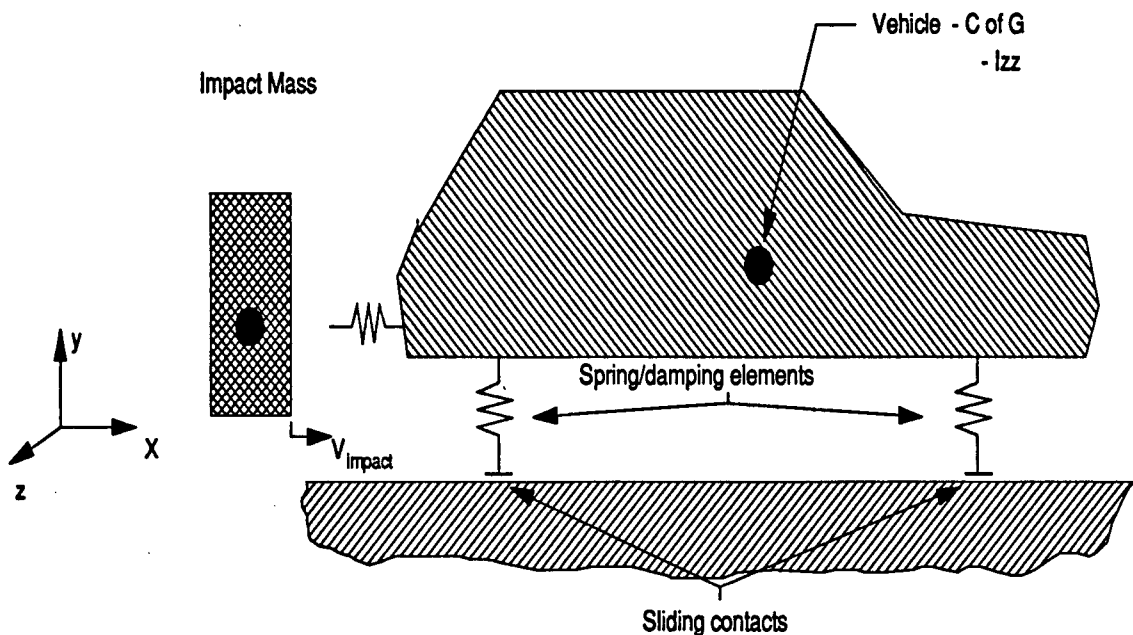


Figure 5.1 - Proposed Model of the Vehicle

Geometrical description of the Volkswagen Rabbit's structure was tedious but not difficult. Reference drawings from repair handbooks [80] (Appendix D) provided measurements used by body repairmen when straightening automotive frames. Physically measuring the vehicle also provided necessary geometry not documented in the repair manuals.

The frame is modelled by beam elements shown in Figure 5.2 that were geometrically arranged to mimic the structural members incorporated into the unibody construction technique. It is important to recognize that the same basic structural designs are employed by all the vehicle manufacturers. Box sections are used to carry most of the load and are generally distributed as

depicted in Figure 5.2. The lower frame members duplicate Volkswagen's construction of the Rabbit, however, the upper frame members have been modified to maintain the Rabbit's mass distribution both longitudinally and vertically.

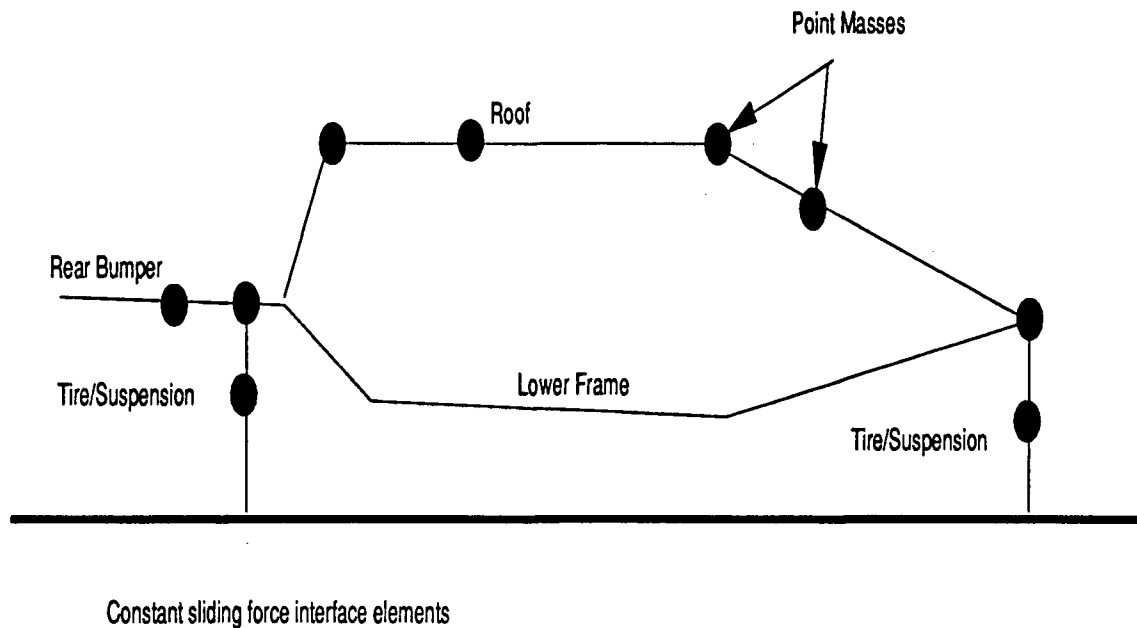


Figure 5.2 - Finite Element Model of the Vehicle

The model was simplified by incorporating the mass of the structures forward of the front wheels into the engine mass. Due to the rigid frame conditions involved, and their distance from the rear bumper, they have no influence on the vehicle's response aside from their mass.

The required mass distribution was determined by weighing various sections of the vehicles obtained from a vehicle wrecking yard. The mass properties of Volkswagen Rabbits were also reported by [81] as test vehicles in their research, listing the total mass and pitch moment of inertia for these cars. Based on this information, the weight was placed in nine lumped masses distributed throughout the model. The resulting model weighed 908 kg, with the center of gravity placed at 1.01 m behind the front axle and 0.53 m above the ground surface.

The published values are 0.92 and 0.52 m, respectively. The mass moment of inertia about the Z axis is reported at about 1000 Nm² compared to the resulting pitching moment of inertia in the model of 940 Nm².

The suspension was modelled using spring-dampers to model the spring and shock above the axle, as well as the tire's spring rate below the axle. The nodes corresponding to spring/frame attachment, axle, and tire/road contact have coupled horizontal degrees of freedom which cause these nodes to move horizontally together as the vehicle moves, but leaves them free to deflect vertically. Wheel contact with the ground was never broken during the test, so representative nodes were restricted to motion in the horizontal direction only.

Deformation characteristics of the shock system, presented in Appendix D, were determined from components removed from a vehicle provided by I.C.B.C.. The spring rates were determined from simple static testing carried out in the Department of Mechanical Engineering. Shock absorbers were tested using incremental loading and monitoring the resulting time/displacement with a linear displacement transducer. A static analysis subjecting the model to the influence of gravity was carried out to determine the stored spring energy when the vehicle is at rest. This initial suspension pre-load, caused by the dead weight of the vehicle, was incorporated into the suspension definition.

The locked wheels in the test vehicles were free to slide on the test floor surface. To replicate these friction effects, drag tests were utilized to determine the coefficient of friction on this surface and values of $\mu_{static} = 0.36$ and $\mu_{dynamic} = 0.32$ were obtained for the floor surface in front of the pendulum. For comparison, these friction values represent approximately 45% of the vehicle's maximum braking capability on an average asphalt road surface ($\mu = 0.71[82]$).

As mentioned in Chapter 4, Volkswagen kindly supplied information on the bumper isolators. Plots of their impact tests and a shop drawing of the component were provided and used to determine the performance characteristics of the isolators. Appendix D describes the parametric definition of the isolator performance employed in the model.

5.3 - IMPLEMENTATION OF THE MODEL

A model is, by definition, the representation of an original physical system in a different medium. The computer software "ANSYS" * was used to implement the modelling parameters described in the preceding section. ANSYS is a finite element modelling (FEM) package that provides the user several predefined element definitions for beams, springs, and other mechanical structures. In this software, a preprocessor is used to define the system geometry, boundary conditions, loading, and material properties of the model. Several analysis options are provided to conduct static, dynamic, and thermal simulations, with or without non-linear modelling options. An extensive post-processor also allows the simulation results to be printed or plotted.

The analysis was conducted using the non-linear transient analysis option which provides iterative solution techniques for the solution of the non-linear components making up the model. A general listing of the ANSYS commands are provided in Appendix B. The general model geometry and mass characteristics were conveniently defined with the available software options, but the direct implementation of some components were not possible and are outlined below.

Movement of the axles relative to the frame was not exactly duplicated. Both the front and rear suspensions pivot on bushings, which causes the wheels to move through an arc, relative to

*ANSYS is a product of Swanson Analysis Systems Inc.

the vehicle structure. However, because the suspension travel is not excessive during the tests (about 6 cm vertically, Figure 4.14) approximation of the suspension system as a vertical spring was not unreasonable.

The retarding forces developed at the tire/ground interface were defined by an element which could duplicate a constant sliding force. Unfortunately, this element definition would not model the initial load developed by static friction. Static friction only occurs in the first milliseconds of impact, and has little influence on the resulting bumper contact forces since the wheels begins to slide before the bumper is fully stroked.

Difficulties were encountered in the translation of the bumper isolator deflection characteristics. As seen in Appendix D, the isolators have a non-linear, non-conservative loading curve. The changing stiffness of the isolators could not be exactly input into the model definition and the approximated force/displacement curve (Figure D.5) was the only possible input allowed in the FEM software. The preload built into the bumper isolator by the manufacturer was simulated as a constant force acting within the isolator.

The last discrepancy between the model and the physical system concerns the pendulum loading. Because of the pendulum's arc, vertical loads on the bumper were introduced. Unfortunately the element definitions available did not allow for this vertical component to be modelled, so only one dimensional loading was explored. To simulate the pendulum, a mass was connected to a linear spring. This spring could be compressed, out of contact with the vehicle, and then released. The original compression would define an impact speed at which the mass would strike the vehicle. With this representation, impact energy was modelled with the equivalent spring constant for a pendulum. If one equates the natural frequency of a pendulum:

$$\omega_n = \sqrt{\frac{g}{l}}$$

with the natural frequency of a spring:

$$\omega_n = \sqrt{\frac{K}{m}}$$

one can write the equivalent spring constant as:

$$K_{eq} = \frac{gm}{l}$$

For the pendulum in the Series II experiments, $m = 929$ kg and $l = 3.3$ m, resulting in an equivalent spring constant of 2761.7 N/m. To recreate a given impact speed, energy methods can be applied to determine spring deflection and an initial restraining force on the pendulum.

$$KE_{impact} = PE_{spring}$$

$$\frac{mass_{pend} v_{impact}^2}{2} = \frac{K_{eq} x^2}{2}$$

From this, initial deflection and thus the original restraining force on the pendulum spring was obtained.

5.4 - SIMULATION CONDITIONS

The current model was used to study the influence of several vehicle and impact parameters on the vehicle response. Of all the variables, the three most important, bumper stiffness, braking forces, and impact energy, were varied in the simulations. The impact conditions modelled reflected those studied in Series II testing. A 929 kg mass represented the pendulum moving at four different impact speeds: 8, 10, 12, and 15 km/h. These speeds were chosen to depict the range of impact speeds which produced no permanent crushing of the vehicle structure. The braking conditions were chosen to duplicate the sliding conditions recorded in the experiments, as well as the case of a free rolling vehicle. This provides two extreme braking situations bounding the documented test conditions with the worst case, a free

rolling vehicle. The last independent variable, bumper stiffness, was varied to represent four conditions: predicted response based on the information provided by Volkswagen, spring stiffness values one half of the predicted values, spring stiffness twice the predicted values, and a rigid bumper link to the vehicle. The use of specification bumper stiffness was employed to verify the model against experimental results, while the one half and two times factory spring stiffness were employed to observe how sensitive vehicle motion was to variations in bumper stiffness. Rigid bumpers were simulated for impact speeds up to 12 km/h to provide the upper bound of bumper stiffness. The 15 km/h impact speed was not simulated with a rigid bumper since frame deformations were beginning to be reported in the empirical data.

Table 5.1: Bumper Stiffness Simulations

Impact Speed	Bumper Stiffness (Braking Vehicle)	Bumper Stiffness (No Vehicle Braking)
8	Rigid	Rigid
8	Half Original	Half Original
8	Twice Original	Twice Original
8	Predicted Original	Predicted Original
10	Rigid	Rigid
10	Half Original	Half Original
10	Twice Original	Twice Original
10	Predicted Original	Predicted Original
12	Rigid	Rigid
12	Half Original	Half Original
12	Twice Original	Twice Original
12	Predicted Original	Predicted Original
15	Half Original	Half Original
15	Twice Original	Twice Original
15	Predicted Original	Predicted Original

To test all the combinations presented by the variations listed above, the simulations listed in Table 5.1 were carried out using the F.E.M. model. The impact simulation time of 1.5 seconds was broken into 3 blocks. The first 85 ms represented the pendulum mass accelerating to speed and only required a limited number of iterations. Just prior to impact, the time step was

changed so that 1000 iterations accommodated the time interval of 0.85 to 1.0 s when the pendulum and vehicle remain in contact. The remainder of the simulation was covered by 1000 iterations as the vehicle moves after pendulum-bumper separation.

5.5 - SIMULATION RESULTS

Comparing the standard bumper to the simulated stroke (Figure 5.3), it can be seen that the model exhibits stiffer spring characteristics. Maximum forces reported by Volkswagen for an 8 km/h impact speed are around 85000N total (both isolators) while those simulated exceeded 98000N. This discrepancy in performance is almost completely due to the oversimplification of the bumper response as a force - deflection curve, removing any time dependent behaviour of the bumper. Damping in the bumper is absent in this representation and is apparent in the high velocity changes by the vehicle reported in Table 5.1. Assuming a perfectly elastic impact, the maximum impact speed for the vehicle is defined by the momentum equation:

$$\sum m_i V_i = \sum m_i V'_i$$

assuming the pendulum stops on impact, the vehicle's post impact speed is thus:

$$V'_{car} = \frac{m_{pend}}{m_{car}} V_{impact} = \frac{929}{910} V_{impact} = 1.02 V_{impact}$$

The values in Table 5.2 suggest that little energy is dissipated as greater than 80% of the impact velocity is achieved by the vehicle. The experimental results indicate a vehicle speed that is 60-70% of the impact speed should be expected. The simplification of the frame does not account for the isolator mounting bolt shift during impact. However, this could not be responsible for the large discrepancies in energy dissipation between the model and those determined experimentally. A review of the errors is presented in Section 5.6.

The horizontal displacements of the vehicle motion in Figure 5.3 indicate that the model does maintain the general kinematic trends recorded in the experiments. The vertical

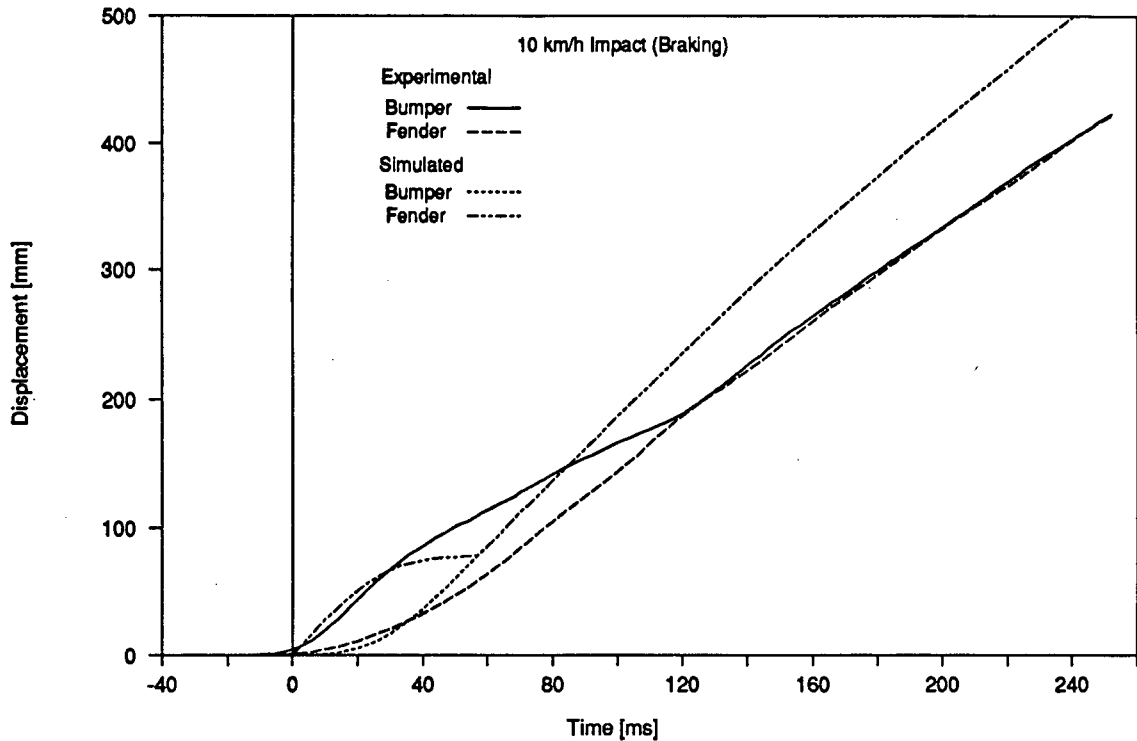


Figure 5.3: Comparison of Experimental and Numerical Response

displacements that occur during simulated impact of the vehicle are shown in Figure 5.4. Here the initial downward motion of the rear vehicle structure is verified by the test results, although the simulation still exhibits a faster response. This suggests the modelling approach has some validity since the general kinematics are duplicated. Refinements to the bumper stiffness will improve the discrepancies in the energy transfer processes and provide more representative simulations.

Figures 5.5 and 5.6 depict the velocity and acceleration trends of 8 and 15 km/h impacts. Compared to the experimental data, peak velocities in the simulations are about 12% higher at 8 km/h, and 42% higher at 15 km/h while corresponding accelerations in this range were 42% and 200% higher, respectively.

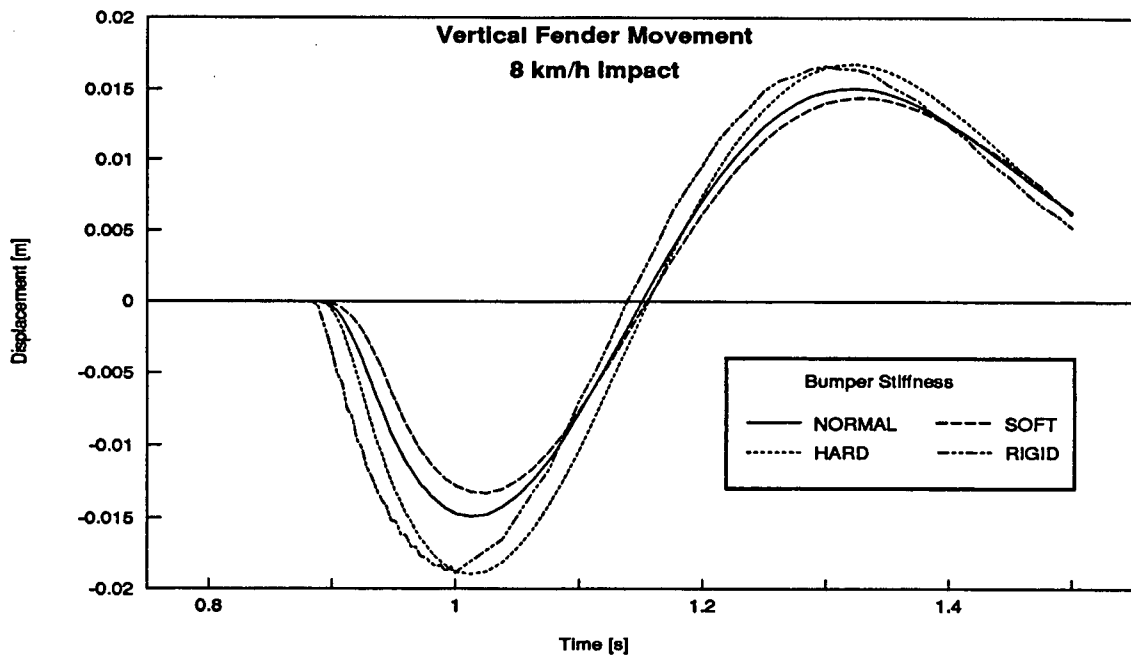


Figure 5.4: Vertical Displacements of the Vehicle

Table 5.2: Performance of Computer Modelled Bumper

	Speed [km/h]	Braking Vehicle		Rolling Vehicle	
		Velocity [km/h]	Acceleration [g]	Velocity [km/h]	Acceleration [g]
Reported Bumper Stiffness	8	6.4	5.1	6.7	5.4
	10	9.3	8.2	9.7	8.3
	12	11.7	10.3	12.1	10.4
	15	14.9	24.2	14.9	17.2
Half Bumper Stiffness	8	5.9	4.2	6.3	4.3
	10	8.8	8.2	9.2	8.3
	12	11.3	15.9	11.6	15.8
	15	14.9	24.2	14.4	21.9
Twice Bumper Stiffness	8	7.8	8.9	8.1	9.1
	10	9.9	11.2	10.1	11.4
	12	11.9	13.9	12.1	14.1
	15	14.9	24.2	15.2	19.8
Rigid Bumper	8	7.9	15.0	8.1	15.2
	10	10.2	19.3	10.3	19.6
	12	12.2	24.2	12.5	24.4

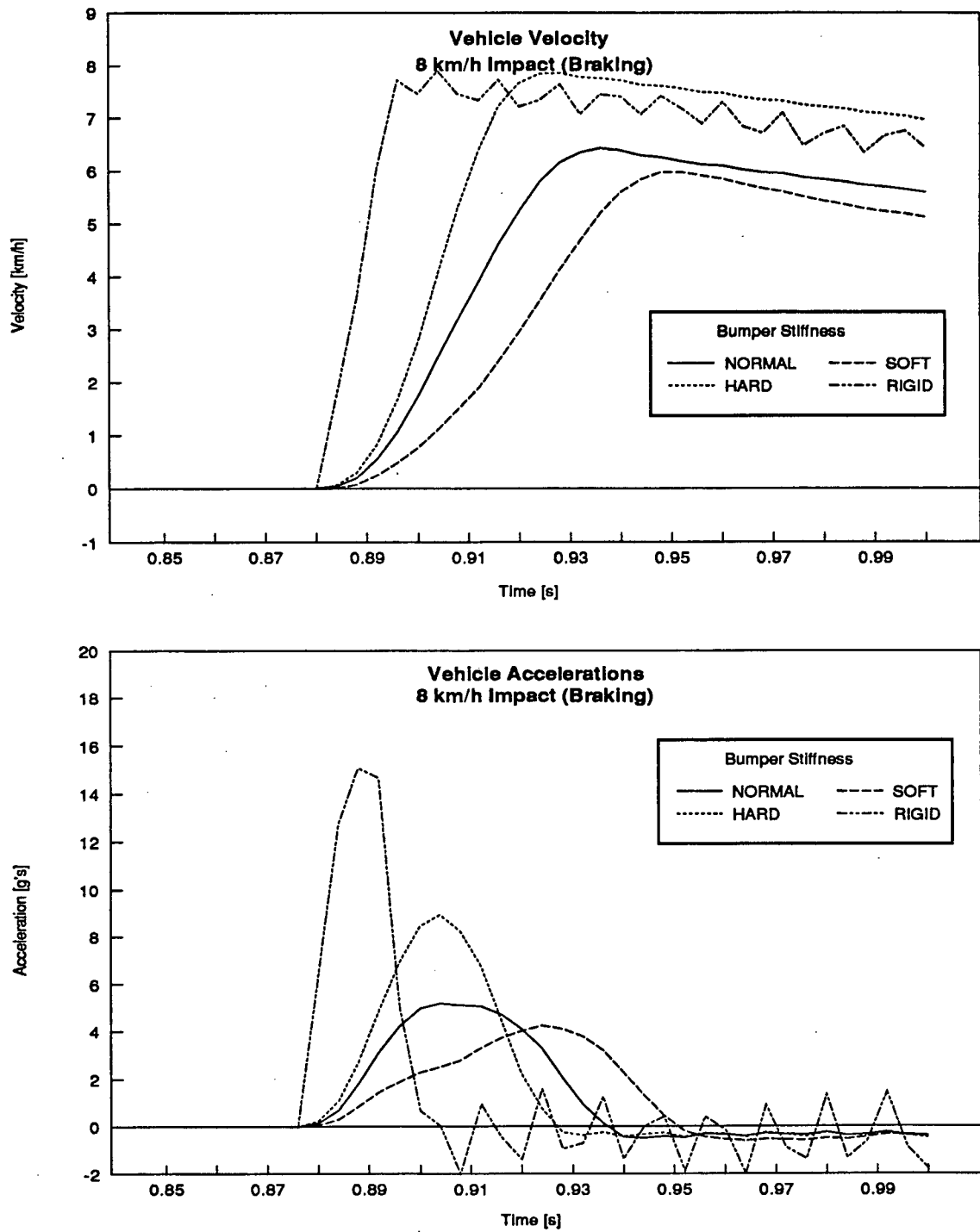


Figure 5.5: Simulated Dynamics of a Vehicle Struck at 8 km/h

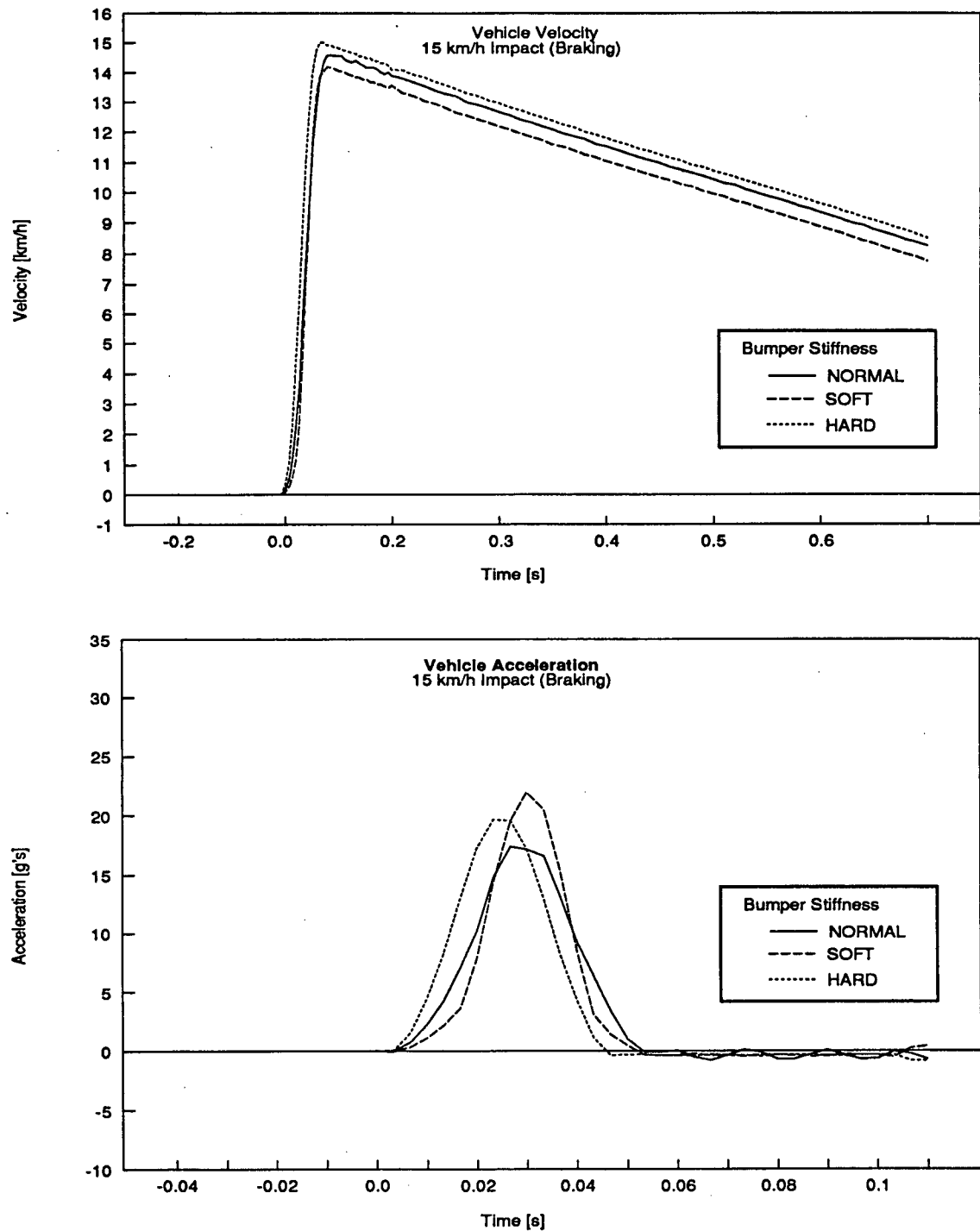


Figure 5.6: Simulated Dynamics of a Vehicle Struck at 15 km/h

Both velocity and acceleration have different roles in the occupant's response. The peak velocity occurs at the time the occupant begins loading the seatback, essentially representing a second impact as the moving seatback strikes the slowly moving torso. However, variations in the stiffness had little influence on this value as seen in Figure 5.5 and 5.6. For example, the peak velocities ranged between 6 and 8 km/h for the bumper stiffnesses simulated, while the accelerations varied between 4.5 and 15.5 g's for the same stiffness variations. Using the simulated response of the original bumper as a reference, this corresponds to a 30% variation in peak velocity, compared to a 190% variation in acceleration. The tendency of acceleration to be more sensitive to stiffness is consistent at higher speeds, although the amount of variance decreases. For a 15 km/h impact, the corresponding range in results drop to 7% for velocity and 29% in acceleration values. As expected, increases in stiffness increased the amplitude, but decreased acceleration pulse width of the vehicle during the impact. The role of vehicle accelerations on the occupant are minor compared to the velocity since the occupant is not appreciably loaded by the compliant vehicle seat during the initial acceleration pulse. The occupant slides in the seat, not fully experiencing the impact until the torso develops significant reaction forces with the seat. At this time the vehicle has reached its maximum speed and is no longer being accelerated by the striking surface.

Of interest is the influence of braking on the vehicle response. Figures 5.7 and 5.8 show the velocity/acceleration history without braking forces. As expected, comparison with Figures 5.5 and 5.6 reveals post impact speeds reach a higher value and remain constant in free rolling conditions but decrease in the presence of a retarding force. The accelerations, however, show the impact pulse into the vehicle is identical in these two situations. This may be due to the small retarding force (2700 N) that develops under braking when compared to the large impact loads generated (98 kN).

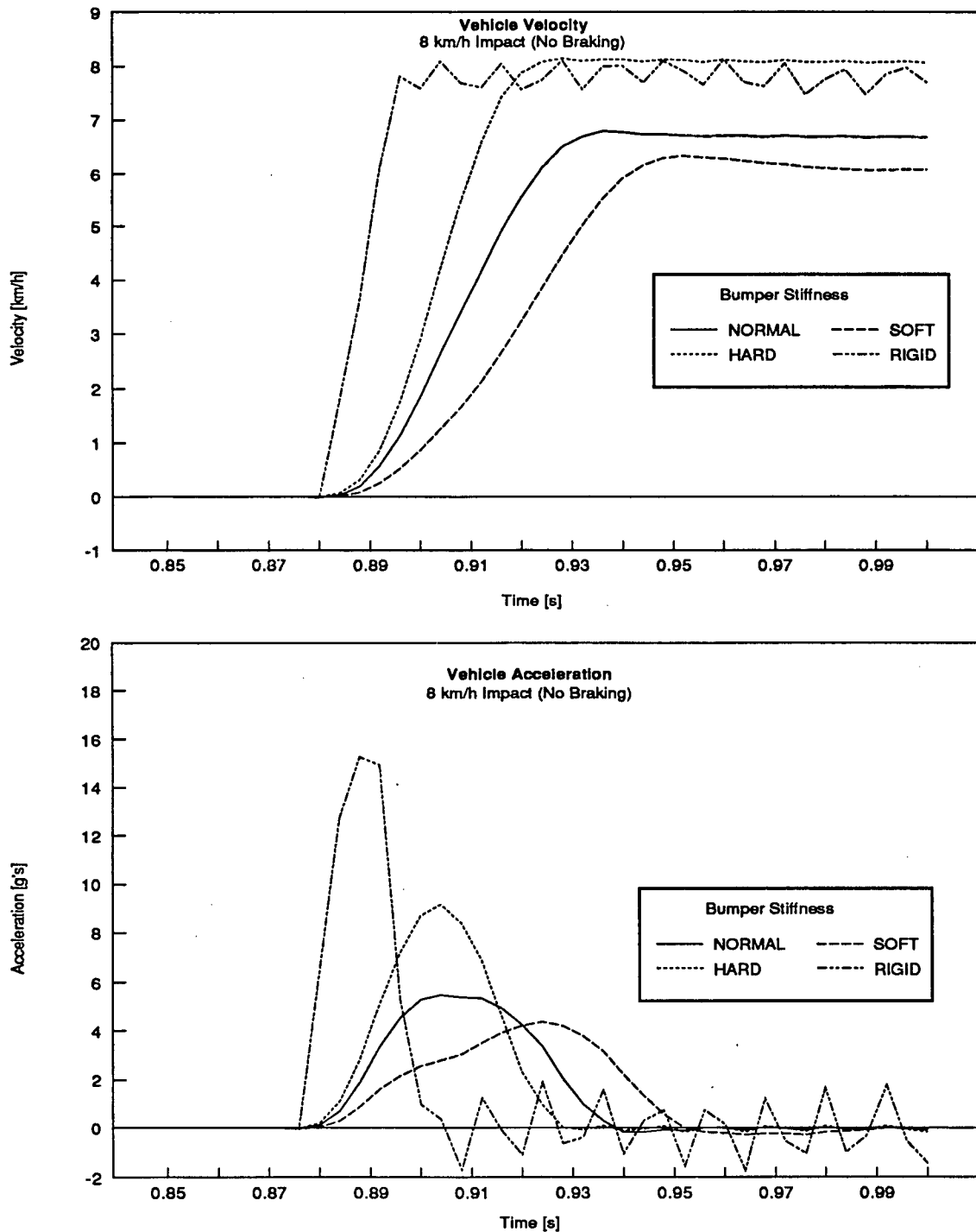


Figure 5.7: Simulated Dynamics of a Free Rolling Vehicle Struck at 8 km/h

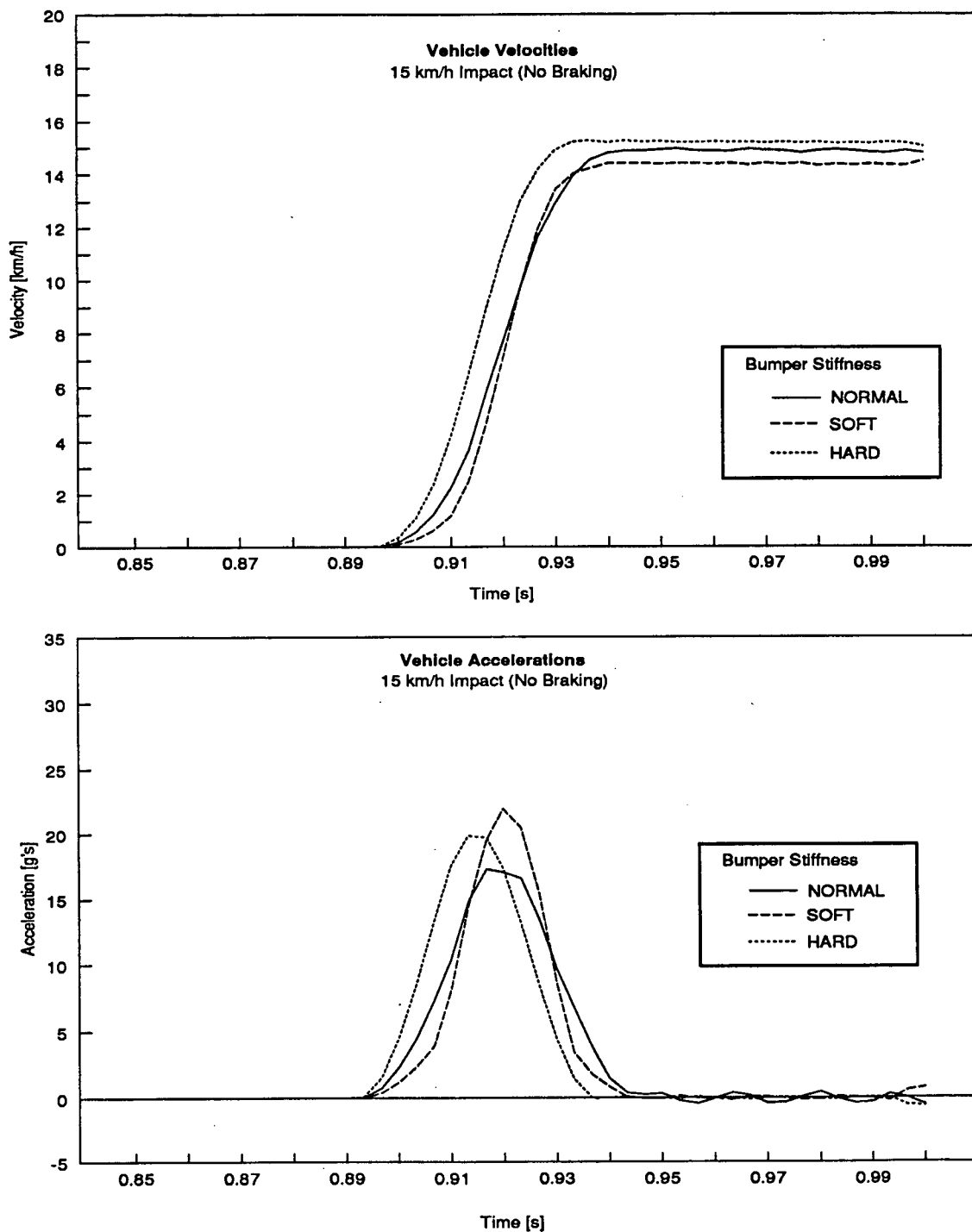


Figure 5.8: Simulated Dynamics of a Free Rolling Vehicle Struck at 15 km/h

5.6 - ERROR ANALYSIS

The response of this model has been shown to be stiffer than the experimental data presented. This error is largely due to the bumper definition employed in the simulations.

The first problem encountered in the bumper definition was the inability to provide a representative spring and damping description of the bumper. It was beyond the resources of this project to analytically define these bumper characteristics. In addition, the modelling options provided by the software also restricted the use of variable damping and stiffness properties. To expedite the modelling program, simple stiffness / displacement criteria (described in Appendix D) were developed. Energy dissipation within the bumper was to be reproduced in the hysteresis of the loading curve.

Two problems were identified with this approach. Without damping, there was no rate sensitive response in the system. As a result, the bumper deflected too rapidly. This is evident in the comparison of experimental and simulated results of Figure 5.3. This rapid response was also a problem in the numerical solution of the simulation. There were 1000 computational iterations defined for the critical 150 milliseconds during impact. Except for the rigid bumper case, this resulted in at least 200 iterations during the bumper stroke. This may not have been enough to allow the simulation to accurately follow the defined bumper response.

The problems produced by insufficient data are highlighted in the results of Table 5.3. Because of available computing resources, only 5% of the calculated values could be stored and used for analysis of bumper contact. As a result, no more than 15 data points were available for review of the total bumper response. This can also be seen in Figures 5.5-5.8 where each available data point is displayed. A review of the data produced the following observation. Integration of the preload in the isolator with the bumper's displacement should result in a value of zero since the bumper's net stroke is also zero. However, this was not the case. In low speed,

Table 5.3: Calculated Energies During Impact

	Impact Speed [km/h]	Energy Change in Pendulum [J]	Energy Change in Vehicle [J]	Braking Energy [J]	Energy Dissipated in Bumper [J]	Efficiency in Dissipating Impact Energy[%]
<u>BRAKING</u>						
Normal	8	2220	1451	373	396	17.8%
Bumper	10	3577	3100	320	156	4.3%
Stiffness	12	5153	4870	243	39	0.7%
	15	8051	7454	239	357	4.4%
Half	8	2206	1253	301	651	29.5%
Bumper	10	3578	2757	266	555	15.5%
Stiffness	12	5149	4532	236	380	7.4%
	15	8038	7054	264	719	9.0%
Twice	8	2248	2173	127	-52	-2.4%
Bumper	10	3574	3445	210	-81	-2.3%
Stiffness	12	5152	4997	158	-2	-0.1%
	15	8053	7903	179	-29	-0.4%
Rigid	8	2279	2196	22	60	2.7%
Bumper	10	3572	3684	39	-150	-4.2%
	12	5138	5250	39	-152	-3.0%
<u>ROLLING</u>						
Normal	8	2205	1616	0	589	26.7%
Bumper	10	3571	3366	0	204	5.7%
Stiffness	12	5153	5191	0	-38	-0.8%
	15	8047	7859	0	188	2.4%
Half	8	2174	1407	0	766	35.3%
Bumper	10	3578	2993	0	584	16.3%
Stiffness	12	5144	4784	0	359	7.0%
	15	8030	7349	0	681	8.5%
Twice	8	2247	2329	0	-81	-3.6%
Bumper	10	3574	3630	0	-55	-1.6%
Stiffness	12	5151	5216	0	-65	-1.3%
	15	8052	8153	0	-100	-1.3%
Rigid	8	2279	2313	0	-34	-1.5%
Bumper	10	3572	3754	0	-181	-5.1%
	12	5137	5560	0	-423	-8.2%

low bumper stiffness situations - cases where several data points were available - this integral was close to zero. When the impact speed increased and the data was limited, the preload force was found to produce non-zero work values. Thus, the total energy calculations reported in Table 5.3 are too low. It should be noted again that these values are derived from 5% of the

simulation output. These values are expected to be higher if the entire simulation data set could be employed, although these values would still underestimate the energy dissipation of the bumper.

5.7 - DISCUSSION OF MODELLING PROGRAM

This modelling attempt provided a first, exploratory step towards modelling vehicle impacts. ANSYS proved to be too restrictive when modelling highly non-linear, time dependent spring characteristics and two dimensional impact loading. Better results are likely possible with a more flexible mechanical modelling software package or by generating new simulation programs. Limitations of this initial model and the inability to easily incorporate the necessary modifications within the time frame of this project curtailed modelling efforts.

The results from this numerical representation of a collision illustrates the difficulties of modelling complex dynamic events. In general, the model was much stiffer, responding faster and more violently than the vehicles tested. This stiff behaviour can be attributed to the material property definition for the bumper stiffness. The restriction to force - deformation information precluded the damping (thus time dependent) effects present in the bumper resulting in faster and stiffer bumper response. It is also evident from the low amounts of dissipated energy during the simulations (Table 5.2) that the non-conservative bumper characteristics were under-estimated by the analysis.

The material definitions studied in this model show that the bumper stiffness variations studied had little influence on vehicle velocity, but acceleration pulses were markedly affected. Also observed was the minimal influence of braking on the peak vehicle and acceleration values.

Compared to the kinetic energy in the pendulum before impact, the frictional dissipation is less than 17% for an 8 km/h impact. This supports Emori's [11] experimental results which suggest peak acceleration values are not significantly affected in the presence of braking.

One other conclusion that may be drawn from the simulation work is that changes in the bumper's stiffness had little influence on the overall response of the vehicle. These results suggest that improvements in bumper design require alterations to the entire system (such as length of isolator stroke and amount of elastic recovery) to significantly improve bumper performance.

Chapter 6 CONCLUSIONS AND RECOMMENDATIONS

The goal of this research was to develop a coordinated program to investigate whiplash injuries arising from low speed rear impacts. After breaking the problem into the three areas of study: 1) energy transfer between striking vehicles 2) energy transfer through the vehicle to seat, and 3) occupant interaction with the seat; an experimental program was developed to address the first two areas and provide some preliminary information on the third. A numerical modelling approach was then applied to help understand vehicle impact dynamics.

The review of previous literature demonstrated that there are weaknesses in the current understanding of the whiplash injuries. In particular, there are deficiencies in current whiplash documentation, especially in the low speed (below 20 km/h) impact regime. How can an injury arise from a low speed accident? What are the requirements for a neck injury? Can we determine if whiplash occurred from the evidence resulting from an accident? These and similar questions are being asked more often by doctors, lawyers, engineers, and insurance representatives. This research program has provided some of the information necessary to begin answering these questions.

The main objective of the program was to develop and conduct a concentrated research program on low speed rear impacts. A facility was developed, instrumentation was designed and collected, and a test program was arranged to record information on this accident type. In addition, numerical simulation work was attempted to supplement this information. As a result, information on over 50 rear impact tests and 30 computer simulations has been compiled. From this work, the following conclusions were found:

Vehicle Impact Response

- The severity of impact required to begin structural damage to the tested vehicle (Volkswagen Rabbit) is equivalent to a 14-15 km/h impact with a moving, rigid barrier.
- The vehicle's bumper system typically absorbs 50% of the impact energy transferred to the bumper for impact speeds below 15 km/h. However, if the bumper's elastic recovery is not controlled, it continues to load the vehicle even when the vehicle has begun to move faster than the striking object.

The reviewed literature did not reveal any documentation of the full scale response of modern vehicles to low speed - rear impacts. No previous testing has documented the dynamics and accompanying damage produced in vehicles impacted at speeds between 8 and 20 km/h. The quantification of bumper response has not been undertaken by individuals other than the manufacturer. Information obtained in this project provides a database required by accident reconstructionists to correlate post-impact evidence with collision severity. In addition, this data can be applied to evaluate current legislation regarding bumpers and seatbacks in the vehicle safety standards.

Occupant Impact Response

- The motions encountered by an anthropomorphic dummy corresponding to these impacts exhibited speeds and accelerations higher than those of the car. In addition, the occupant's head and neck move relative to each other, increasing the loading on the neck and the potential for injury.
- Frame deformations for the impact speed range studied occurred before the occupant was able to begin responding to the impact. Typically, the occupant did not experience any significant loading until the vehicle accelerations had subsided.
- Occupant surrogate positioning prior to impact significantly increases the dynamic loading on the occupant and will likely increase the potential for injury. As the occupant increases their offset from the seat prior to impact, the severity of their response is increased.

It is apparent from Chapter 2 that correlation of the occupant response with collision severity has not been addressed in the current literature. Previous research has utilized sled-test equipment, numeric models, or has been conducted at speeds predominantly above 30 km/h. Sled testing and numerical modelling have typically employed modified seats that are stiffer than production equipment or do not have a head restraint. Full scale test information for impact speeds below 20 km/h is restricted to altered or outdated vehicle designs.

The present program has quantified occupant response for low speed - rear impacts of known severity. The vehicle response and damage can thus be compared to this data, providing a means to estimate the occupant's injury potential during an impact as well as evaluate the safety equipment of the vehicle. Differential rebound of the occupant's head and torso off the seat back and increased impact loading when the passenger's initial posture is inclined forward of the seatback were both observed in this project. These trends have been previously documented but for atypical vehicle configurations and have not been extensively described.

Safety Equipment

- The highly elastic performance of the seatback amplifies the acceleration levels of the vehicle to those experienced by the occupant.
- The adjustable head restraint does not provide proper protection when improperly positioned for the occupant. Occupant ramping up the seatback allowed the occupant's head to rotate over top of the seat.
- Seatbelts attached to the frame of the car did not spool up the slack developed as the occupant and seat deflected rearwards. This leaves the occupant free to rebound off the seat until the slack is taken up by their forward motion. The subsequent arrest of torso motion causes the occupant's head to experience a flexing motion which may also influence the injury potential.

As mentioned in the occupant dynamics discussion, the information obtained in this program describes the undesirable effects of elastic seatbacks. Previous researchers have observed these response characteristics, but none have isolated and quantified them. Also, the data previously available did not address impact speeds below 20 km/h and was obtained using modified vehicle structures. The program undertaken at U.B.C. has obtained data for unaltered Volkswagen Rabbits exposed to 8-20 km/h impact speeds. This information can be correlated to collision severity, a feature that is necessary to evaluate the safety equipment in regards to expected service conditions.

Vehicle Impact Modelling

- A rigid model of the vehicle frame, with spring/dashpot representation of the suspension was a reasonable approximation for simulating impact speeds below 15 km/h. However, numerical model of the vehicle will require a modelling system that can accommodate the highly nonlinear - time dependent behaviour of the bumper to accurately represent the energy transfer to the occupant's seating location.

The exploratory model developed in this program exposed several obstacles that must be overcome when simulating vehicle impacts. Although the described model produced more violent vehicle dynamics than experimentally observed, useful information was obtained that verified the approach. The model confirmed test results of Emori and Horiguchi [11] showing peak accelerations are not significantly influenced by braking forces. The general kinematics of the vehicle were also reproduced, although at different magnitudes.

The empirical and analytical information obtained in this project highlights several areas of vehicle design that should be modified to offer improved occupant protection during rear impact type accidents. These results have been used to suggest vehicle design improvements presented in the following section.

6.1 - OCCUPANT SAFETY IMPROVEMENTS

The findings of this study highlight two areas of vehicle design that have a strong influence on the occupant's response. The level of energy attenuation within the vehicle, as well as the elastic response of the seat are issues that are not being addressed by the manufacturer, government, or automotive insurer. It is apparent from this study that effective occupant protection during rear impacts has not been fully explored. Several vehicle design changes could be incorporated individually, or in different combinations, to supplement those currently available.

Starting with the rear of the car, an effective bumper design should have a no damage - sacrificial damage threshold. Here, conventional bumpers could provide protection during low impact speeds (below 5 km/h for example) without introducing damage to the vehicle. For speeds where injury becomes a possibility, a sacrificial mounting system could then be developed to encourage the energy dissipation process through plastic deformation. Designed properly, this system could provide cheap but effective protection.

A re-assessment of current seat and belt restraint systems should be investigated. The most significant observation in this study has to be the violent rebound of the occupant as they interact with the seat. As the vehicle component directly loading the occupant, the seat is the most sensitive to design changes, and thus, the most direct means of improving protection. Better control of the occupant rebound should be possible even with present energy levels introduced through the bumper.

The current belt safety system should be re-evaluated for rear impacts. Seatbelts should be integrated with the seat structure so that seat deflections will not introduce slack between the occupant and the belt. Seatbelt pre-tensioners, now used to improve frontal impact protection, could also be incorporated into the restraint system. Having the retractor spool up extra webbing

and then lock the belt upon impact would restrict the passenger from bouncing off the seatback. In addition, proper lap belt placement should be able to restrict the amount of vertical ramping of the occupant. Careful contouring of the seatback cushions could also be used to minimize vertical occupant movements.

The seatback regulations of the government (CMVSS 202) should be reviewed in regards to its present effectiveness. The dynamic testing option should be modified and incorporated as a requirement. Integral head restraints should be mandatory, and of sufficient height to protect the 95 percentile population under dynamic conditions. Also, placement of the head restraint should be as close to the head as possible, eliminating head offsets which aggravate rebound effects.

Structural stiffness of the seat should be increased to offer high speed protection and controlling occupant rebound as discussed by Severy [63] and Berton [66]. In addition, energy dissipation can be introduced into the seat design using the cushioning material or seat structure itself. Three different seat modifications to increase occupant safety can be identified.

The first design is based upon the same principle as air bags. Inflatable comfort cushions within the seat would incorporate pressure relief valves. A sufficient impact with the occupant would bleed off air, dissipating some of the contact forces. The seat could then be re-inflated to its previous state, introducing no repair cost.

The second option would utilize rotary damping or frictional dissipaters in the seatback pivot. Seat back deflections could be used to control some of the occupant's rebound, but rear displacement would be restricted to prevent excessive occupant ramping. Integration of this system with the reclining mechanism should simplify the design.

The last proposal uses a sliding mount between the seat and the frame to absorb energy. A shear pin or similar threshold device maintains normal positioning, but when sufficient loadings are experienced by the seat, the mount slides on rails (or similar equipment) to dissipate impact energy. The advantage of this design is its application to both front and rear impacts.

Although not tested in this project, nor addressed in government regulations, rear passenger protection should be to the same standard as the front seat passengers. Statistically, children are the major occupants of the rear seats and do not require a high seatback. As a result, adults in this seating position do not have adequate head and neck protection. Unfortunately, widespread incorporation of rear seat head restraints will not occur until concerns for rear visibility are addressed. This should not preclude the manufacturer or the safety standard committees from attempting to improve the rear passengers' protection. The deployable head restraint of Melvin [69],[70] is one design solution to this problem.

Accompanying all the proposed designs for the vehicle is a public awareness campaign or education program to demonstrate operation of the equipment along with the dangers of improper usage. It is obvious from surveys on head restraints [20],[68] that the public does not properly position their head restraint, and that instruction of the equipment's function is an important component in any road safety program.

6.2 - WHIPLASH RESEARCH RECOMMENDATIONS

6.2.1 - EXPERIMENTAL STUDY

In general, the protocol developed for these experiments was able to satisfy the analytical requirements of this program. Information on a wide range of impact configurations was obtained without omitting any essential data. As is always the case, an increased number of tests

should be conducted to increase this database and is discussed in the last section on future research. To improve on the facility, Table 6.1 has been constructed - presenting the components of experimental procedures, materials, and instrumentation.

Table 6.1: Suggested Improvements to Low Speed Test Facility

Item	Comments
1) Instrumentation	
High Speed Video Accelerometers	- improved scaling and digitizing processes should be investigated using high contrast markers for auto-digitization schemes
Load cells	- methods to better attach the sensors to the vehicle are needed to reduce the high frequency vehicle vibrations
Speed Transducers	- accurate documentation of the contact forces requires a force measuring sensor
	- an independent source of test vehicle and pendulum speeds after impact would supplement and help validate the video records
2) Facility	
Pendulum Geometry	- adapt the rigid pendulum face to accommodate a more bumper-like surface to observe the effects of bumper geometry and energy dissipaters of both vehicles
3) Test Materials	
Occupant Surrogate (Test Dummy)	- a more biofidelic neck arrangement should be acquired or designed to more accurately simulate the neck response of the occupant
Test Vehicles	- a numerical model could be employed to interpret the torso loadings of a dummy with a poor neck to improve neck response
	- a greater variety of vehicle types should be available to test the variations between manufacturers
	- a vehicle surrogate or 'bogey' which can conveniently accommodate new bumper and seat designs would allow these new systems to be evaluated under controlled conditions

The incorporation of these features to the existing facility would present a unique opportunity to study vehicle impacts at U.B.C. This upgraded facility would be capable of undertaking research programs involving many aspects of low speed impact protection including front and side impact conditions.

6.2.2 - NUMERICAL MODELLING PROGRAM

The analytical modelling employed in this study had limited success. Representation of the vehicle frame and suspension as a rigid body and spring/dashpots, respectively, appears valid for impact speeds below 15 km/h. The whole body motion was reproduced in this initial model, requiring some refinement of the suspension's characteristics to better simulate the pitching movement of the vehicle.

The stiffness/displacement approach employed to define the bumper must be re-assessed. Even with the proper incorporation of hysteresis to dissipate energy, a damping element is required to provide the time dependent response of the original isolator. Implementation of this model with F.E.M. software should be attempted only if the analytical definitions can be faithfully incorporated.

6.2.3 - RECOMMENDATIONS FOR FUTURE WORK

This research has answered several questions regarding whiplash injuries in low speed collisions. In the process, additional questions regarding the biological criteria for an injury, influence of the striking vehicle's bumper, and the biomechanics of occupant - seat interactions have been raised. It is important to recognize the present research program as the beginning of a broader research project. Thus, it is advantageous to use the experiences from this research to suggest future programs to expand the knowledge of low speed - rear impacts. The following outline of proposed research topics are the most noticeable areas of deficiencies. This is not an exhaustive list, only an initial attempt to describe weaknesses in the area.

Survey Descriptions of Head Restraint Effectiveness and Vehicle Damage in Motor Vehicle Accidents

Statistics on whiplash and head restraint positioning have been carried out with sample sizes below 1000 and before 1980. Current opinions on whiplash and other soft tissue injuries vary considerably in regards to representation in total injury claims, number of genuine injuries, and relationships between vehicle damage and injury. A survey to document the influential parameters in whiplash accidents - type of head restraint, location of head restraint, type of car, damage to the car (location and repair cost), occupant age, sex and position at the time of the impact - could indicate the risk of injury in a given situation.

Biomechanics of Whiplash Injuries

Current information on whiplash injuries suggest that it is a family of soft tissue injuries involving the neck structures. Documentation of the tissues involved, as well as the frequency these tissues are represented in the injury population would provide insight into the neck motions producing the injury. Knowledge of the neck motion and loading required for injury is necessary when designing safety equipment and estimating tolerable occupant motions during an impact.

Studies on the Occupant and Seatback Interaction

Only a few authors have described the occupant's interaction with the seatback. The information obtained in this report highlights the undesirable seat characteristics that have not been adequately addressed. The production seats in use today can be categorized with respect to construction, strength, and size. A testing program that documents the occupant impact response with these various seat configurations should then be explored, beginning with the further analysis of data obtained in these recent test programs. The proposed seat designs in Section 6.2 could also be evaluated and optimized for most efficient and economical occupant protection.

Variation on Rear Impact Response Between Vehicles Struck

Rear impact response of the vehicle itself is governed by the bumper's spring and damping characteristics, and the stiffness of the rear structures. Since bumpers come in varying configurations, a database of the different bumper categories could be developed, providing a useful tool for accident reconstruction as well as design. A current undergraduate program studying the isolator's performance (as a single component) should continue to document the performance of the gas filled isolator, expanding to include other bumper types. After the bumper and isolator have been characterized, the vehicle's structure should be evaluated. Merging of this data could be used to predict performance of different vehicle and bumper combinations.

Influence of the Striking Vehicle: Structure and Impact Configuration

The present project studies one impact configuration with one striking "vehicle". To understand the significance of the striking vehicle, impacts with different striking bumpers and impact angles could be simulated. The present bumper standards requires the bumper to have adequate lateral and bending strengths. However, these strengths do not consider the occupant inside. Thus, documentation of this type could provide data for improved vehicle to vehicle impact modelling, as well as identify the limitations of current bumper designs.

Documentation of Rear Impact Speeds Below 8 km/h

The present program has explored impacts above 8 km/h because of the high damage threshold of the test vehicle. However, impact speeds below 8 km/h may still introduce hazardous occupant loading depending on the impact configuration. Impact speeds below 8 km/h should be conducted to observe the range of occupant loadings possible. This information will be important if compliance regulations based on possibility of injury are developed. Results of biomechanic research and surveys of whiplash injuries could be combined with this data to produce effective legislation.

Complete understanding of the whiplash injury still eludes the medical, engineering, and insurance communities. This research project has made a contribution in regards to vehicle performance, providing documentation of the vehicle and occupant loading during low speed rear impacts for researchers in this area. However, additional research is required to better

understand this phenomenon which is increasingly presenting itself in accident statistics.

Appendix A: PENDULUM DESIGN

The pendulum system criteria are outlined in Section 3.1. The maximum test vehicle expected for this facility is a large passenger car with a mass of 1980 kg to be impacted at 20 km/h. This worst case loading was used to design the pendulum.

The dynamic loading consists of a centrifugal loading and an impact load. Referring to Figure A.1, centrifugal loading amounts to:

$$a_{cent} = V^2/R$$

where: a_{cent} = centrifugal acceleration

V = tangential velocity of the pendulum

R = pendulum radius

The centrifugal force then equals:

$$F_{cent} = (a_{cent} + g)m_{pend}$$

where: F_{pend} = centrifugal force

m_{pend} = pendulum mass

g = gravity

thus for 1820 kg mass and 20 km/h (5.6 m/s) impact conditions:

$$F_{cent} = \left(\frac{(5.6)^2}{3.3} + 9.81 \right) (1820)$$

$$F_{cent} = 35.150kN$$

Impact loading is calculated by the following, refer to Figure A.1

Assuming: $I_1 = 17.8 \text{ kg/m}^2$ $I_2 = 97.8 \text{ kg/m}^2$
 $m_1 = 23.7 \text{ kg}$ $m_2 = 1820 \text{ kg}$ $m_3 = 1820 \text{ kg}$
 $\omega_1 = 1.7 \text{ m/s}$ $V_1 = 2.5 \text{ m/s}$ $V_2 = 5.6 \text{ m/s}$
 $\Delta t = 0.005 \text{ s}$
 $F_{fric} = \mu m_3 g = (0.6)(1820)(9.81) = 10.71 \text{ kN}$

Conservation of Angular Momentum (primes indicating post-impact value):

$$\sum H_{pre-impact} = \sum H_{post-impact}$$

$$M_1 V_1 r_1 + \omega(I_1 + I_2) + M_2 V_2 r_2 - F_{fric} r_2 \Delta t = M_1 V'_1 r_1 + \omega'(I_1 + I_2) + M_2 V'_2 r_2$$

knowing:

$$\omega = \frac{V_2}{r_2} \quad \text{and} \quad V_1 = V_2 \left(\frac{r_1}{r_2} \right)$$

$$(23.7)(2.5)(1.5) + (1.7)(97.8 + 17.8) + (3.3)(1820)(5.6) - (10712.5)(3.3)(0.005) =$$

$$(23.7)(V'_2) \left(\frac{1.5}{3.3} \right) (1.5) + (3.3)(1820)(V'_2) + \frac{(V'_2)}{3.3} (17.8 + 97.8) + (1820)(V'_3)(3.3)$$

$$33742.2 = 16.2V'_2 + 6006V'_2 + 35V'_2 + 6006V'_3$$

$$33742.2 = 6057V'_2 + 6006V'_3$$

For a perfectly elastic impact $e = 1$:

$$V_2 = V'_2 - V'_3$$

$$\therefore 33742.2 = 6057(V'_2) + 6006(5.6 + V'_2)$$

$$33742.2 = 6057V'_2 + 6006V'_2 + 33633.6$$

$$108.6 = 12063V'_2$$

$$V'_2 \approx 0.01 \text{ m/s}$$

and

$$V'_3 \approx 5.6 \text{ m/s}$$

From the speed calculation, it is possible to calculate the reaction forces at A:

$$\sum H_{pre-impact} = \sum H_{post-impact}$$

$$\omega(I_1 + I_2) + V_1 M_1 r_1 - R_x \Delta t r_2 = \omega'(I_1 + I_2) + V'_1 m_1 r_1$$

$$(1.7)(97.8 + 17.8) + (23.8)(2.5)(1.8) - 3.3R_x \Delta t = \left(\frac{0.01}{3.3}\right)(17.8 + 97.8) + (23.8)(1.5)\left(\frac{1.5}{3.3}0.01\right)$$

$$(3.3)(0.005)R_x = 304.1$$

$$R_x = 18.43 \text{ kN}$$

Based on these calculations, a cable stayed frame as shown in Figure 3.1 was designed anticipating a maximum loading of 40 kN vertically and 20 kN horizontally. The material used, 10 cm x 10 cm x .5 cm square steel tubing, withstands the imposed loads with a 1.5 - 2.0 factor of safety. The frame is pin jointed to the floor to eliminate bending moments at the base, as well as to allow easy installation.

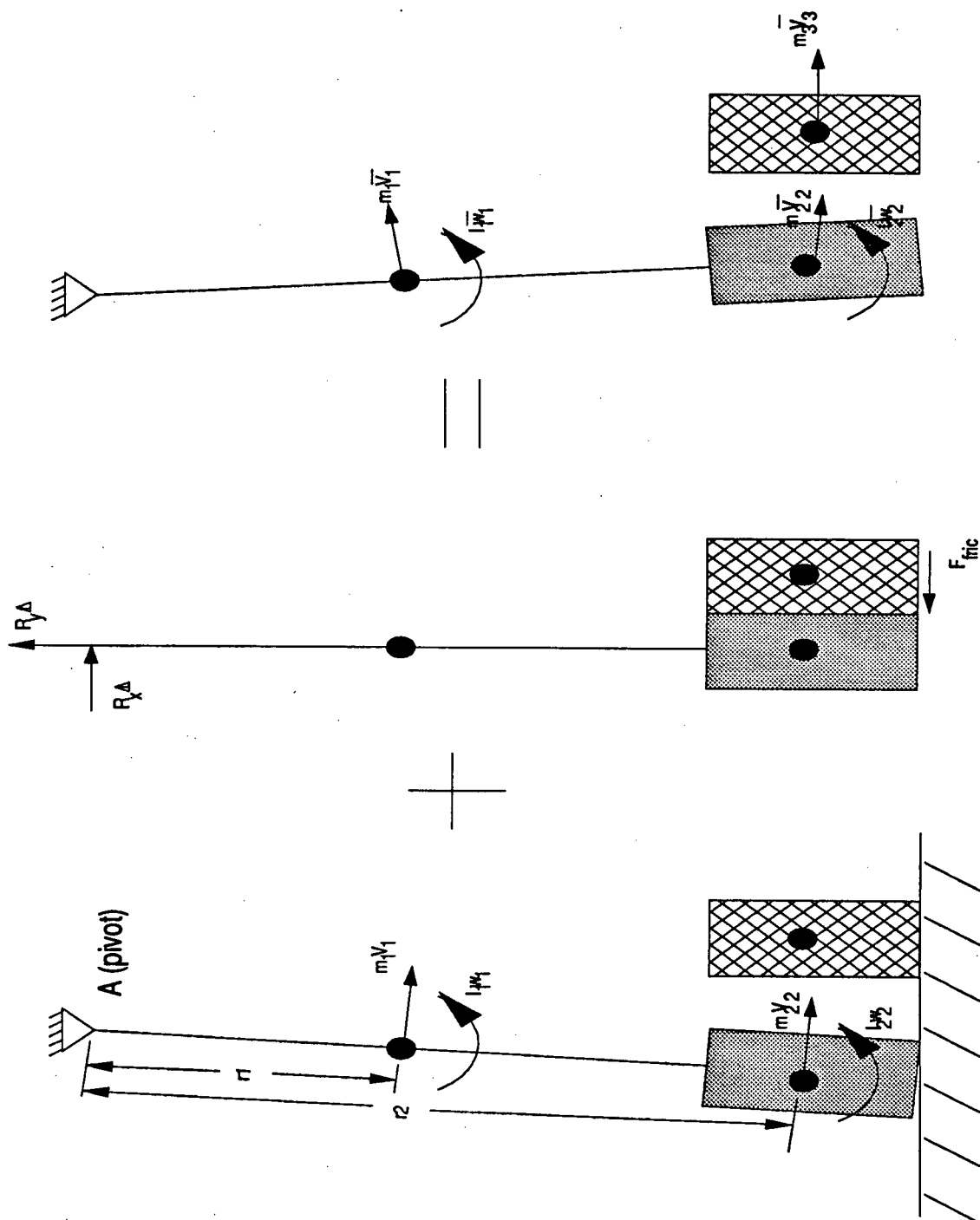


Figure A.1: Free Body Diagram of Pendulum

Appendix B: FEM MODEL DEFINITION

/TITLE, 2-D VEHICLE RESPONSE 8 KM/H IMPACT - STANDARD BUMPER (BRAKING)

/COM, NONLINEAR - TRANSIENT DYNAMIC ANALYSIS OPTION

KAN,4

KAY,5,2 *SET TO 0 INITIAL VELOCITY

KAY,9,2 *USE MODIFIED NEWTON-RAPHSON SOLUTION

*SET,HT,.8 *DEFINE HEIGHT OF THE VEHICLE

*SET,VEL,8 *SET IMPACT VELOCITY [KM/H]

/COM, SET GRAVITY FIELD

ACEL,,9.81

/COM, ELEMENT 1 MASS ELEMENT - NO ROTARY EFFECTS

ET,1,21,,4

/COM, ELEMENT 2 IS 2-D ELASTIC BEAM

ET,2,3

/COM, ELEMENT 3 IS A COMBINATION ELEMENT FOR THE SUSPENSION

ET,3,40,,2,,1

/COM, ELEMENT 4 IS A SPRING ELEMENT

ET,4,14,,2

/COM, ELEMENT TYPE 5 IS A COMBINATION ELEMENT FOR THE BUMPER
AND BRAKING FORCES ELEMENTS

ET,5,40,,,,1

/COM, ELEMENT TYPE 8 IS A CONTROL ELEMENT FOR THE BUMPER

ET,6,37,1,,,,1,,,,

/COM, PLACING THE COORDINATE SYSTEM ORIGIN TO ASSIST IN GEOMETRY DEFINITION

LOCAL,11,,,,450

N,10

N,9,-.058

/COM, PLACING PENDULUM AND BUMPER NODES

N,1000,-0.13186

N,1001,-1

N,1002,-0.13186

/COM, PLACING FRAME NODES

LOCA,12,,678,.405

N,20

N,5,-.168

LOCAL,13,,723,.404

N,30

LOCAL,14,,901,.288

N,40

LOCA,15,,965,.251

N,50

LOCAL,16,,1.850,.229

N,60

LOCAL,17,,1.950,.222

N,70

LOCAL,18,,2.336,.216

N,80

LOCA,20,,3.10,.223

N,100

LOCAL,19,,3.078,.405

N,90

N,6,-.135

LOCAL,25,,965,HT

N,250

LOCAL,26,,1.95,HT

N,260

```
CSYS
FILL,10,20,2
FILL,250,260,2
FILL,260,90,2

/COM, PLACE THE TIRE AND FRICTION NODES
N,1,.,677
N,2,.,677
N,3,3.077
N,4,3.077

/COM, REAL CONSTANTS FOR VEHICLE

Rsize,12

/COM, FRICTION COEFFICIENTS
*SET,MUS,0.36
*SET,MUD,0.32

/COM, DEFINE WEIGHT DISTRIBUTION
*SET,WFRO,5103
*SET,WREA,3775

/COM, MASS COMPONENTS
R,1,68
R,2,62
R,3,50
R,4,62
R,5,140
R,6,82
R,7,320

/COM, BEAM GEOMETRY
R,8,1,.,0833,.,5

/COM, FRONT SUSPENSION STIFFNESS
R,10,30.9E3,1618

/COM, REAR SUSPENSION STIFFNESS
R,11,26.9E3,1618

/COM, TIRE STIFFNESS
R,12,4.7E5

/COM, SPAR CROSS SECTION AREA
R,13,1

/COM, YOUNGS MODULUS FOR STEEL
EX,1,2E8

/COM, ENGINE MASS
R,14,241.5

/COM, PENDULUM EQUIVALENT STIFFNESS
R,15,2761.7,.,929

/COM, FRONT TIRE BRAKING FORCE
R,17,1E7,.,.,MUD*WFRO
/COM, *REAR TIRE BRAKING FORCE
R,18,1E7,.,.,MUD*WREA
```

```
/COM, BUMPER CHARACTERISTICS  
R,20,22.7E5,,,0045,50.3E3 * INITIAL STIFFNESS AND SLIDING  
R,21,22.2E5,,,0.04253, * FINAL STIFFNESS  
R,23,,,0.0,0.062,2000 * PRETENSION
```

```
/COM, MESHING THE BUMPER/PENDULUM  
TYPE,5  
REAL,15  
E,1000,1001 *ELEMENT 1  
REAL,20  
E,1000,1002 *ELEMENT 2 K1/SLIDE  
REAL,21  
E,1000,1002 * K2  
TYPE,6  
REAL,23  
E,1000,1002,1000,1002
```

```
/COM, MESHING THE FRAME  
TYPE,2  
MATE,1  
REAL,8  
E,10,13  
E,13,16  
E,16,20  
E,30,20  
E,30,40  
E,40,50  
E,50,60  
E,60,70  
E,70,80  
E,80,90  
E,30,250  
E,250,253  
E,253,256  
E,256,260  
E,260,204  
E,204,90
```

```
/COM, PLACING POINT MASSES  
/COM, ZONE,1  
TYPE,1  
REAL,1  
E,16
```

```
/COM, ZONE 2  
REAL,2  
E,20  
E,250  
REAL,3  
E,5
```

```
/COM, ZONE 3  
REAL,4  
E,253
```

```
/COM, ZONE 4  
REAL,5  
E,260
```

```
/COM, ZONE 5  
REAL,6  
E,204
```

/COM, ZONE 6,7

REAL,7
E,90
REAL,4
E,6

/COM, PLACING THE FRICTION SPRINGS

TYPE,5
REAL,18
E,1,2
REAL,17
E,3,4

/COM, PLACING THE TIRE SPRINGS

TYPE,4
REAL,12
E,2,5
E,4,6

/COM, PLACING THE FRONT AND REAR SUSPENSION SPRINGS

REAL,10
E,90,6
REAL,11
E,20,5

/COM, DEFINING THE RESTRICTED DEGREES OF FREEDOM

D,1,UY,0,,4,1,
D,1001,UX,,,,UY
D,1000,UY,0,,1002,2

/COM COUPLING THE MOTIONS OF THE WHEEL HUB AND TIRE CONTACT PATCH

CP,1,UX,2,5,20
CP,2,UX,4,6,90

/COM, COUPLE THE LOADING NODE (1002) WITH THE BUMPER)

CP,3,UX,1002,10

/COM, DEFINING LOAD STEPS

/COM, RAISING PENDULUM

ITER,1,1,1
F,1000,FX,VEL*(-444.9)

/COM, PRETENSIONING THE SUSPENSION

D,1,UX,-0.738598E-01
F,20,FY,WREA
F,5,FY,-WREA
F,6,FY,-WFRO
F,90,FY,WFRO
KBC,2
LWRITE

/COM, RELEASING - PENDULUM SWING

ITER,80,20,20
D,3,UX,-0.738567E-01
TIME,,8
KBC,1
CNVR,,.001
F,1000,FX,0
PRRF,-1
LWRITE

/COM, REFINE ANALYSIS TIME STEP DURING CONTACT

ITER,1000,20,20

TIME,1

KBC,1

PRRF,-1

LWRITE

/COM, DECREASE TIME STEP AFTER CONTACT IS BROKEN TO FINAL TIME

ITER,1000,25,25

TIME,1.5

KBC,1

PRRF,-1

LWRITE

/COM, WRITE ANALYSIS FILE

AFWRIT

FINI

/COM, SUBMIT FOR ANALYSIS

Appendix C: SOFTWARE DESCRIPTIONS

Software employed in Series I testing sorted the digitized data, scaled the information to full size, and then smoothed the data. The data was first processed with the FORTRAN program "MESSAGE.FOR" to collate the data points for each benchmark. Lotus 123 was used to determine the scales for the different marker distances which was read into the "SCALE.FOR" program. The data files were transmitted to the U.B.C. MTS system where the least square curve fitting routines "DOLSF" and "DOLNT" were used. The latter routine also generated the first derivatives of fitted data and was used to provide velocity and acceleration values. The FORTRAN program "CURVE.FTN" read in the data files and submitted it to the subroutines for processing.

The second series of tests required new software because of the different equipment employed. The "ACCEL.FOR" program contains subroutines to convert the accelerometer output voltage to acceleration values and to apply a sixth-order Butterworth low pass filter to the data. The filtering routine was written previously by Bruce Lehmann, U.B.C. Mechanical Engineering and use of this is appreciated.

Video processing in Series II was carried out using Lotus 123 and the "VIDEO.FOR" program. Transformation constants between the image and full size coordinates were calculated in a Lotus spread sheet and exported to a reference text file. The "VIDEO.FOR" program then read in the data points and their corresponding distances from the camera. These distances were cross-referenced to the appropriate transformation constants allowing digitized distances to be scaled to full size. A least squares curve fitting routine and low pass filter (mentioned above) were used to smooth the data. Finally, a numeric differentiation algorithm was used to generate the velocity and acceleration values from the time / displacement data.

A copy of this software is stored in the office of Dr. Doug Romilly in the Department of Mechanical Engineering at the University of British Columbia.

Appendix D: VEHICLE INFORMATION

Geometric and Mass Properties of the Test Vehicles

Vehicle test weights measured at the I.C.B.C. Test Centre ranged from 773 to 943 kg. This data was compared to the information reported in Tables D.1-3. A vehicle mass of 840 kg was adopted and combined with the Hybrid II mass of 68 kg to produce a total mass of 908 kg.

Table D.1: Inertial Measurements of 1979 VW Rabbits

(from [81])

Vehicle No.	Weight [kg]	C of G (vertical) [m]	I_{zz} [Nm ²]
1	840.9	0.51	944.5
2	840.9	0.52	995.9
3	840.9	0.52	970.2
4	840.9	0.54	1062.3
5	840.9	0.53	1023.0
Average	840.9	0.52	999.2

Note: occupant not included

Table D.2: Mass Properties of a Modified 1977 VW Rabbit

(from [79])

Vehicle Mass	1041 kg
Center of Gravity	0.92 m behind front axle 0.51 m vertical
I_{zz}	1270 Nm ²

Table D.3: General Dimensions of 1980 Volkswagen Rabbit

(from Transport Canada Vehicle Specifications Database - U.B.C. Accident Research Team)

Wheel Base	240 cm
Overall Length	395 cm
Overall Height	160 cm
Curb Weight	833 kg

The information used by autobody repairmen was used to derive the geometry of the model. The dimensions shown in Figure D.1 are based on factory specifications.

Volkswagen reported that the models from 1976-1982 were identical in construction except for cosmetic changes.

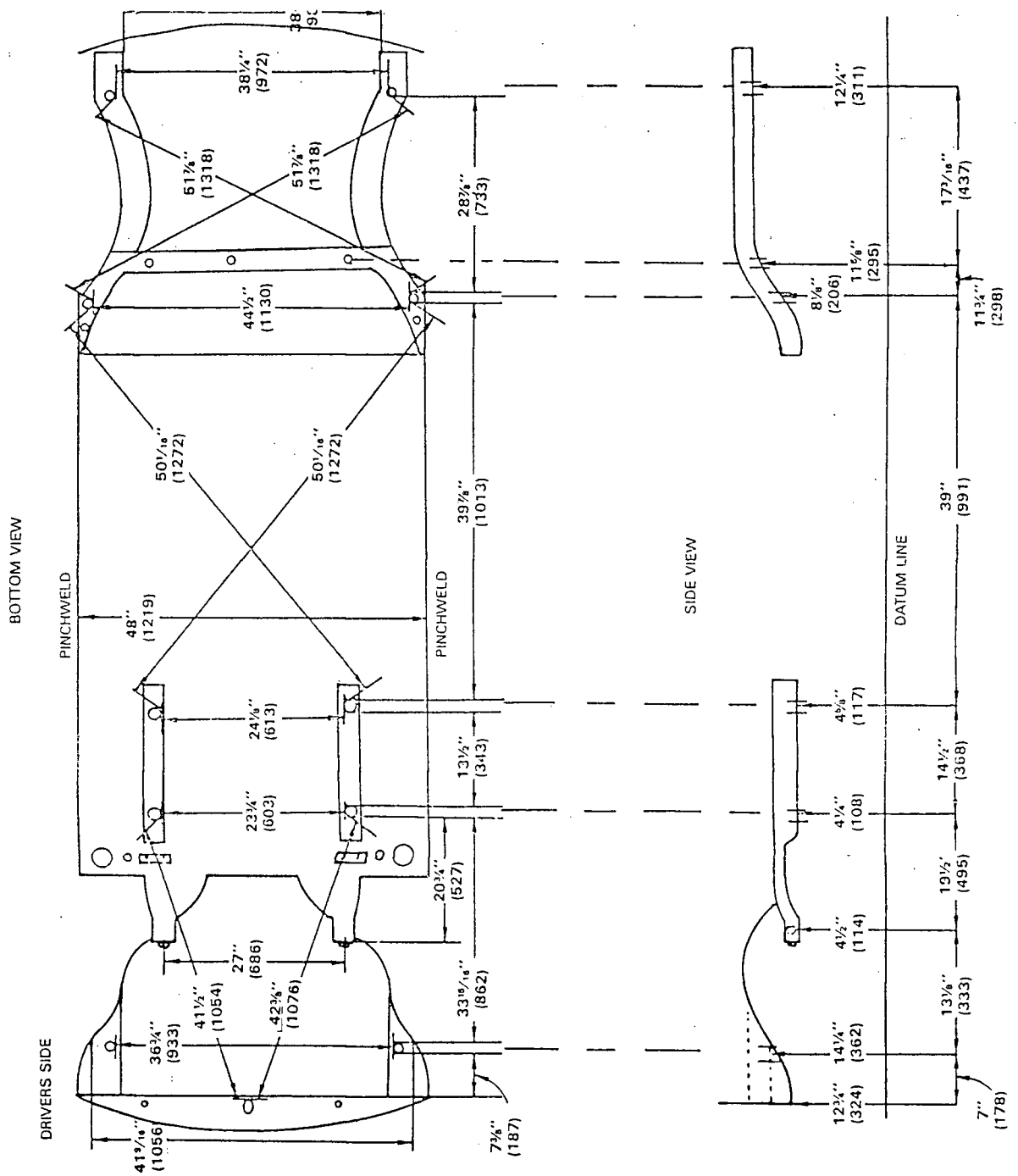


Figure D.1: Volkswagen Frame Dimensions
(from [80])

Suspension Parameters

Mechanical performance characteristics for the suspension components were not available from Volkswagen. A front and rear suspension spring, as well as the rear shock absorber was removed from a Rabbit and tested at U.B.C.. The results are listed in the following tables and graphs.

Table D.4: Spring Characteristics of Volkswagen Suspension

	Front Spring	Rear Spring
Spring Constant	15.4 kN/m	13.4 kN/m
Corrected For Two Parallel Springs	30.9 kN/m	26.8 kN/m

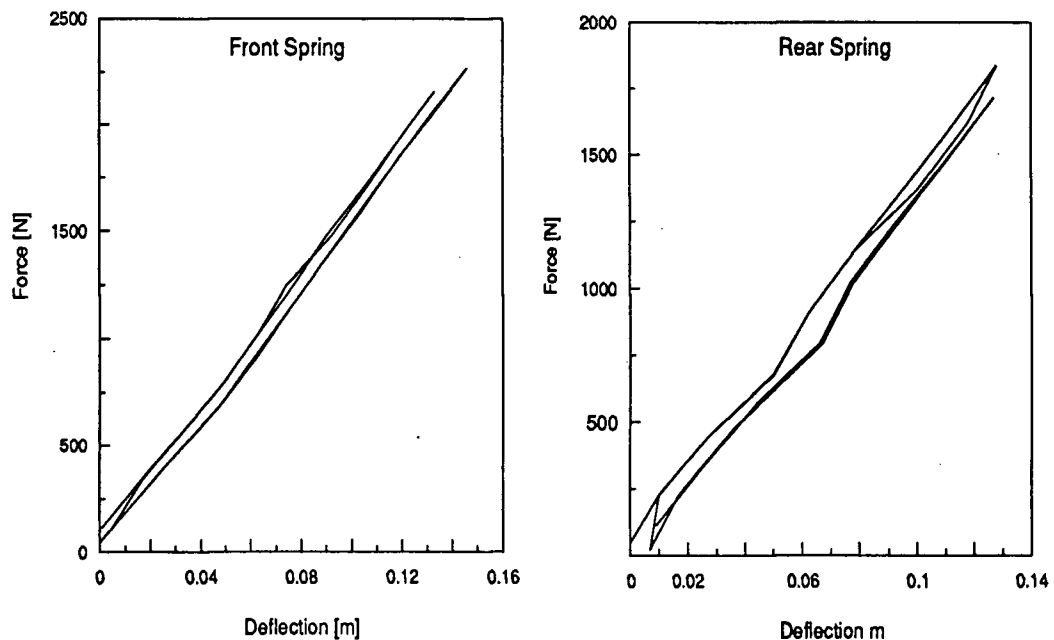


Figure D.2: Force / Deflection Curves for Suspension Springs

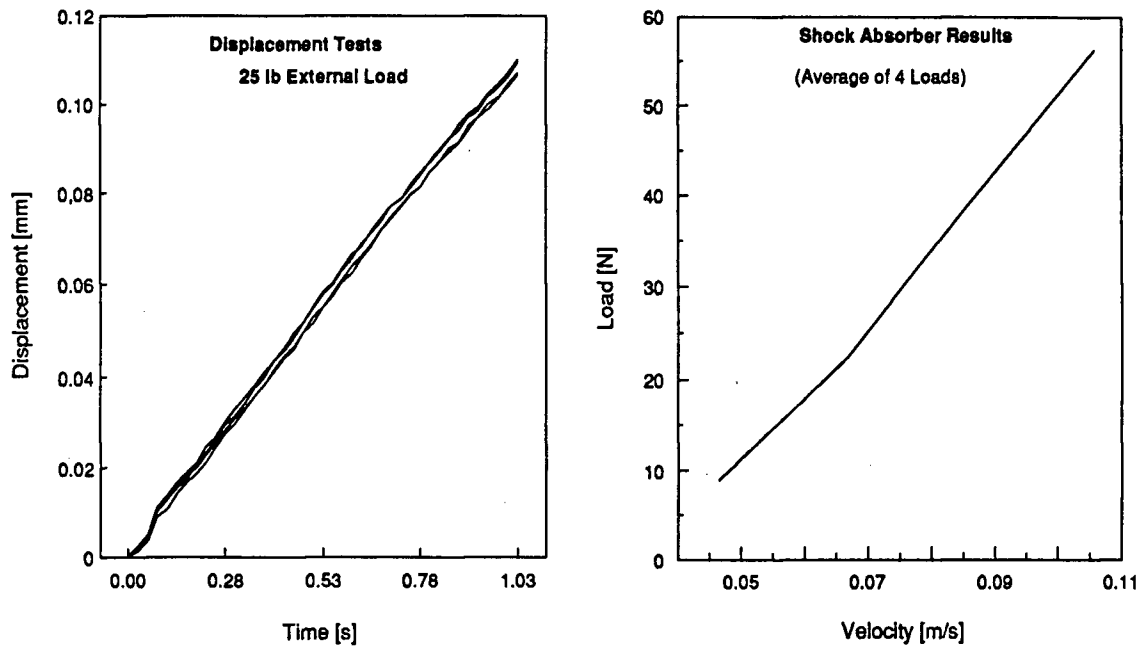


Figure D.3: Damping Characteristics of the Suspension

The damping coefficient, obtained from the slope of the load vs velocity curve, is 809.0 kg/s which is 1618 kg/s when corrected for two parallel shocks.

The compliance of steel belted radial tires is given in reference [83] as 23.5 kN/m per tire.

Bumper Characteristics

Bumper isolator response curves, documenting a 475 kg weight striking an individual isolator at four different impact speeds (7.3, 8.0, 8.1, 8.37 km/h), were supplied by Volkswagen. Figure D.4a presents the force-time and force-time behaviour of the isolators and Figure D.4b represents the corresponding force-displacement relationship for the same test. The nonlinearities present in these figures make application of $F = kx + c\dot{x}$ infeasible. The best approximation of the bumper could be achieved with the force deflection curves. These were described with key points connected with straight lines, as in Figure D.5. The dissipated energy was calculated (Table D.5) and incorporated into the bumper approximations. The value of the key points and dissipated energies at higher speeds were predicted using linear regressions, similar to that shown in Figure D.6.

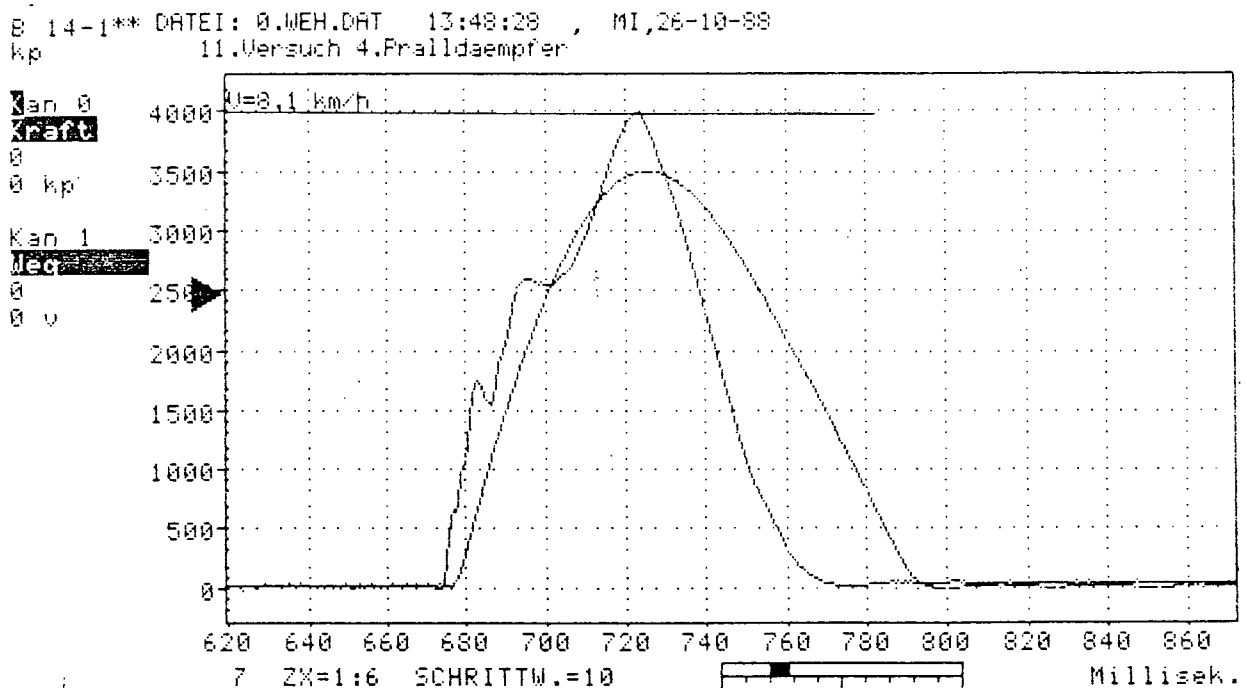


Figure D.4a: Bumper Deflection and Force Response with Time

B 14-19 ATEI: 0.WEH.DAT 13:48:28 , MI,26-10-88
 mm 11.Versuch 4.Pralldaempfer

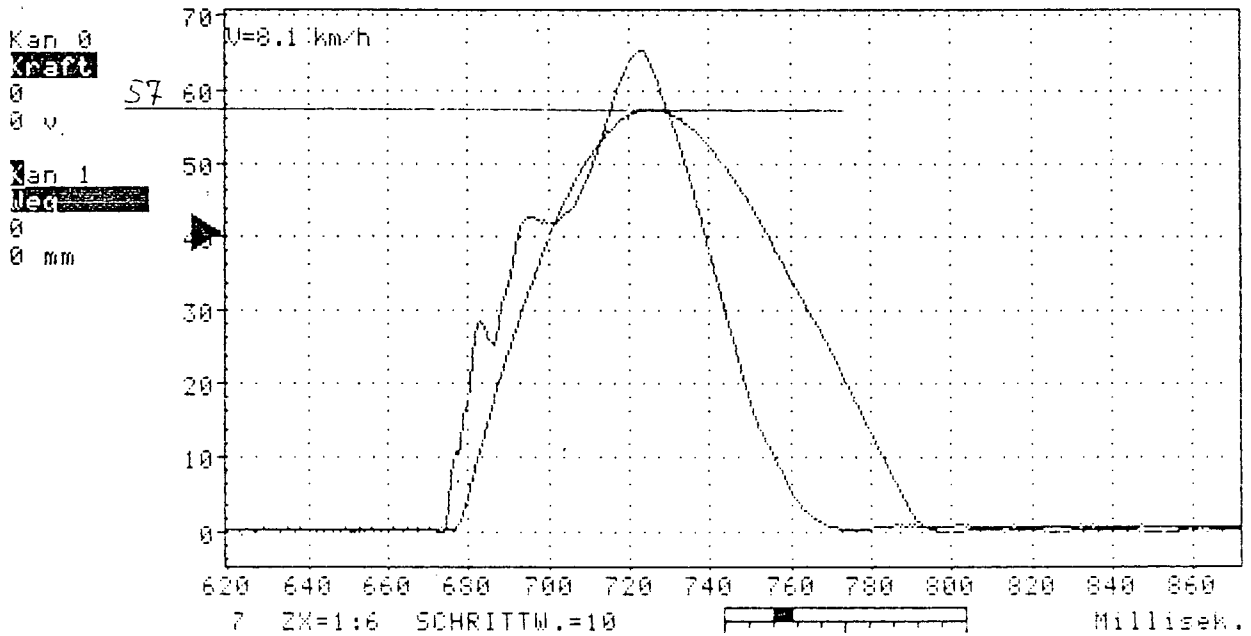


Figure D.4b: Bumper Force/Deflection Response

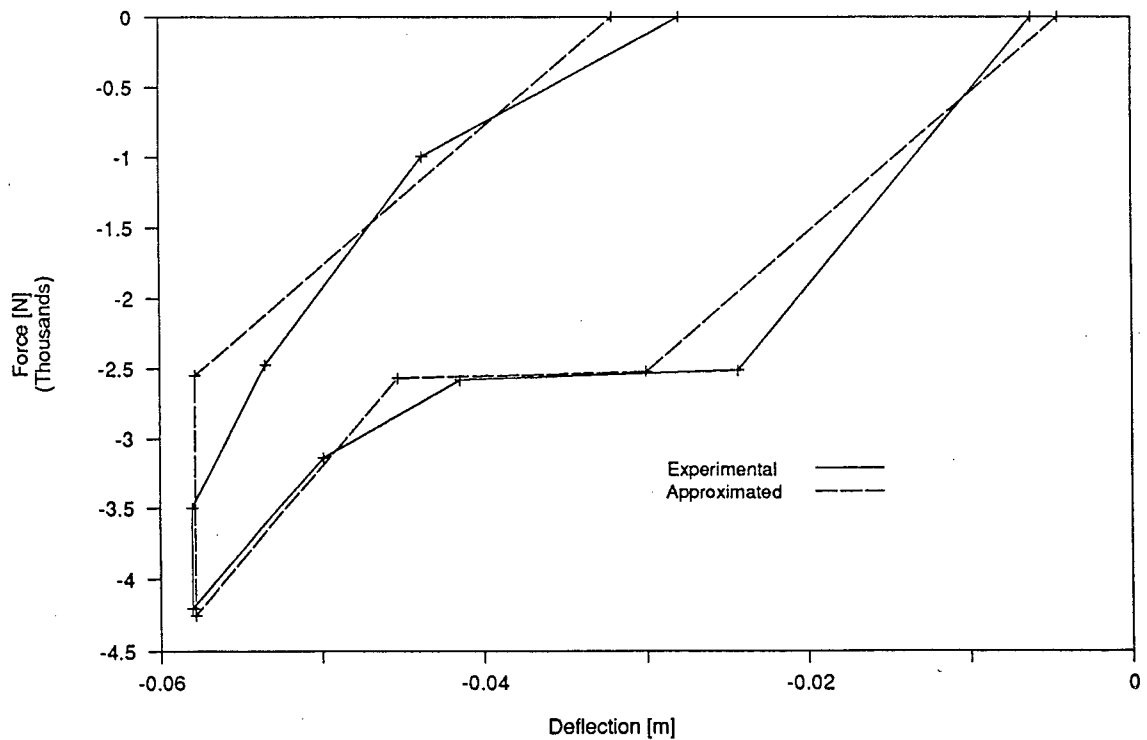


Figure D.5: Approximated Bumper Force/Deflection Curve

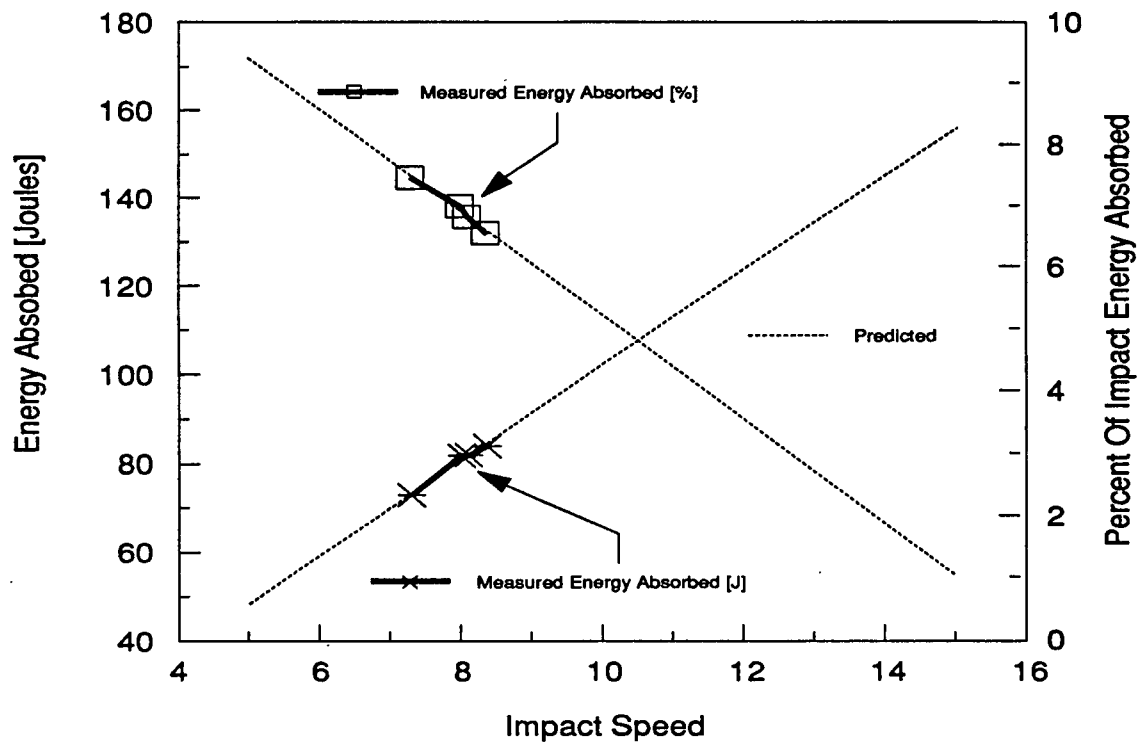


Figure D.6: Predicted Energy Dissipation

Table D.5: Absorbed Energy for Different Impact Speeds

Speed [km/h]	Energy [J]
7.3	1456
8.0	1637
8.1	1637
8.37	1679

Appendix E: PHOTOGRAMMETRY

The principles of coordinate transformation can be applied to the photographic images to obtain the full size measurements of the image. A mathematical relationship can be derived, as shown in Moffit and Mikail [84], based on Figure E.1. MacInnis and Siegmund [85] suggest solving the 8 transformation constants from known reference measurements in the image. A Lotus 123 spreadsheet was used to solve this series of equations with the values obtained in the experiments.

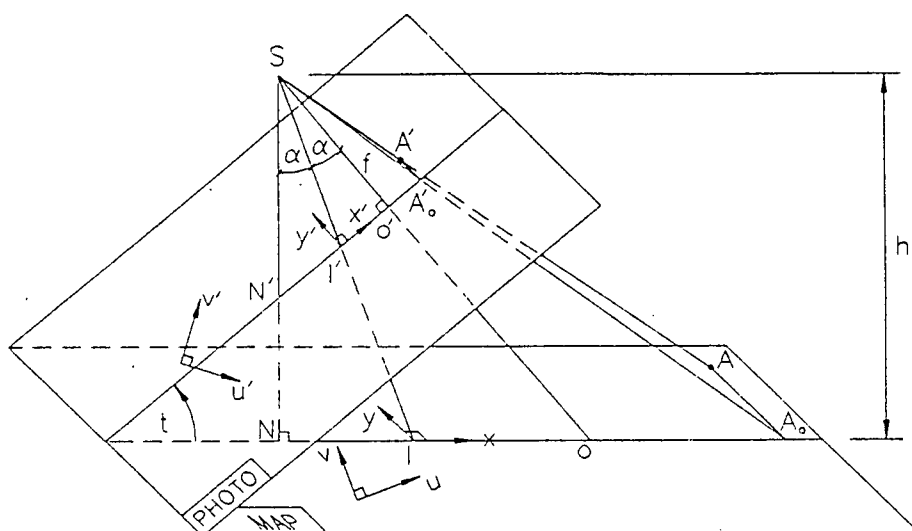


Figure E.1: Photographic - Full Size Image Transformation
(from [83])

S = Camera Focal Point

(u,v),(u',v') = Coordinate System of Map and Photo Plane, respectively

$$u = \frac{a_1 u' + b_1 v' + c_1}{a_0 u' + b_0 v' + 1}$$

$$v = \frac{a_2 u' + b_2 v' + c_2}{a_0 u' + b_0 v' + 1}$$

Appendix F: CANADIAN MOTOR VEHICLE SAFETY STANDARDS

CMVSS 202

202. (1) In this section, "manikin" means a manikin described in SAE Recommended Practice J826 Manikins For Use In Defining Vehicle Seating Accommodation, (November 1962).

(2) A head restraint shall be provided at each outboard front designated seating position on a vehicle

(a) when tested during a forward acceleration of not less than 8g on the seat supporting structure, limits rearward angular displacement of the head reference line to 45 degrees from the torso reference line; or

(b) when adjusted to its fully extended design position,

(i) has an overall height of not less than 27.5 inches when measured perpendicularly to a line that passes through the seating reference point and is perpendicular to the torso line,

(ii) has a lateral width of not less than 10 inches in the case of a bench-type seat or 6.75 inches in the case of an individual seat when measured either 2.5 inches below the top of the head restraint or 25 inches above the seating reference point,

(iii) does not allow the rearmost portion of the head form to be displaced more than 4 inches perpendicularly rearward of the extended displaced torso reference line during the application of the test load, and

(iv) withstands an increasing load until either failure of the seat or seat back occurs or the load so increased is equal to 200 pounds,

(3) The test referred to in paragraph (2)(a) shall be carried out as follows:

(a) the head restraint shall be in its fully extended design position;

(b) reference lines shall be established on the exterior profile of the head and torso of a dummy or an approved equivalent test device by

(i) positioning the dummy's back on a horizontal flat surface with the lumbar joints in a straight line,

(ii) rotating the head of the dummy rearward until the back of the head contacts the surface referred to in subparagraph (i),

(iii) positioning the back of a two-dimensional manikin against the surface referred to in subparagraph (i) and alongside the dummy in such a manner that the H-point of the manikin is aligned with the H-point of the dummy,

(iv) establishing the torso line of the manikin in the manner set out in SAE Aerospace-Automotive Drawing Standards Section 2.3.6, P. E1.01, (September 1963),

(v) establishing the dummy torso reference line by superimposing the torso line of the manikin on the torso of the dummy, and

(vi) establishing the head reference line by extending the dummy torso reference line onto the head;

(c) the dummy referred to in paragraph (b) shall have the weight and seated height of a 95th percentile adult male and an approved representation of a human articulated neck structure;

(d) at each designated seating position having a head restraint, the dummy shall be placed in the manufacturer's recommended design seated position and snugly restrained by a Type 1 seat belt referred to in section 209 of this Schedule;

(e) a forward acceleration shall be applied to the structure supporting the seat in such a manner that when graphically depicted the magnitude of the acceleration curve shall not be less than that of a half-sine wave having an amplitude of 8g and a duration of 80 milliseconds and not more than that of a half-sine wave having an amplitude of 9.6g and a duration of 96 milliseconds; and

(f) the maximum rearward angular displacement of the head reference line from the dummy torso reference line shall be measured.

(4) The test referred to in paragraph (2)(b) shall be carried out as follows:

(a) a test device having the back pan dimensions of the three-dimensional manikin and the centreline of the head room probe in the full back position shall be placed at the manufacturer's recommended design seated position;

(b) the displaced torso reference line shall be established by applying a rearward moment of 3,300 pound-inches about the seating reference point to the seat back through the back pan of the test device so placed;

(c) the back pan shall be removed and using a 6.5-inch diameter spherical head form or a cylindrical head form having a 6.5-inch diameter in plan view and a 6-inch height in profile view a rearward initial load shall be applied perpendicular to the displaced torso reference line and 2.5 inches below the top of the head restraint sufficient to produce a 3,300 pound-inches moment about the seating reference point; and

(d) the initial load shall be gradually increased to 200 pounds or until the seat or seat back fails, whichever occurs first.

CMVSS 215

Bumpers

215. (1) Every vehicle that is impacted at its unloaded vehicle weight by a pendulum-type testing device in accordance with subsections (3) to (5) shall, where prior to each impact in any test described in this section it had

(a) its front wheels parallel to the vehicle's longitudinal centreline,

(b) its tires inflated to the vehicle manufacturer's recommended pressure indicated on the placard pursuant to subsection 110(5) for the specified loading condition,

(c) its brakes disengaged and the transmission in neutral, and

(d) trailer hitches and licence plate brackets removed from the vehicle,

have, during and after each impact in any test described in this section,

(e) each lamp or reflective device, except licence plate lamps, free of cracks and meeting the visibility requirements of section 108 or 108.1, whichever is applicable,

(f) the aim of each headlamp to which section 108 is applicable adjustable to within the beam aim inspection limits specified in SAE Recommended Practice J599d (December 1974) measured with a mechanical aimer that meets the requirements of SAE Standard J602c (December 1974),

(g) the aim of each headlamp to which section 108.1 is applicable adjustable to within the beam aim inspection limits required under that section,

(h) the hood, trunk and doors operating in the normal manner,

(i) no leaks in the fuel and cooling systems and no constricted fluid passages and all sealing devices and caps operating in the normal manner,

(j) no leaks or constrictions in the exhaust system, and

(k) the propulsion, suspension, steering and braking systems in adjustment and operating in the normal manner.

(2) Every vehicle that, after being impacted by a pendulum-type testing device in accordance with subsections (3) to (5), is impacted into a fixed-collision barrier that is perpendicular to the line of travel of the vehicle while it is travelling longitudinally forward at 8 km/h (5 mph) and longitudinally rearward at 8 km/h (5 mph), with its engine operating at idle speed and subject to the conditions set out in paragraphs (1)(a) to (d) shall, during and after each impact, meet the requirements of paragraphs (1)(e) to (k).

(3) Every vehicle shall be impacted on the front surface and rear surface two times each with the impact line at any height between 500 mm (20 inches) and 400 mm (16 inches) in accordance with the following longitudinal impact test procedure:

(a) for impacts at a height between 500 mm (20 inches) and 400 mm (16 inches), place the test device shown in Figure 2 to this section so that plane A is vertical and the impact line is horizontal at a height within the range;

(b) for each impact, position the test device so that the impact line is at least 50 mm (2 inches) apart in vertical direction from its position in any prior impact, unless the midpoint of the impact line with respect to the vehicle is to be positioned more than 300 mm (12 inches) apart laterally from its position in any prior impact;

(c) for each impact, align the vehicle so that it touches, but does not move, the test device, with the vehicle's longitudinal centreline perpendicular to the plane that includes plane A of the test device and with the test device at any position inboard of the vehicle corner test position specified in subsection (4);

(d) move the test device away from the vehicle, then release it so that plane A remains vertical from release until the onset of rebound, and the arc described by any point on the impact line is constant, with a radius of not less than 3.3 m (11 feet), and lies in a plane parallel to the vertical plane through the vehicle's longitudinal centreline;

(e) impact the vehicle with the test device moving at 8 km/h (5 mph) at the moment of impact; and

(f) perform the impacts at intervals of not less than 30 minutes.

(4) Every vehicle shall be impacted on a front corner and a rear corner once each with the impact line at a height of

500 mm (20 inches) in accordance with the following corner impact test procedure:

(a) for an impact at a height of 500 mm (20 inches) place the test device shown in Figure 1 to this section so that plane A is vertical and the impact line is horizontal at the specified height;

(b) for each impact align the vehicle so that a vehicle corner touches, but does not move, the lateral centre of the test device, with plane A of the test device forming an angle of 60 degrees with a vertical longitudinal plane;

(c) move the test device away from the vehicle, then release it so that plane A remains vertical from release until the onset of rebound, and the arc described by any point on the impact line is constant, with a radius of not less than 3.3 m (11 feet), and lies in a vertical plane at an angle of 30 degrees to the vertical plane through the vehicle's longitudinal centreline; and

(d) impact each corner with the test device moving at 4.8 km/h (3 mph) at the moment of impact.

(5) For the purposes of subsections (3) and (4),

(a) the test device consists of a block with one side contoured as specified in Figures 1 and 2 to this section with the impact ridge made of hardened steel;

(b) with plane A vertical, the impact line shown in the said Figures 1 and 2 is horizontal at the same height as the test device's centre of percussion;

(c) the effective impacting mass of the test device is equal to the mass of the tested vehicle; and

(d) when impacted by the test device, the vehicle is at rest on a level, rigid concrete surface.

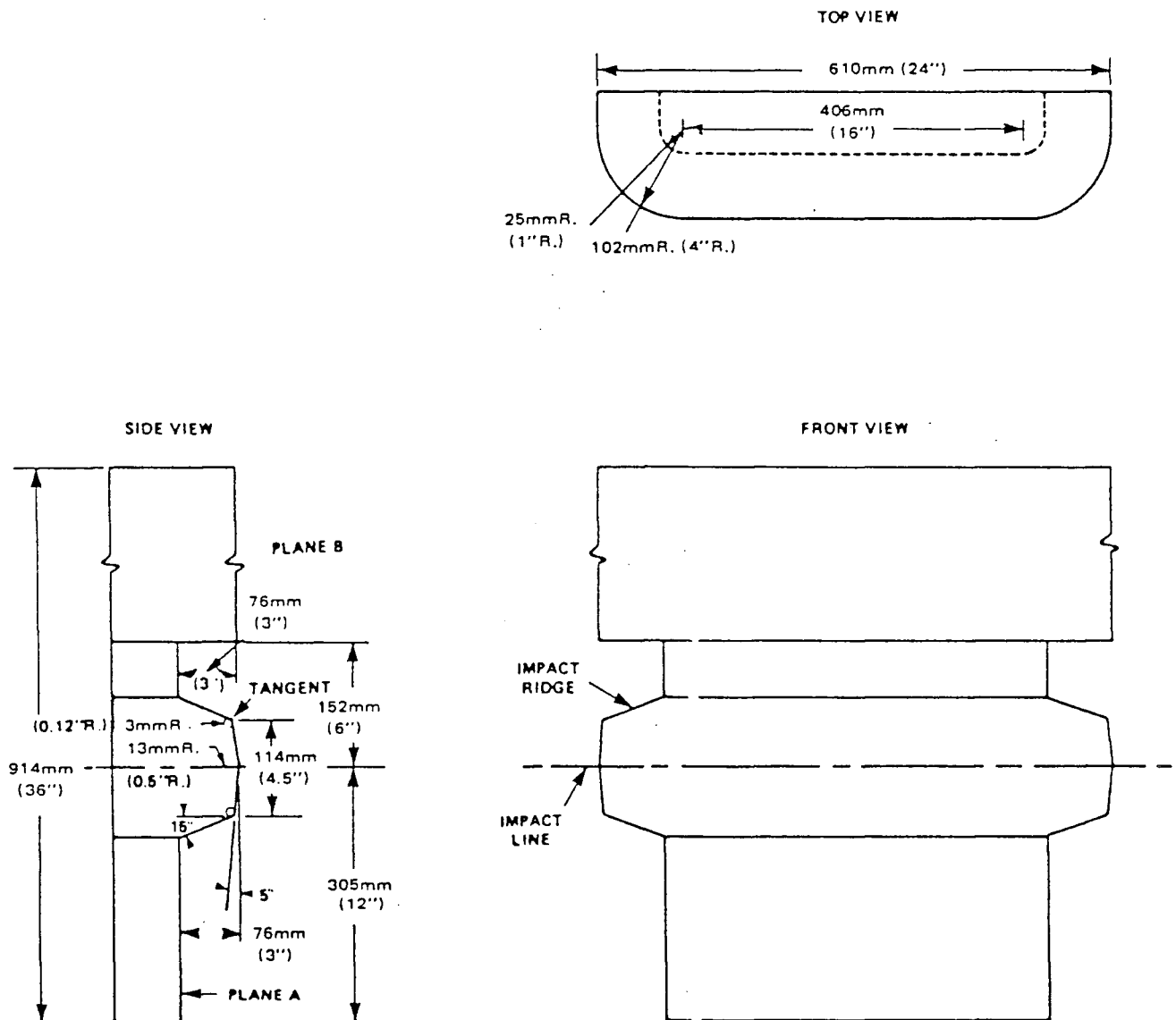


FIGURE 1



REFERENCES

- 1 Mercer, G.W. " Whiplash Producing Casualty Traffic Accidents: Trends, Characteristics, Persons Involved, and Consequences, British Columbia 1987", Counter Attack Program, Ministry of Labour and Consumer Services, British Columbia, Canada, 1988
- 2 "Human Tolerance to Impact Conditions as Related to Motor Vehicle Design", SAE J885 Apr80, SAE Information Report
- 3 Foreman, S.M., Croft, A.C., Whiplash Injuries. The Cervical Acceleration/Deceleration Syndrome, Williams and Wilkens Co., 1988
- 4 Sehmer, J., Lubin, S. Private communication
- 5 Anatomical Chart Co., Chicago, Ill. (c) 1947
- 6 Macnabb, I., "Acceleration-Extension Injuries of the Cervical Spine", The Spine, W.B. Saunders Co., 1982
- 7 Huelke, D.F., "Anatomy of the Human Cervical Spine and Associated Structures", The Human Neck - Anatomy, Injury Mechanisms, and Biomechanics, SAE SP438, Pa. 790130, 1973
- 8 Mulligan, G.W.N., Thom, R., Dyck, K., Sobie, C., "Whiplash Injuries To The Neck, Acute Cervical Sprain, Hyperextension Injury; A Continuing Enigma for Physicians and a Frequent Dilemma for Litigants", University Of Manitoba, 1988
- 9 Severy, D.M., Mathewson, J.H., Bechtol, C.O., "Controlled Automobile Rear-End Collisions, An Investigation of Related Engineering Phenomena", Canadian Services Medical Journal, Vol. 11, November, 1955
- 10 Whiplash Symposium II, Richmond, B.C., 1989
- 11 Emori, R.I., Horiguchi, J., "Whiplash in Low Speed Vehicle Collisions", SAE Pa. 900542, 1990
- 12 Kipp, W.I., "Impact-With-Rebound: An Advanced Tool for Laboratory Crash Simulation", SAE Pa., 700406
- 13 Transport Canada TP 3322, "1987 Canadian Motor Vehicle Traffic Accident Statistics"
- 14 "Motor Vehicle Safety Test Methods", Transport Canada, TP 3666-E

- 15 Tarriere, C., Fayon, A., Harteman, F., "The Contribution of Physical Analysis of Accidents Towards Interpretation of Severe Traffic Trauma", Nineteenth Stapp Car Crash Conference, SAE Pa. 751176, 1975
- 16 Bosio, A.C., Bowman, B.M., "Simulation of Head and Neck Dynamic Response in -Gx and +Gy", Proceedings of the Thirtieth Stapp Car Crash Conference, SAE Pa. 86
- 17 Mertz, H.J., "Neck Injury", SAE Conference Proceedings P-49, Human Tolerance to Biomechanics, Impact and its Application to Automotive Design, 1973
- 18 States, J.D., Korn, M.T., Masengill, J.B., "The Enigma of Whiplash Injury", New York State Journal of Medicine 70:24 P2971-2978, 1970
- 19 Roaf, R., "A Study of the Mechanics of spinal Injury ", Journal of Bone and Joint Surgery, 1960
- 20 States, J.D., Baclerak, J.C., Williams, J.S., Morris, A.T., Babcock, W., Polvino, R., Riger, P., Dawley, R.F. "Injury Frequency and Head Restraint Effectiveness in Rear End Impact Accidents", Sixteenth Stapp Car Crash Conference, Pa. 720967, 1972
- 21 O'Neil, B., Haddon, W., Kelley, A.B., Sorenson, W., "Automobile Head Restraint - Frequency of Neck Injury Claims in Relation to the Presence of Headrests", American Journal of Public Health 62:399-406 1972
- 22 Garrett, J.W., Morris, D.F., "Performance Evaluation of Automobile Head Restraints", SAE Pa. 720034, 1972
- 23 Stapp, J., "Historical Review of Impact Injury", Impact Injury to the Head and Spine, Charles C. Thomas Publ., pp.5-40, 1983
- 24 Proceedings of the Fifth Stapp Automotive Crash and Field Demonstration Conference, University of Minnesota, 1962
- 25 Mertz, H.J., Patrick, L.M., "Investigation of Kinematics and Kinetics of Whiplash", SAE Transactions Vol 76, Paper 670919, 1967
- 26 Mertz, H.J., Patrick, L.M. "Strength and Response of the Human Neck", Fifteenth Stapp Car Crash Conference Pa. 710855, 1971
- 27 Bowman, B.M., Robbins, D.H., "Parameter Study of Biomechanical Quantities in Analytical Neck Models", Proceedings of Sixteenth Stapp Crash Car Conference, P14-44, 1972 Society of Automotive Engineers

- 28 Seemann, M.R., Lustick, L.S., Frisch, G.D., "Mechanism for Control of Head and Neck Dynamic Response", Naval Biodynamics Laboratory, Proceedings Of the Twenty-Eighth Stapp Car Crash Conference Pa. , 1984
- 29 Tarriere, C., Sapin, C., "Biokinetic Study of the Head to Thorax Linkage", SAE Transactions Vol. 78 Pa. 690815, 1969
- 30 Ewing, C.L., Thomas, D.J., "Human Head and Neck Response to Impact Acceleration", NAMRL Monograph 21, 1972
- 31 Foust, D.R., Chaffin, D.B., Snyder, R.G., Baum, J.K., "Cervical Range of Motion and Dynamic Response and Strength of Cervical Muscles", Seventeenth Stapp Car Crash Conference, SAE Pa. 730975, 1973
- 32 Clemens H.J., Burow, K., "Experimental Investigation on Injury Mechanisms of the Cervical Spine at Frontal and Rear-Frontal Impacts", Sixteenth Stapp Car Crash Conference, Pa. 720960, 1972
- 33 Ewing, C.L., "Injury Criteria and Human Tolerance for the Neck", Aircraft Crashworthiness, University of Virginia, 1975
- 34 Hodgson, V.R., "Role of Impact Location in Reversible Cerebral Concussion" SAE Pa. 831618, Proceedings of the Twenty Seventh Stapp Car Crash Conference, 1983
- 35 Culver, C.C., Neathery, R.F., Mertz, H.J., "Mechanical Necks with Humanlike Responses", SAE Pa. 1972
- 36 Melvin, J.W., McElhaney, J.H., Roberts, V.L., "Improved Neck Simulation for Anthropometric Dummies", Sixteenth Stapp Car Crash Conference, Paper 720958, 1972
- 37 Mintes, J.M., Goldsmith, W., "Response of An Advanced Head-Neck Model to Transient Loading", Journal of Biomechanical Engineering, Vol.105, 1983
- 38 Muzzy, W.H., Lustick, L., "Comparison of Kinematic Parameters Between Hybrid II Head and Neck System with Human Volunteers for -Gx Acceleration Profiles", SAE Paper 760801, 1976
- 39 Foster, J.F., Kortge, J.O., Wolanin, M.J., "Hybrid III - A Biomechanically Based Crash Dummy", Proceedings of the Twenty-First Stapp Car Crash Conference, SAE Pa. 770938, 1977

- 40 Viano, D.C., Melvin, J.W., McCleary, J.D., Madeira, R.G., Shee, T.R., Horsch, J.D., "Measurement of Head Dynamics and Facial Contact Forces in the Hybrid III Dummy", Proceedings of the Thirtieth Stapp Car Crash Conference, SAE Pa. 861891, 1986
- 41 Martinez and Garcia, "A Model for Whiplash", Journal of Biomechanics, Vol. 1 No. 1, 1968
- 42 McKenzie, J.A., Williams, J.F., "The Dynamic Behaviour of the Head and Cervical Spine During Whiplash", Journal of Biomechanics, Vol.4, No.6, 1971
- 43 Prasad, P., Mital, M., King, A.I., Patrick, L.M., "Dynamic Response of the Spine During + Gx Acceleration", Proceedings of the Seventeenth Stapp Car Crash Conference, SAE Pa. 751172, 1975
- 44 Reber, J.G., Goldsmith, W., "Analysis of Large Head-Neck Motions", Journal of Biomechanics, Vol. 12 No. 3, 1979
- 45 Merrill, T., Goldsmith, W., Deng, Y.C., "Response of a Lumped Mass Parametric Head-Neck Model Due to Impact and Impulsive Loading", Journal of Biomechanics 17:2, 1984
- 46 Lin, K.H., "A Rear End Barrier Impact Simulation Model for Unibody Passenger Cars", SAE Pa. 730156
- 47 Greene, J.E., "Computer Simulation of Car-to-Car Collisions", SAE 770015, 1977
- 48 Tomassoni, J.E., "A Study of the Effect of Strain Rate on the Automobile Crash Dynamic Response", Collection of Technical Papers: 19th AIAA-ASME Structures and Structural Dynamics Material Conference (Published by American Institute of Aeronautics and Astronautics, NY), 1978, No. 474
- 49 Kurimoto, K., Mantus, M., Pifko, A., "Modelling and Simulation of Frontal Crash Impact Response", SAE Pa. 811306, 1981
- 50 Okamoto, T., Shibo, F., Yamada, M., "Rear-End Crash Characteristics and Fuel System Safety", SAE Pa. 770815, 1977
- 51 Arima, K., Seo, K., Arakawa, T., "Rear Body Construction of Sub-Compacts and Fuel System Integrity in Rear End Collisions", SAE Pa. 770171, 1977
- 52 Tani, M., Funahashi, A., "Energy Absorption by the Plastic Deformation of Body Structural Members", SAE Pa. 780368, 1978

- 53 Peterson W., "Application of Finite Element Method to Predict Static Response of Automobile Body Structures, SAE Pa. 710263, 1971 Note:
- 54 Borowski, V.J., Steury, R.L., Lubkin, J.L., "Finite Element Dynamic Analysis of an Automotive Frame Publisher", SAE Paper 730506, 1973
- 55 Kirioka, K., Katto, Y., Saji, H. "Elasto - Plastic Analysis of Automobile Body Structures by the Finite Element Method", SAE Pa. 740039, 1974
- 56 Ishiyama, S., Nishimura, T., Tsuchiya, Y., "Impact Response of Thinwall Plane Frame Structures", International Journal of Impact Engineering Vol1. No.3, 1983
- 57 Yanaoka, H., Sakai, H., Ariyoshi, T., Fujii, M., "Computer Simulation of Automobile Body Crash Response Publisher", SAE Pa. 851685, 1985
- 58 Arima, K., Seo, K., Arakawa, T., "Rear Body Construction of Sub - Compact Vehicles and Fuel System Integrity in Rear End Collisions", SAE Pa. 77017, 1977
- 59 Winter, R., Mantus, M., Pifko, A.B., "Finite Element Crash Analysis of a Rear-Engine Automobile", SAE Pa. 811306, 1981
- 60 Prasad, P., and Chou, C.C., "A Review of Mathematical Occupant Simulation Models", Proceedings of Crash Performance Standards and the Biomechanics of Impact: What are the Relationships?", AAAM-IRCBI, 1990
- 61 Nakamura, K., Yashuom W., "Analytical Technique for Predicting of Car Body Structural Components and its Application", SAE Pa. 840450, 1984
- 62 Severy, D.M., Brink, H.M., Baird, J.D., "Backrest and Head Protection for Rear End Collisions Protection", SAE Paper 680079
- 63 Severy, D.M., Harrison, M.B., Baird, J.D., "Vehicle Design for Passenger Protection from High-Speed Rear-End Collisions", SAE Pa. 680774, 1968
- 64 Severy, D.M., Blaisdell, D.M., Kerkoff, J.F., "Automotive Seat Design and Collision Performance", SAE Transactions Vol. 85, Pa. 760810, pp.2551-2565, 1976
- 65 Strother, C.E., James, M.B., "Evaluation of Seat Back Strength and Seat Belt Effectiveness in Rear End Impacts", SAE Pa. 872214, 1987
- 66 Berton, R.J., "Whiplash, Tests of the Influential Variables", SAE Pa. 680080, 1968
- 67 Hu, A., Bean, S.P., Zimmerman, R.M., "Response of Belted dummy and Cadaver to Rear Impact", 1978, NTIS PB275/472

- 68 McKay, M., "Occupant Protection and Vehicle Design", Proceedings of Crash Performance Standards and the Biomechanics of Impact: What are the Relationships?", AAAM-IRCOBI, 1989
- 69 Melvin, J.W., McElhaney, J.H., Roberts, V.L., Portnoy, H.D., "Deployable Head Restraints - A Feasibility Study", Proceedings of the Fifteenth Stapp Car Crash Conference, SAE Pa. 710853, 1971
- 70 Melvin, J.W., McElhaney, J.H., "Occupant Protection in Rear-End Collisions", SAE Pa. 720033, 1973
- 71 Shibabuma, K., Tanaka, H., Nishiwaki, N., "Occupant Safety by use of Variable Energy Absorbing Bumpers", SAE Paper 850511, 1985
- 72 Shieh, R.C., "Strain Rate Sensitivity Effects on Crash Response and Dynamic Yield Moment Formulas for Crash Prediction of Automobile Bumpers", AIAA/ASME/SAE 16th Structures, Structural Dynamics, and Materials Conference, Pa. No. 75-791, 1975
- 73 Severy, D.M., Brink, H.M., Blaisdeck, D.M., "Smaller Vehicle versus Larger Vehicle Collisions", SAE Paper 710861, 1971
- 74 Naab, K., "Basic Research into Crashworthiness II. Low Speed Impact Tests of Unmodified Vehicles", NTIS PB212/924, 1972
- 75 SAE Handbook, Volume 4 "On Highway Vehicles and Off Highway Machinery", SAE 1984
- 76 "Repeatability of Setup and Stability of Anthropometric Landmarks and Their Influence on Impact Response of Automobile Crash Test Dummies"; Backaitis, S., SAE Paper 770260, 1977
- 77 "Sensitivity Study of Occupant Response in Simulated Crash Environment"; Backaitis, S.H., SAE Paper 740117, 1974
- 78 Burden, R.L., Faires, J.D., Reynolds, A.C., Numerical Analysis, Second Edition, PWS Publishers, 1978
- 79 Private communication - Ivar Lall, Volkswagen Canada, Inc., August 1989 and April 1990
- 80 KLM Automotive Publishing Inc. 1981
- 81 Holt, C., Brown, C., Totante, N., Hensen, A., "Validation of a Surrogate Vehicle for Certification Testing of Transformer Base Luminaire Supports", U.S. Dept. of Transportation Report FHWA/RD-87/034

- 82 Mark's Standard Handbook for Mechanical Engineers, Eighth Edition, McGraw-Hill Book Co., 1978
- 83 "Mechanics of Heavy-Duty Trucks and Truck Combinations", University of Michigan, July 13-17, 1987
- 84 Moffit, F.H., Mikhail, E.M., Photogrammetry, Third Edition, Harper and Row, 1980
- 85 MacInnis, D.D., Siegmund, G.P., "Application of Photogrammetry to Accident Reconstruction", Canadian Multidisciplinary Road Safety Conference VI, P. 289-298, 1989